ROLE OF CADHERINS IN SYNAPSE-SPECIFIC PLASTICITY

by

Raunak Basu

A dissertation submitted to the faculty of
The University of Utah
in partial fulfillment of the requirements for the degree of

Doctor of Philosophy

Department of Neurobiology and Anatomy

The University of Utah

May 2017

Copyright © Raunak Basu 2017

All Rights Reserved

The University of Utah Graduate School

STATEMENT OF DISSERTATION APPROVAL

The dissertation of **Raunak Basu**

has been approved by the following supervisory committee members:

Megan E. Williams	, Chair	**12/12/2016** Date Approved
Karen S. Wilcox	, Member	**12/12/2016** Date Approved
Jason Shepherd	, Member	**12/12/2016** Date Approved
Scott W. Rogers	, Member	**12/12/2016** Date Approved
Andres Villu Maricq	, Member	**12/12/2016** Date Approved

and by **Monica L. Vetter**, Chair/Dean of

the Department/College/School of **Neurobiology and Anatomy**

and by David B. Kieda, Dean of The Graduate School.

ABSTRACT

Single neurons often receive synapses with distinct properties. However, the molecules regulating these distinct properties remain largely unknown. This dissertation focuses on deciphering such molecules using the mammalian hippocampus as the model system. Hippocampal CA3 neurons form synapses with CA1 neurons at two distinct layers, stratum oriens (SO) and stratum radiatum (SR). SO synapses possess higher levels of long-term potentiation (LTP) and large headed dendritic spines (mushroom spines) compared to SR synapses. Results in Chapter 3 discuss the identification of a synaptic specificity molecule cadherin-9 that is expressed in the CA3 neurons. Genetic deletion of cadherin-9 resulted in reduction of the enhanced levels of LTP and mushroom spines in CA1 SO synapses without affecting the SR synapses. Using in vitro studies cadherins-6 and 10, expressed specifically in the CA1 neurons, were identified to be the postsynaptic binding partners of cadherin-9. Further, deletion of the postsynaptic cadherins resulted in reduced LTP and mushroom spines specifically in the CA1 SO layer similar to the phenotypes observed by deletion of cadherin-9. These results describe a novel functional heterophilic interaction between cadherins-6, 9, and 10 that regulate unique properties specific to one set of synapses without affecting other synapses in the same neuron.

This dissertation is dedicated to my family and Binku Da

TABLE OF CONTENTS

LIST OF FIGURES

ACKNOWLEDGEMENTS

First, I would like to thank my mentor, Dr. Megan Williams, for providing me with immense freedom to think, design experiments, and shape my own project. Her balanced mix of pragmatism and enthusiasm helped me to both stay on track as well as greatly enjoy graduate school. I also want to thank the current and previous members of the Williams Lab for making working in the lab an enjoyable experience. I especially want to thank Mr. Matthew R. Taylor, Mrs. E. Anne Brogdon, Dr. Randi Rawson, Dr. Shruti Muralidhar, and Mr. Zhirong Wang for their numerous intellectually stimulating discussions that have helped me improve as a scientist. I also want to thank Mrs. Jennifer Hunter and Mr. Keegan Wade Teeder for their immense help with various experiments that have accelerated the completion of my dissertation.

I want to thank the members of thesis committee, Dr. Karen S. Wilcox, Dr. Jason Shepherd, Dr. Scott Rogers, and Dr. Andres Villu Maricq, for providing insightful discussions during committee meetings and helping me streamline my project. I want to thank Dr. Peter J. West for his immense help with the LTP studies. I also want to thank the administrative staff of the Department of Neurobiology and Anatomy, especially Mrs. Nicole Cheleste Caldwell and Mrs. Karen Evans, for their extremely efficient handling of paperwork.

I want to thank my parents, Mr. Rana Basu and Mrs. Anjana Basu, for instilling in me

the value of education and for constantly encouraging me to pursue a career in academics. I want to thank my grandmother, Mrs. Bela Rani Basu, for her unconditional love and my sister, Ms. Shreya Basu, for a unique friendship that made my childhood a memorable experience. I also want to thank my wife, Dr. Haimasree Bhattacharya, for providing a home several thousand miles away from Kolkata. Her constant companionship helped me get through the numerous ups and downs of Ph.D. life.

I want to thank my cousins, Mr. Sayantan and Mr. Iman Ghoshdastidar, whose constant encouragement motivated me to become a curious human being and Mrs. Ushasi Das for always being a close confidante and source of support.

Finally, I want to thank my friends, Mr. Somshubhro Banerjee, Mr. Jishnu Batabyal, Mr. Reeshav Chatterjee, Mr. Nirjhar Banerjee, and Dr. Debanjan Mukherjee, for a fun-filled childhood, unparalleled moral support, and a deep friendship that has immensely influenced various facets of my character. I also want to thank my friend Mr. Niladri Sinha, whose consistent enthusiasm and extreme rigor for science has inspired me to think and work harder and become a better scientist.

CHAPTER 1

INTRODUCTION

Every cognitive and motor activity critically depends on precise communication between specialized cell types called neurons in the brain. Neurons are highly polarized cells that send out information through long thin processes called axons and receive information on shorter and thicker processes called dendrites. The major site of communication between two neurons is a specialized junction, called a synapse, formed between the axon of the sender neuron and dendrite of the receiving neuron. Importantly, normal brain function requires synaptic specificity whereby synapses form between appropriate partner neurons, at the appropriate subcellular location and with a repertoire of molecular constituents specific to the unique demands of a given synapse. Despite decades of study, we know remarkably little about the system of rules that guide neurons to build specific kinds of synapses between appropriate partners during normal brain development and how these systems may go awry in disease.

The fundamental process of synaptic specificity can be conceptualized by a sequence of three steps (Sanes and Yamagata, 2009; Williams et al., 2010):

1) During development, axons from the presynaptic neuron are guided to the correct postsynaptic target.
2) The two cells recognize their correct partners amongst many incorrect targets.
3) Subsequently, specific molecular recruitment forms the correct type of synapse with its characteristic properties.

The first step entails guiding the presynaptic axon along the correct path, which leads to the second step where the axon recognizes its target postsynaptic neuronal membrane. This step majorly comprises holding the pre- and postsynaptic membranes together. Successful adhesion among the two membranes leads to the third step where various

signaling cascades are initiated. This results in recruitment of different synaptic factors like scaffolding proteins, synaptic vesicles, and various neurotransmitter receptors (Friedman et al., 2000). Although several classes of molecules have been implicated in these processes, the most abundant class are cell adhesion molecules (CAMs). CAMs are integral membrane proteins (or membrane-associated proteins in certain cases) that have an extracellular domain (ECD) that binds to its partner CAM residing in the juxtaposed membrane. Moreover, these proteins generally have an intracellular domain (ICD) that can trigger downstream signaling (Dalva et al., 2007). This domain architecture makes CAMs ideally suited to relay extracellular information to the intracellular milieu. The major aim of this dissertation is to investigate the role of classic cadherins, a particular family of CAMs, in regulating characteristic properties of specific synapses (discussed in detail in Chapter 3). While a detailed review of current literature describing the role of cadherins in synaptic specificity is provided in Chapter 2, here I will give a brief overview of the role of various non-cadherin CAMs in the three phases of synaptic specificity outlined above. In the first section, I will highlight how CAMs have been implicated in guidance and target recognition of axons. In the subsequent section, I will give examples of CAMs that regulate characteristic properties of specific synapses.

CAMs are instrumental in guidance and target recognition of axons

Guiding an axon to the correct target entails different axonal pathfinding solutions. Very long-range axons can be guided to an overall correct target region by a combination of attractive and repulsive guidance cues. In this case, CAMs often function as a coarse guidance system steering an axon away from wrong routes. Alternatively, axons and their

correct dendritic partners may both be progressing towards each other through a narrow stretch of neuropil until they find each other. In other systems, axons may need to find the correct target neuron among incorrect neurons in the vicinity. In both cases, “finding” is hypothesized to be dependent on binding the correct partner through an adhesive code mediated by matching CAMs present on the pre- and postsynaptic membranes. Finally, axons are further targeted to the correct subcellular destination of their target neurons. Here, CAMs may act as adhesives (to bind the axon to the correct destination) or as repellants (to exclude the axons from wrong subcellular layers). Below, I will describe some of the seminal discoveries identifying the role of CAMs in each of the discrete steps outlined above.

As an example of long-range axon guidance, corticospinal axons emanating from the neocortex cross over to the contralateral side just before entering the spinal cord and continue down to synapse onto motor neurons. In mammals, this process is orchestrated by the Eph-Ephrin family of CAMs, which actively prevent the axons from re-crossing over to the ipsilateral side. Receptor tyrosine kinase (RTK) EphA4 expressed in corticospinal axons binds to EphrinB3 expressed along the midline (Kullander and Klein, 2002). Subsequent intracellular signaling via the RTK domain of EphA4 repels the axons away from the midline, thereby preventing re-crossing.

In the vertebrate retina, two classes of interneurons, bipolar cells and amacrine cells, synapse with retinal ganglion cells (RGCs) that relay visual information to the brain. Both the interneurons and RGCs can be further subdivided into several functional subtypes. Each particular subtype of RGC only synapses with a restricted and specific subset of interneurons. Interestingly, this complex synaptic specificity is achieved within

a narrow layer called the inner plexiform layer (IPL). In the IPL, the dendrites of a particular RGC and the axons of its partner interneuron arborize and form synapses in specific sublayers. Work from Joshua R. Sanes lab (Krishnaswamy et al., 2015; Yamagata and Sanes, 2008) showed that this layer specificity is mediated by expression of specific immunoglobulin superfamily CAMs (IgCAMs) . They found that four IgCAM members, Sidekick1, Sidekick2, Dscam, and DscamL, are expressed in non-overlapping subsets of interneurons and RGCs. These IgCAMs undergo homophilic interactions, implying that the proteins bind in trans across juxtaposed membranes. Interestingly, each synapsing pair of neurons expresses a specific IgCAM. This led to a model where the IgCAMs act as specific adhesives that hold together axons and dendrites of matching pairs of neurons. This model, however, does not explain a more complex situation where an RGC arborizes into multiple IPL sublayers. In Chapter 2, I will discuss the role of cadherins in mediating synaptic specificity in such complex circuits.

In most cases, axons may need to choose their correct partners among other incorrect choices in the vicinity. One such example is the *drosophila* olfactory system, which is comprised of approximately 50 different types of olfactory receptor neurons (ORNs) that synapse with around 50 different types of projection neurons (PNs). Interestingly, these synapses are not random; each class of ORNs synapses with a particular class of PNs at a discrete glomerulus in the olfactory bulb. This extreme synaptic specificity provides an ideal model to find mechanisms that prevent axons from one ORN class promiscuously synapsing with neurons in multiple adjacent glomeruli. Hong et al. (2012) through an ingenious genetic screen identified two homophilic CAMs, teneurin-a and teneurin-m, that mediate the connection between specific ORN-PN pairs. Genetic labeling studies

showed that two glomeruli, VA1d, and VA1lm, and their corresponding ORNs specifically expressed elevated levels of teneurin-m while an adjacent glomerulus DA1 and its corresponding ORN specifically expressed teneurin-a. RNAi and ectopic expression experiments confirmed that specific teneurin expression patterns are necessary for targeting the ORN axons to their correct PNs. The fact that flies express only two teneurins suggests that additional CAMs may mediate the specific wiring of other ORN-PN pairs.

Finally, I will review the roles of CAMs in targeting axons to the correct subcellular destination. Synapses formed at different parts of a neuron can have differential impact on the cell body and thus determine how the neuron integrates its incoming activity. Hence, it is imperative that axons form synapses at the correct subcellular location of postsynaptic neurons. One well-studied example of such a system is the Purkinje cell (PC) in the mammalian cerebellum. PCs receive inhibitory inputs onto their axon initial segment (AIS) from basket cells and on their dendrites from stellate cells. Ango et al. (2004) showed that PCs express an adhesion molecule Neurofascin186, a member of L1 immunoglobulin family, specifically at the cell body and AIS. This molecule captures the basket cell axons near the cell body, which then climb towards the AIS following the Neurofascin186 gradient. They further showed that disruption of this gradient causes mislocalization of basket cell synapses into other regions of PCs. The stellate cell axons, on the other hand, are guided towards the PC dendrites by their interaction with another cerebellar cell type called Bergman glia. In a follow-up paper, Ango and colleagues identified another member of the L1 immunoglobulin family, close homologue of L1 (CHL1), which is expressed in both Bergman glia and the stellate axons (Ango et al.,

2008). Targeted mutation of CHL1 results in the inability of stellate axons to follow the Bergman glial processes. Hence, it was hypothesized that homophilic interaction between CHL1 molecules in both cell types facilitates the stellate axon guidance.

A different mechanism of subcellular specificity was reported in hippocampal CA3 neurons, which receive inputs from dentate gyrus granule cells (DGs) specifically in a synaptic layer proximal to the cell body called stratum lucidum (SL). Suto et al. (2007) showed that CA3 neurons express a transmembrane semaphorin, Sema6A, throughout their dendrites that repels away the DG axons expressing a Sema6A receptor PlexinA4. However, expression of a different Sema6A receptor PlexinA2 specifically in SL attenuates the repulsion, thereby permitting DG axonal innervation specifically in that layer. Genetic deletion of PlexinA2 or PlexinA4 results in mistargeting of DG axons to incorrect dendritic layers of CA3 neurons (Suto et al., 2007).

Although seminal discoveries have identified the role of various CAMs in axon guidance (as highlighted above), a fundamental question still remains: Are the identified molecules enough to achieve the wiring complexity found in different parts of the nervous system? For example, it is conceivable that two members of the teneurin family, or a few members of the IgCAM superfamily, are not enough to explain the complex wiring scheme present in the olfactory bulb and retina. Future studies, therefore, will need to identify the molecular signatures of the variety of cell types comprising these complex systems. Recently, Shekhar et al. (2016) used single cell mRNA profiling to identify 15 different classes of bipolar cells in the mammalian retina. Similar studies, when extended to the downstream target RGCs, will help elucidate the molecular adhesion code that mediates specific synapse formation among all RGCs and bipolar cells

Role of CAMs in formation of correct type of synapses with characteristic properties

It can be argued that once axons are correctly targeted, "generic" synaptogenic factors can build the synapses. However, synapses releasing same neurotransmitters (e.g., glutamatergic synapses) can have unique properties (Arai et al., 1994; Nicholson et al., 2006; Nicoll and Schmitz, 2005). This leads to the hypothesis that individual classes of synapses use synaptic specificity factors to confer these distinct properties. Further, the disruption of these factors may only affect one particular class of synapses, but not other synapses in the cell that use other factors. In this chapter, I will discuss recent reports describing the role of three distinct classes of CAMs in hippocampal synaptic specificity.

Hippocampal CA1 neurons receive excitatory synapses in three distinct layers, stratum oriens (SO), stratum radiatum (SR), and stratum lacunosum-moleculare (SLM). Major inputs to SO and SR layers originate from hippocampal CA3 neurons while the inputs to SLM arrive from entorhinal cortex layer III neurons. DeNardo et al. (2012) showed that Netrin-G Ligand-2 (NGL-2), a leucine-rich repeat (LRR) domain containing CAM, is required for proper functioning of CA1 SR excitatory synapses but not SLM synapses. Genetic deletion or RNAi-mediated silencing of NGL-2 results in impaired synaptic transmission and less dendritic spines in CA1 SR layer but it does not affect the SLM synapses. Further, over-expression studies revealed that NGL-2 specifically localizes to CA1 SR dendrites but not to SLM dendrites. This study resulted in a model where NGL-2 in CA1 SR dendrites binds its receptor Netrin-G2 in CA3 axons to regulate functional properties of CA1 SR but not SLM synapses.

In a different study, Anderson et al. (2015) were investigating synapses formed by

CA1 neurons with subiculum neurons. Subiculum neurons are the major hippocampal targets of CA1 neurons and are comprised of two functionally distinct pyramidal cell types, normal firing (NF) and burst firing (BF). In this study, ß-Neurexins were shown to be important for functioning of synapses between CA1 and BF neurons but not between CA1 and NF neurons. Neurexins, typically localized to the presynaptic terminals, are a family of synapse inducing CAMs known to regulate multiple aspects of synapse function (Krueger et al., 2012). Deletion of ß-Neurexins specifically from CA1 neurons resulted in reduced presynaptic release probability of CA1-BF synapses through an endocannabinoid-dependent signaling mechanism, but the deletion did not affect the CA1-NF synapses.

CA1 pyramidal neurons send their projections not only to downstream excitatory neurons but also to local interneurons that provide feedback inhibition to the CA1 network. Although originating from the same presynaptic cell type, these pyramidal cell-interneuron synapses have distinct functional presynaptic properties based on the identity of the postsynaptic interneuron. For example, synapses between CA1 pyramidal neurons and oriens-lacunosum moleculare (O-LM) interneurons have low synaptic release probabilities whereas synapses between CA1s and parvalbumin positive (PV) interneurons have high release probabilities. Sylwestrak and Ghosh (2012) showed that the low release probability of CA1-OLM synapses can be attributed to an LRR domain containing CAM named Elfn1 that is specifically expressed in the OLM interneurons. Acute knockdown of Elfn1 in OLM interneurons increases release probability of CA1-OLM synapses whereas its overexpression in PV interneurons reduces the release probability of CA1-PV synapses. Thus, Elfn1expression in a postsynaptic cell is

sufficient to confer unique release properties of presynaptic axons. Collectively, the studies highlighted in this section provide evidence that synaptic specificity molecules act downstream of axon guidance to confer specific properties to specific synapses.

Dissertation overview

In the current chapter, I provided a brief overview of the roles of various CAMs in different stages of synaptic specificity. In Chapter 2, I will review some relevant literature on the role of cadherins, a family of CAMs, in synaptic specificity. Subsequently, in Chapter 3, I will describe my research investigating the role of three cadherins, cadherins-6, -9 and -10, in mediating enhanced synaptic potentiation observed specifically in a set of hippocampal CA1 synapses. In Chapter 4, I will describe my results investigating a possible presynaptic role of these cadherins. Finally, in Chapter 5, I will propose different models that describe the possible mechanism by which these cadherins may function.

References

Anderson, G.R., Aoto, J., Tabuchi, K., Földy, C., Covy, J., Yee, A.X., Wu, D., Lee, S.-J., Chen, L., Malenka, R.C., et al. (2015). β-Neurexins control neural circuits by regulating synaptic endocannabinoid signaling. Cell *162*, 593–606.

Ango, F., di Cristo, G., Higashiyama, H., Bennett, V., Wu, P., and Huang, Z.J. (2004). Ankyrin-based subcellular gradient of neurofascin, an immunoglobulin family protein, directs GABAergic innervation at purkinje axon initial segment. Cell *119*, 257–272.

Ango, F., Wu, C., Van der Want, J.J., Wu, P., Schachner, M., and Huang, Z.J. (2008). Bergmann glia and the recognition molecule CHL1 organize GABAergic axons and direct innervation of Purkinje cell dendrites. PLoS Biol. *6*, e103.

Arai, A., Black, J., and Lynch, G. (1994). Origins of the variations in long-term potentiation between synapses in the basal versus apical dendrites of hippocampal neurons. Hippocampus *4*, 1–9.

Dalva, M.B., McClelland, A.C., and Kayser, M.S. (2007). Cell adhesion molecules: signalling functions at the synapse. Nat. Rev. Neurosci. *8*, 206–220.

DeNardo, L.A., de Wit, J., Otto-Hitt, S., and Ghosh, A. (2012). Ngl-2 regulates input-specific synapse development in CA1 pyramidal neurons. Neuron *76*, 762–775.

Friedman, H.V., Bresler, T., Garner, C.C., and Ziv, N.E. (2000). Assembly of new individual excitatory synapses: time course and temporal order of synaptic molecule recruitment. Neuron *27*, 57–69.

Hong, W., Mosca, T.J., and Luo, L. (2012). Teneurins instruct synaptic partner matching in an olfactory map. Nature *484*, 201–207.

Krishnaswamy, A., Yamagata, M., Duan, X., Hong, Y.K., and Sanes, J.R. (2015). Sidekick 2 directs formation of a retinal circuit that detects differential motion. Nature *524*, 466–470.

Krueger, D.D., Tuffy, L.P., Papadopoulos, T., and Brose, N. (2012). The role of neurexins and neuroligins in the formation, maturation, and function of vertebrate synapses. Curr. Opin. Neurobiol. *22*, 412–422.

Kullander, K., and Klein, R. (2002). Mechanisms and functions of eph and ephrin signalling. Nat. Rev. Mol. Cell Biol. *3*, 475–486.

Nicholson, D.A., Trana, R., Katz, Y., Kath, W.L., Spruston, N., and Geinisman, Y. (2006). Distance-dependent differences in synapse number and AMPA receptor expression in hippocampal CA1 pyramidal neurons. Neuron *50*, 431–442.

Nicoll, R.A., and Schmitz, D. (2005). Synaptic plasticity at hippocampal mossy fibre synapses. Nat. Rev. Neurosci. *6*, 863–876.

Sanes, J.R., and Yamagata, M. (2009). Many paths to synaptic specificity. Annu. Rev. Cell Dev. Biol. *25*, 161–195.

Shekhar, K., Lapan, S.W., Whitney, I.E., Tran, N.M., Macosko, E.Z., Kowalczyk, M., Adiconis, X., Levin, J.Z., Nemesh, J., Goldman, M., et al. (2016). Comprehensive classification of retinal bipolar neurons by single-cell transcriptomics. Cell *166*, 1308–1323.e1330.

Suto, F., Tsuboi, M., Kamiya, H., Mizuno, H., Kiyama, Y., Komai, S., Shimizu, M., Sanbo, M., Yagi, T., Hiromi, Y., et al. (2007). Interactions between plexin-A2, plexin-A4, and semaphorin 6A control lamina-restricted projection of hippocampal mossy fibers. Neuron *53*, 535–547.

Sylwestrak, E.L., and Ghosh, A. (2012). Elfn1 regulates target-specific release probability at CA1-interneuron synapses. Science *338*, 536–540.

Williams, M.E., de Wit, J., and Ghosh, A. (2010). Molecular mechanisms of synaptic specificity in developing neural circuits. Neuron *68*, 9–18.

Yamagata, M., and Sanes, J.R. (2008). Dscam and Sidekick proteins direct lamina-specific synaptic connections in vertebrate retina. Nature *451*, 465–469.

CHAPTER 2

THE CLASSIC CADHERINS IN SYNAPTIC SPECIFICITY

Reprint of: Basu, R., Taylor, M.R., and Williams, M.E. (2015). The classic cadherins in synaptic specificity. Cell Adh Migr *9*, 193–201. Reprinted with permission.

REVIEW

Cell Adhesion & Migration 9:3, 193–201; May/June 2015; Published with license by Taylor & Francis Group, LLC

The classic cadherins in synaptic specificity

Raunak Basu[†], Matthew R Taylor[†], and Megan E Williams*

Department of Neurobiology and Anatomy; University of Utah; Salt Lake City, UT USA

[†]These authors equally contributed to this work.

Keywords: classic cadherins, cognitive disorders, molecular identity, synaptic specificity

Abbreviations: EC, extracellular cadherin; DG, dentate gyrus; RGCs, retinal ganglion cells; DN-cadherin, Drosophila N-cadherin; SNPs, single nucleotide polymorphisms; ADHD, attention deficit/hyperactivity disorder; BC, bipolar cell; EGF, epidermal growth factor.

During brain development, billions of neurons organize into highly specific circuits. To form specific circuits, neurons must build the appropriate types of synapses with appropriate types of synaptic partners while avoiding incorrect partners in a dense cellular environment. Defining the cellular and molecular rules that govern specific circuit formation has significant scientific and clinical relevance because fine scale connectivity defects are thought to underlie many cognitive and psychiatric disorders. Organizing specific neural circuits is an enormously complicated developmental process that requires the concerted action of many molecules, neural activity, and temporal events. This review focuses on one class of molecules postulated to play an important role in target selection and specific synapse formation: the classic cadherins. Cadherins have a well-established role in epithelial cell adhesion, and although it has long been appreciated that most cadherins are expressed in the brain, their role in synaptic specificity is just beginning to be unraveled. Here, we review past and present studies implicating cadherins as active participants in the formation, function, and dysfunction of specific neural circuits and pose some of the major remaining questions.

Introduction

Molecules of the cadherin superfamily are defined by the presence of calcium binding, extracellular cadherin (EC) repeats. Members of the cadherin superfamily include the classic cadherins, protocadherins, desmosomal, Fat, and 7-pass transmembrane cadherins.[1] Cadherin superfamily members are conserved across species and most are expressed in the nervous system where they function in several aspects of neural development from neurogenesis and cell migration to synapse formation and plasticity.[1-4] By definition the classic cadherins contain precisely 5 extracellular EC repeats (and no other conserved extracellular motifs) and an intracellular catenin-binding domain (**Fig. 1**). For reference, other cadherin superfamily members have varying numbers of EC repeats, often in combination with other extracellular protein motifs, and do not bind the catenins.[3] The classic cadherins have been subject to investigation for many years, yet their role in the nervous system is still unclear. This review focuses on the role of the classic cadherins in target selection and synaptic specificity and aims to unify work spanning several decades starting from early suggestions that cadherins regulate specific circuit development based on their remarkably selective neuronal expression patterns to recent work that directly tests the role of individual cadherins in identified circuits using newly available genetic and imaging tools. For more information regarding the general role of cadherins and cadherin signaling in neural development, synapse formation, and plasticity we refer to several excellent reviews.[5-8]

© Raunak Basu, Matthew R Taylor, and Megan E Williams
*Correspondence to: Megan E. Williams; Email: megan.williams@neuro.utah.edu
Submitted: 06/12/2014; Revised: 08/04/2014; Accepted: 12/15/2014
http://dx.doi.org/10.1080/19336918.2014.1000072
This is an Open Access article distributed under the terms of the Creative Commons Attribution-Non-Commercial License (http://creativecommons.org/licenses/by-nc/3.0/), which permits unrestricted non-commercial use, distribution, and reproduction in any medium, provided the original work is properly cited. The moral rights of the named author(s) have been asserted.

The Development of Synaptic Specificity

At the turn of the 20th century, Ramón y Cajal famously documented the existence of specific neural connections through his detailed anatomical drawings of neuronal cell types and their orderly and selective axonal projections.[9] The term "synaptic specificity" describes the fact that neural connections do not form randomly, but instead are highly organized. Neurons often synapse only with specific types of partner neurons. This requires that presynaptic axons identify correct partners within a complex environment containing a myriad of incorrect cell types. Then neurons must build the appropriate types of synapses relevant to the types of neurons being connected.

The extreme specificity of neural connections is now well established but the molecular mechanisms responsible for generating synaptic specificity are only just beginning to be understood. Many cellular factors contribute to the development of synaptic specificity. These factors include temporal and spatial constraints, genetically specified molecular identities, and neural activity. Moreover, these factors are often inextricably linked. For example, genetically specified molecules can encode spatial constraints on growth[10] and neural activity can influence gene

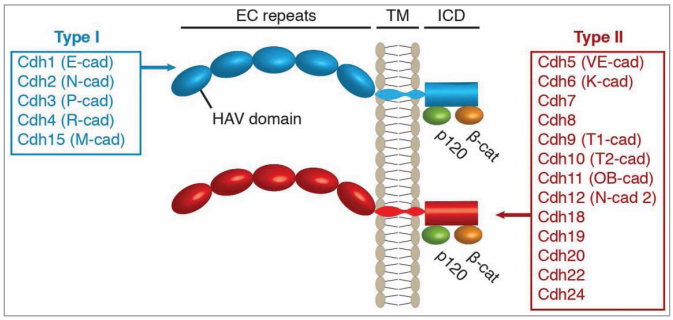

Figure 1. Structure of the classic cadherin protein family in humans. All classic cadherins have 5 extracellular cadherin (EC) repeats, a transmembrane (TM) domain, and an intracellular domain (ICD) that binds p120-catenin and β-catenin. The classic cadherins are sub-divided into Type I and Type II depending on the presence of a histidine-alanine-valine (HAV) motif in the first EC domain. Human Type I and Type II cadherins are indicated as annotated in the HUGO Gene Nomenclature Committee database with common names noted in parentheses.

expression to provide neurons with a specific molecular identity.[11] The role of neural activity in circuit formation has been a particularly active area of investigation since Hubel and Wiesel's classic experiments showing that visual experience shapes the functional connectivity of visual circuits.[12] Subsequently, many studies have shown that neural activity mediates the removal of synapses from incorrect targets and the pruning of excessive synapses from correct targets.[13] Although activity plays a significant role in circuit refinement, many initial steps in target selection and synapse formation proceed normally in the complete absence of neural activity.[14-17] Thus, synaptic specificity is initially mapped out in a large part because neurons are genetically programmed to express unique molecular features allowing them to be identified by other neurons. This idea is rooted in John Langley's early studies on nerve regeneration in cats and was elegantly conceptualized in Roger Sperry's "chemoaffinity hypothesis".[18,19] Sperry predicted that synaptic specificity is based on matching cytochemical tags expressed on pre and postsynaptic neurons. The extreme interpretation of this is that every neuron expresses a unique molecular identity that matches one to one with its correct synaptic partner.

Remarkably, neurons have a unique individual molecular identity that, in vertebrates, is encoded by members of the cadherin superfamily known as the clustered protocadherins. Clustered protocadherins are single-pass transmembrane proteins with 6 extracellular EC domains and intracellular domains with no clear homology or conserved binding domains.[20,21] In mice, 58 protocadherin genes are arranged in 3 clusters. Single cell RNA analysis of Purkinje neurons shows that individual neurons express about 1–3 isoforms from each cluster and expression is monoallelic and stochastic.[22-24] This means that there are hundreds of thousands of possible combinations, which afford many unique molecular identities.

Given that clustered protocadherins are located at synapses,[25,26] their discovery generated excitement because it was thought Sperry's one-to-one cytochemical tags allowing neurons to recognize correct synaptic partners had been found. Recent work, however, shows that the unique molecular labels provided by clustered protocadherins have an important but alternative function. They are not directly required for synapse formation between 2 different neurons, but instead mediate self-recognition to prevent dendrites on the same cell from interacting.[27,28] Clustered protocadherins are homophilic and their binding mediates repulsion, not adhesion.[28] The only dendrites a neuron is likely to contact with a strict homophilic match to its clustered protocadherins are its own dendrites and the repellent signaling causes the dendrites to spread apart from one another. Drosophila neurons use a similar mechanism of dendritic self-avoidance, but it is mediated by a completely different molecular family called Downs Syndrome cell adhesion molecules (DSCAMS).[29-31] Thus, studies indicate that neurons use their individual molecular identity to recognize themselves but not their synaptic partners.

Therefore, if not the clustered protocadherins, then what molecules mediate trans-cellular recognition among correct versus incorrect synaptic partners? The answer to this question is not yet solved and is likely to be a very complicated answer. Organizing the brain is an extremely complex process that requires the concerted action of many molecules, neural activity, and temporal events. However, new and increasing evidence suggests that one particularly important molecular family in regulating target recognition and synaptic specificity is the classic cadherins.

The Classic Cadherins

The mammalian classic cadherins, referred to from here as simply "cadherins," consist of approximately 20 genes that each encode a single-pass transmembrane protein with 5 EC repeats and intracellular binding domains for p120-catenin and β-catenin[32] (**Fig. 1**). Catenins are accepted as the primary intracellular mediators of cadherin signaling although other signaling mechanisms have been reported.[5-8] For comparison, other members of the cadherin superfamily, including the protocadherins, do not bind catenins.[21] Mammalian cadherins can be further subdivided into type I and type II based on sequence homology in the first EC domain; a domain critical for trans-cellular cadherin-cadherin binding[3,33,34] (**Fig. 1**). The human genome contains 5 type I and 13 type II cadherins[35] (**Fig. 1**). Like the clustered protocadherins, type I and type II cadherin binding is largely homophilic,[36] however, heterophilic interactions between cadherins of the same subtype have been observed in vitro.[37-41]

Cadherins are found in dendrites, axons, and growth cones of young neurons. Live imaging studies suggest they preferentially

cluster in pre and postsynaptic compartments at nascent synapses and then are maintained at pre and postsynaptic structures as synapses mature.[42] Synaptic localization has been shown for several different cadherin molecules by light and electron microscopy in brain sections, cultured neurons, and slice cultures.[43-50] More specifically, cadherins are commonly found at puncta adherentia, structures analogous to adherens junctions that are located adjacent to the synaptic active zone,[44,45,51] but cadherins have also been shown to associate directly with the postsynaptic density.[52] Crystal structures of several cadherin extracellular domains suggest that trans-cellular cadherin interactions are the perfect length (~40 nm) to span the synaptic cleft.[39,53,54] Thus, cadherins are expressed at the right place and time to function throughout synapse development.

Many Cadherins Have Circuit-Specific Expression in the Brain

The cadherins have been postulated to provide a molecular code to guide the formation of specific synaptic connections since the late 1980s and 90s when many cadherin family members were cloned and their expression patterns analyzed.[55-61] Although some cadherins, particularly those of the type I class, are widely expressed in the vertebrate brain, most type II cadherins are differentially expressed by subpopulations of neurons. Intriguingly, expression of type II cadherins often follows functional connections within circuits.[59,62-64] Takeichi and collegues provided an early demonstration of this when they injected a fluorescent dye in regions of the cortex expressing either cadherin-6 or cadherin-8 and retrograde uptake of the dye resulted in selective labeling of cadherin-6 or cadherin-8-expressing thalamic neurons respectively.[62] This indicated that neurons are selectively connected to other neurons that express matching cadherins and suggests that the cadherins themselves may be responsible for guiding the connectivity.

However, the idea that cadherins guide selective connectivity fell out of favor for many years because experiments investigating cadherins in the nervous system failed to provide conclusive evidence to support this role. In hindsight, this likely resulted from several reasons. First, analyses of cadherin function in the nervous system have overwhelmingly centered on the role of N-cadherin (also known as cadherin-2) in cultured neurons.[6,8] N-cadherin is a type I cadherin that is broadly expressed by most neurons and, with some exceptions, studies largely suggest N-cadherin has a primary role in general synapse function and plasticity rather than in synaptic specificity. Second, a common approach to study cadherins in the brain has been to simultaneously ablate the function of all cadherins using dominant negative constructs or catenin knockouts.[65-67] These first 2 strategies led to important discoveries about the general functions of cadherins in neural development, but by design they do not permit analysis of specificity. Third, overlapping and combinatorial cadherin expression along with potential functional redundancy with other synaptic specificity molecules ensures high fidelity of circuit formation but also means that chances are great that the loss of 1 or 2 cadherin genes will not result in obvious connectivity defects.

Differentially Expressed Cadherins in Synaptic Specificity

Other than the expression data mentioned above, there had been some findings that suggested but did not directly test a role for cadherins in specificity. This includes the finding that overexpression of cadherin-11 increases synapse density in cultured neurons whereas overexpression of either cadherin-13, cadherin-9, or N-cadherin does not.[51,65,68] Axons of hippocampal dentate gyrus (DG) neurons grow longer on an N-cadherin substrate compared to a cadherin-8 substrate[69] and motor neurons use differential expression of type II cadherins to sort into topographically defined motor pools.[63] It was also shown that high frequency stimulation capable of inducing long term potentiation in the medial molecular layer of the hippocampus selectively decreases cadherin-8 from this layer but does not alter N-cadherin expression.[70] Together, these observations suggest that different cadherins function distinctly at different types of synapses.

Recent technological advances in neuron and synapse labeling, imaging, and gene manipulation have facilitated more direct and detailed investigations of the role of cadherins in specificity. As a result, studies from the last few years have begun to provide strong evidence that the cadherins play important roles in directing synaptic specificity in the mouse. For example, one study investigated axon targeting of non-image forming retinal ganglion cells (RGCs). Here, the authors observed that among the many neuronal target areas of RGCs, cadherin-6 is selectively expressed by a unique subset of targets used in non-image forming visual processes.[71] Furthermore, a subpopulation of RGC axons that expresses cadherins-3 and -6 selectively projects to cadherin-6-expressing targets but not to other nearby RGC target areas. These RGC axons have a variety of projection defects in cadherin-6 knockout mice, often overshooting targets.[71] The results suggest cadherin-6 is required for these axons to accurately identify their specific target areas in the brain, likely via cadherin-6 homophilic interactions between this subset of RGC axons and their matching target areas.

Another study in the visual system showed that differentially expressed cadherins are necessary for proper laminar targeting of retinal bipolar cells.[72] Experiments with cell-type specific markers revealed that cadherin-8 and cadherin-9 are selectively and specifically expressed in 2 distinct populations of bipolar cells (BCs) that are part of a direction-selective visual circuit. Cadherin-8 is expressed in so called BC2s while cadherin-9 is expressed in BC5s.[72] Axons from BC2 and BC5 cells target different synaptic laminae within the inner plexiform layer. Using knockout mice, the authors showed that cadherin-8 and cadherin-9 loss-of-function leads to aberrant laminar targeting and functional connectivity defects only in BC cells that normally express the missing cadherin.[72] Furthermore, ectopic overexpression of cadherin-8 in BC5s or cadherin-9 in BC2s is sufficient to redirect axons to the

wrong synaptic layer.[72] These results provide evidence that differentially expressed type II cadherins play an instructive role in targeting axons to correct laminar targets.

Studies have also examined type-II cadherin mediated specificity at the synaptic level. In the hippocampus, principal cells receive synaptic input from different types of neurons and these different synapses can be identified in cultured hippocampal neurons using unique molecular markers.[51] Screening candidate genes for a role in the formation of distinct subtypes of synapses in vitro led to the identification of cadherin-9. Cadherin-9 is strongly expressed in hippocampal DG and CA3 neurons and not by any other types of hippocampal neurons.[51,58] Knockdown of cadherin-9 in vitro caused specific reduction of DG-CA3 synapses leaving other hippocampal synapses intact whereas an in vivo knockdown of cadherin-9 resulted in severely altered morphology of DG-CA3 mossy fiber synapses.[51] These results suggest that cadherin-9 is selectively required to regulate pre- and postsynaptic development of hippocampal mossy fiber synapses. This is likely mediated via homophilic interactions between DG axons and CA3 dendrites.

In the pontocerebellar circuit, pontine nucleus axons synapse onto granule cells and not with nearby Purkinje neurons. Kuwako et al. showed that cadherin-7 is specifically present in pontine nucleus and granule neurons.[73] Knockdown of cadherin-7 in pontine nucleus neurons in vivo causes some pontine nucleus axons to incorrectly invade the Purkinje cell layer. In addition, knockdown of cadherin-7 in vitro causes impaired synapse formation between pontine nucleus and granule neurons.[73]

Taken together, data from several studies now supports the hypothesis that cadherins participate in directing the development of synaptic specificity. The primary mechanism used by cadherins to mediate synaptic specificity in the vertebrate brain is likely via differential expression of type II cadherin genes (**Fig. 2**). This model postulates that when neurons encounter another neuron expressing the same cadherin, synapse formation is more likely to occur than if a neuron encounters another neuron in which cadherin expression does not match. Transcriptional mechanisms that control the differential expression of cadherins is an interesting unsolved question and is an active area of investigation.[74] Moreover, it remains unclear whether the actual signal to build a synapse is directly mediated by cadherin intracellular signaling or indirectly mediated by cadherins via increased axo-dendritic adhesion leading to activation of other synaptogenic molecules. Studies on N-cadherin suggest that both possibilities may be correct. On one hand, N-cadherin/catenin signaling can directly recruit synaptic vesicles to the presynapse[75,76] and, on the other hand, N-cadherin can indirectly affect synapse formation by enhancing the function of neuroligin, a highly synaptogenic transsynaptic molecule.[77,78]

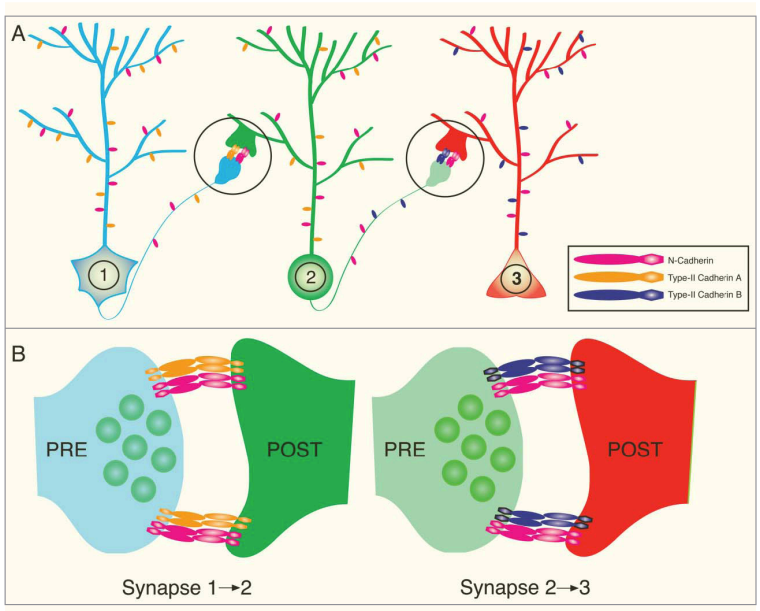

Figure 2. Model of Type II cadherin mediated synaptic specificity. (**A**) Illustration depicting a 3 neuron circuit with specific connections from neuron 1 to neuron 2 and then neuron 2 to neuron 3. (**B**) Expanded view of synaptic areas circled in A. Note that all 3 neurons express the Type-I N-cadherin (pink), which is present and required for function of most synapses. However, the neurons express different kinds of Type II cadherins (orange or purple) to restrict synapse formation to select synaptic partners that express the matching Type II cadherin.

Broadly Expressed Cadherins in Synaptic Specificity

The concept that differentially expressed (primarily type II) cadherins regulate synaptic specificity based on locating appropriate partner neurons that express matching cadherins has been technically difficult to test until recently but represents a straightforward mechanism of differential adhesion leading to specific connectivity. Interestingly, studies in Drosophila provide evidence that broadly-expressed cadherins can also

regulate synaptic specificity but the mechanisms may be distinct from those used by differentially expressed cadherins in the mammalian brain.

The Drosophila genome has only 3 classic cadherins; E-cadherin, N-cadherin, and the less understood N-cadherin2. Notably, the sequences of these cadherins are significantly different from their vertebrate counterparts.[3,79] Drosophila N-cadherin (DN-cadherin) has 15 EC repeats, a fly classic cadherin box region, and several EGF-like repeat regions.[3,79] Nonetheless, like vertebrate N-cadherin, DN-cadherin is widely expressed in most neurons and plays many roles in neural development including synaptic specificity. How does DN-cadherin regulate synaptic specificity when it is ubiquitously expressed and does not provide a target-specific cue? One mechanism is that DN-cadherin expression is temporally regulated. It is known that Drosophila axons from the R8 class of photoreceptor cells terminate in the medulla layer known as M3. In contrast, R7 photoreceptor axons terminate in the more distal layer M6. All the axons and target cells express DN-cadherin, but it was shown that differential expression of a zinc-finger transcription factor drives high levels of DN-cadherin expression earlier in R8 cells compared to R7 cells.[80] DN-cadherin is thought to cause R8 axons to stop growing and adhere at the peak of DN-cadherin expression that happens to occur when axons arrive at the M3 layer.[80] In contrast, R7 axons have lower adhesion and continue growing to the M6 layer.[80] Thus, although eventually most neurons express DN-cadherin, they express it at different time points in development when the axons are encountering different synaptic partners. A similar mechanism could also occur in mammalian neurons. In cultured rat and mouse neurons, N-cadherin has different functions depending on the age of the neurons. Blocking cadherin function in neurons prior to synapse maturation has strong effects on synapse density whereas blocking cadherin function after synapse formation does not affect synapse density.[81] In addition, although N-cadherin is broadly expressed in the mammalian cortex, it is enriched in specific brain regions at different developmental time points. In particular, the enrichment of N-cadherin in cortical layer IV in early postnatal animals may play a role in directing thalamacortical axons precisely to this layer during development.[82]

In addition to tightly controlled temporal expression of N-cadherin, it is possible that broadly expressed cadherins regulate specificity through differential subcellular localization or regulated surface trafficking. This remains to be conclusively tested, but there is correlative evidence to support each possibility. For example, as rodent neurons mature, N-cadherin is retained at excitatory synapses and excluded from inhibitory synapses.[45,46] Conversely, E-cadherin localizes to and is required for inhibitory synapse formation.[45,83] It is possible that the selective retention of N- and E-cadherin at excitatory vs. inhibitory synapses is primarily mediated by other synaptic specificity molecules like the neuroligins. Different neuroligin genes are well known to have a strong bias toward excitatory (neuroligin-1) versus inhibitory (neuroligin-2) synapses and cadherins have been shown to associate with neuroligins via intracellular synaptic scaffolds.[84-86] Although this idea remains to be directly tested, it emphasizes the complex nature of synaptic specificity, which is likely mediated by a network of synaptic molecules. A second example of regulated surface trafficking of cadherins was shown in Drosophila. Photoreceptor cell targeting is disrupted in Rab6 (a GTPase) and Ric-1 homolog (Rich, a Rab6 binding protein) mutants.[87] Rab6 regulates vesicle transport and causes a specific reduction of DN-cadherin expression at synapses suggesting that regulated trafficking of cadherins is another way that broadly-expressed N-cadherin can influence synaptic specificity.[87] One mechanism that does not appear to play a major role in cadherin-directed synaptic specificity is alternative splicing. DN-cadherin has up to 12 isoforms, but the isoforms do not have biochemical differences and isoform diversity is not required for R7/R8 photoreceptor targeting.[88,89] Vertebrate cadherins have few splice forms and evidence suggests that the classic cadherin gene family diversified by gene duplication events rather than alternative splicing mechanisms.[3]

Combinatorial Coding Increases the Selectivity and Fidelity of Neural Circuits

There are billions of neurons in the human brain that must assemble and organize into countless numbers of specific circuits and microcircuits. One question that often arises about the cadherins is how such a relatively small number of cadherin molecules could possibly accomplish this task? Each cadherin is independently transcribed from an individual gene locus and expression studies indicate most neuronal cell types express more than one cadherin. Thus, from a purely mathematic perspective there are hundreds of thousands of unique combinations that the 18 classic cadherins or just the 13 classic type II cadherins can generate. This level of diversity is not necessarily even needed given that a developing brain goes through many stages prior to synapse formation. By the time an axon has been guided to the correct area where it will make a synapse, it is faced with a much simpler problem of choosing between a few cell types in the local area. For this task, the diversity of the classic cadherins is more than sufficient to identify specific target cell populations and construct different types of synapses. It is important to distinguish that although cadherins may theoretically be capable of providing a unique cellular identity, there is little evidence for this and we favor a model in which the cadherins provide a population identity. This is based on in situ and expression studies showing that cadherin expression levels vary substantially between different cell types but not between individual neurons of the same type.[58,90] How does a neuron choose between one cell and another cell of the same type? This aspect of specificity is likely to occur independent of the cadherins and although the mechanism is not known, timing, spatial constraints, randomization, and neural activity may all play a role in refining circuits at this level.

Although the cadherins may be capable of providing molecular diversity to wire the entire brain, the most realistic answer is that they likely do not – at least not on their own. As mentioned throughout this review, it is almost certain

that the cadherins function together with other cell adhesion, axon guidance, and synaptogenic molecules on the neuronal cell surface. Interactions between cadherins and other cell adhesion systems can take several forms. First, cadherins act redundantly with other adhesion systems whereby both sets of molecules signal to accomplish the same task. For example, DN-cadherin and a 7-pass transmembrane cadherin Flamingo act redundantly to polarize Drosophila photoreceptor growth cones toward correct synaptic partners.[91] Cadherins can also act in a complementary push-pull manner with other cell surface proteins. In this case, the cadherins are usually the positive adhesive cues promoting appropriate synapse formation while repellent cues push an axon or dendrite away from incorrect synaptic partners. An example of this type of mechanism was reported in the Drosophila medulla where DN-cadherin mediates adhesion between an axon and its correct synaptic target zone while Sema/Plexin signaling provides a simultaneous repellent signal to keep the axon out of nearby incorrect synaptic areas.[92]

Cadherins also affect synaptic specificity through their ability to modulate synaptogenic signals. In most cases, cadherins are necessary, but not sufficient, to induce de novo synapse formation.[51,65,81,93-95] However, recent work showed that N-cadherin modulates recruitment of neuroligin-1. Previous studies found an indirect biochemical link between neuroligins and N-cadherin via S-SCAM and β-catenin[84-86] and more recent results from 2 different groups show that N-cadherin is necessary to cluster neuroligin-1 at synaptic sites.[77,78] Thus, overexpression of neuroligin-1 is synaptogenic, but only in the presence of N-cadherin.[77,78] Together, these 2 cell adhesion systems promote the clustering of synaptic vesicles and increase the probability of synaptic vesicle release.[77,78] As discussed in the previous sections, almost all individual neurons (certainly all cortical and hippocampal neurons) also express other classic cadherins in addition to N-cadherin. An unanswered question is whether other classic cadherins also synergize with synaptogenic molecules like neuroligin? One intriguing possibility is that different cadherins may synergize with different cell adhesion molecules to organize distinct classes of synapses. Future studies are needed to understand how specific members of the classic cadherin family interact with neuroligins and other synaptogenic cues.

Combinatorial coding among the cadherins themselves and with other synaptic molecules is expected to dramatically increase the fidelity of neural circuit formation. It also is likely a major reason why direct evidence showing that cadherins regulate synaptic specificity has been so sparse. In the hippocampus, each class of excitatory neuron expresses 4–5 different cadherins.[58,90] This provides each cell type with a unique extracellular identity but there is enough overlap among them that the global loss or overexpression of any one cadherin may do little to significantly alter the molecular adhesion or identity of synaptic partners. Depleting all cadherin signaling by knocking out cadherin signaling molecules reveals synaptic defects[67,86] but also obscures any analysis of specificity. One experimental paradigm that may overcome this conundrum is to sparsely deplete individual cadherins from neurons using viral transfections, in utero electroporation, or conditional genetic techniques. As recently shown for neuroligin, sparse deletion can put individual cells at a competitive disadvantage and reveal the function of a molecule when global changes in gene expression do not.[96]

Cadherins, Synaptic Specificity, and Neurodevelopmental Disorders

The cadherins are emerging as important regulators of synapse form and function. Therefore, it is not surprising that cadherin genes are implicated in the etiology of a variety of neurological disorders. Supporting a role for cadherins in synaptic specificity, alterations in different cadherin genes are associated with distinct neurological disorders in humans. Genetic deletions or copy number variations of cadherin-8 and the GPI-linked cadherin-13 were identified in patients with autism and learning disability.[97,98] Single nucleotide polymorphisms (SNPs) within the cadherin-13 gene associate with attention deficit/hyperactivity disorder (ADHD) and alcoholism and a SNP between cadherin-9 and -10 associates with autism.[99-101] In addition, a chromosomal rearrangement involving cadherin-9 was identified in a family with non-syndromic mental retardation.[102] Finally, analysis of a monozygotic twin pair discordant for schizophrenia identified a genetic deletion between cadherins-12 and -18.[103]

So far, at least 2 of these genetic associations have led to follow up studies supporting their role in disease. First, in a study of over 7,000 participants, the high-risk autism SNP between cadherin-9 and cadherin-10 correlates with lower communication traits in the general population.[104] This interesting finding suggests isolated genetic aberrations are important, but need to accumulate or undergo environmental stresses before behavioral impairments are severe enough to reach functional and clinical significance.[105] Second, in a cohort of 238 children, the presence of the ADHD-associated SNP in cadherin-13 was found to specifically correlate with a defect in verbal working memory, but not with spatial working memory.[106] This finding provides the first glimpse that cadherins may also regulate circuit specificity in humans. It suggests that cadherin-13 may be required for the formation of specific circuits involved with verbal working memory but not for circuits specific to spatial working memory or other cognitive functions. It is important to note that most of these studies identified SNPs or deletions in non-coding genomic regions associated with a cadherin. These alterations may be located in regulatory regions affecting expression of the nearby cadherin gene, but more studies are required to determine whether or not expression of individual cadherins are actually affected by these genomic alterations.

Conclusions and Future Directions

Experiments over the last 10 years provide increasing evidence that cadherins are important mediators in the formation of

specific neural circuits, however, many questions remain. One major unresolved issue is the nature of cadherin heterogeneity. While it is likely all cadherins undergo strong homophilic interactions, in vitro binding assays indicate that some cadherins form heterophilic interactions with other cadherin family members.[37-41] Moreover, cadherins are differentially expressed throughout the brain, but not in an exclusive manner. Most neurons express multiple cadherins yet little is known about how adhesion is affected when single cells express multiple cadherins. Do all cadherins have to match for binding to occur, or just a few? Does adhesion depend on the expression levels of each cadherin? Do different cadherins segregate to different subcellular compartments? Our understanding of how multiple classic cadherins function within the context of a single cell is very limited. We do not yet know if different cadherins segregate to different synapses or if they are all present at every synapse made by a single cell.

Equally important for understanding the role of different cadherins in synaptic specificity is to understand how they signal. Is specificity governed exclusively by adhesive extracellular matching or are distinct intracellular signaling mechanisms required? By definition, all classic cadherins bind the catenins and catenins are critical for synapse formation, but some cadherins have been shown to interact directly and indirectly with other synaptic proteins including glutamate receptors (AMPA, NMDA, and kainate type), scaffolding proteins (AKAP79/150, GRIP), and signaling molecules (Vangl2, p38 MAPK).[95,107-111] Nonetheless, the precise signaling mechanisms used by cadherins during the process of synaptic specificity remain unknown. Another unresolved question is at what stage in synapse development are cadherins required? Are they activated at the moment of axo-dendritic contact or are they recruited some time later? This answer is likely to be complex because previous work suggests the role of the cadherins changes as neurons mature.[81]

In conclusion, although cadherin and cadherin-signaling has been extensively studied since the first cadherin was cloned in 1980 (resulting in tens of thousands of published manuscripts), there is still much more to learn about the role of cadherins in the brain. Now that cadherins are becoming established as important molecules in the development of synaptic specificity, future experiments can be aimed at elucidating the specialized mechanisms used by cadherins to wire the brain during neural development.

Disclosure of Potential Conflicts of Interest

No potential conflicts of interest were disclosed.

Acknowledgments

We thank Dr. Joris DeWit and Anne Martin for comments on the manuscript.

Funding

This work was supported by grants from the Whitehall, Edward Mallinckrodt Jr., and Sloan foundations (M.E.W).

References

1. Angst BD, Marcozzi C, Magee AI. The cadherin superfamily: diversity in form and function. J Cell Sci 2001; 114:629-41; PMID:11171368
2. Takeichi M. The cadherin superfamily in neuronal connections and interactions. Nat Rev Neurosci 2007; 8:11-20; PMID:17133224
3. Nollet F, Kools P, van Roy F. Phylogenetic analysis of the cadherin superfamily allows identification of six major subfamilies besides several solitary members1. J Mol Biol 2000; 299:551-72; PMID:10835267; http://dx.doi.org/10.1006/jmbi.2000.3777
4. Zipursky SL, Sanes JR. Chemoaffinity revisited: dscams, protocadherins, and neural circuit assembly. Cell 2010; 143:343-53; PMID:21029858; http://dx.doi.org/10.1016/j.cell.2010.10.009
5. Tai C-Y, Kim SA, Schuman EM. Cadherins and synaptic plasticity. Curr Opin Cell Biol 2008; 20:567-75; PMID:18602471; http://dx.doi.org/10.1016/j.ceb.2008.06.003
6. Arikkath J, Reichardt LF. Cadherins and catenins at synapses: roles in synaptogenesis and synaptic plasticity. Trends Neurosci 2008; 31:487-94; PMID:18684518; http://dx.doi.org/10.1016/j.tins.2008.07.001
7. Hirano SS, Takeichi MM. Cadherins in brain morphogenesis and wiring. Physiol Rev 2012; 92:597-634; PMID:22535893; http://dx.doi.org/10.1152/physrev.00014.2011
8. Brigidi GS, Bamji SX. Cadherin-catenin adhesion complexes at the synapse. Curr Opin Neurobiol 2011; 21:208-14; PMID:21255999; http://dx.doi.org/10.1016/j.conb.2010.12.004
9. Sotelo C. Viewing the brain through the master hand of Ramón y Cajal. Nat Rev Neurosci 2003; 4:71-7; PMID:12511863
10. Vrieseling E, Arber S. Target-induced transcriptional control of dendritic patterning and connectivity in motor neurons by the ETS gene Pea3. Cell 2006; 127:1439-52; PMID:17190606
11. Serizawa S, Miyamichi K, Takeuchi H, Yamagishi Y, Suzuki M, Sakano H. A neuronal identity code for the odorant receptor-specific and activity-dependent axon sorting. Cell 2006; 127:1057-69; PMID:17129788; http://dx.doi.org/10.1016/j.cell.2006.10.031
12. Espinosa JS, Stryker MP. Development and plasticity of the primary visual cortex. Neuron 2012; 75:230-49; PMID:22841309; http://dx.doi.org/10.1016/j.neuron.2012.06.009
13. Kano M, Hashimoto K. Synapse elimination in the central nervous system. Curr Opin Neurobiol 2009; 19:154-61; PMID:19481442; http://dx.doi.org/10.1016/j.conb.2009.05.002
14. Verhage M, Maia AS, Plomp JJ, Brussaard AB, Heeroma JH, Vermeer H, Toonen RF, Hammer RE, van den TK, Berg, et al. Synaptic assembly of the brain in the absence of neurotransmitter secretion. Science 2000; 287:864-9; PMID:10657302
15. Nevin LM, Taylor MR, Baier H. Hardwiring of fine synaptic layers in the zebrafish visual pathway. Neural Dev 2008; 3:36; PMID:19087349; http://dx.doi.org/10.1186/1749-8104-3-36
16. Godinho L, Mumm JS, Williams PR, Schroeter EH, Koerber A, Park SW, Leach SD, Wong ROL. Targeting of amacrine cell neurites to appropriate synaptic laminae in the developing zebrafish retina. Development 2005; 132:5069-79; PMID:16258076; http://dx.doi.org/10.1242/dev.02075
17. Mumm JS, Williams PR, Godinho L, Koerber A, Pittman AJ, Roeser T, Chien C-B, Baier H, Wong ROL. In vivo imaging reveals dendritic targeting of laminated afferents by zebrafish retinal ganglion cells. Neuron 2006; 52:609-21; PMID:17114046; http://dx.doi.org/10.1016/j.neuron.2006.10.004
18. Langley JN. Note on regeneration of Pr -ganglionic fibres of the sympathetic. J Physiol (Lond) 1895; 18:280-4; PMID:16992254
19. Sperry RW. Chemoaffinity in the orderly growth of nerve fiber patterns and connections. Proc Natl Acad Sci USA 1963; 50:703-10; PMID:14077501
20. Kohmura N, Senzaki K, Hamada S, Kai N, Yasuda R, Watanabe M, Ishii H, Yasuda M, Mishina M, Yagi T. Diversity revealed by a novel family of cadherins expressed in neurons at a synaptic complex. Neuron 1998; 20:1137-51; PMID:9655502; http://dx.doi.org/10.1016/S0896-6273(00)80495-X
21. Wu Q, Maniatis T. A striking organization of a large family of human neural cadherin-like cell adhesion genes. Cell 1999; 97:779-90; PMID:10380929; http://dx.doi.org/10.1016/S0092-8674(00)80789-8
22. Esumi S, Kakazu N, Taguchi Y, Hirayama T, Sasaki A, Hirabayashi T, Koide T, Kitsukawa T, Hamada S, Yagi T. Monoallelic yet combinatorial expression of variable exons of the protocadherin-α gene cluster in single neurons. Nat Genet 2005; 37:171-6; PMID:15640798; http://dx.doi.org/10.1038/ng1500
23. Kaneko R, Kato H, Kawamura Y, Esumi S, Hirayama T, Hirabayashi T, Yagi T. Allelic gene regulation of Pcdh- and Pcdh- clusters involving both monoallelic and biallelic expression in single purkinje cells. J Biol Chem 2006; 281:30551-60; PMID:16893882; http://dx.doi.org/10.1074/jbc.M605677200
24. Hirano K, Kaneko R, Izawa T, Kawaguchi M, Kitsukawa T, Yagi T. Single-neuron diversity generated by Protocadherin-β cluster in mouse central and peripheral nervous systems. Front Mol Neurosci 2012; 5; PMID:22969705; http://dx.doi.org/10.3389/fnmol.2012.00090
25. Phillips GR, Tanaka H, Frank M, Elste A, Fidler L, Benson DL, Colman DR. γ-Protocadherins are

targeted to subsets of synapses and intracellular organelles in neurons. J Neurosci 2003; 23:5096-104; PMID:12832533

26. Junghans D, Heidenreich M, Hack I, Taylor V, Frotscher M, Kemler R. Postsynaptic and differential localization to neuronal subtypes of protocadherin β16 in the mammalian central nervous system. Eur J Neurosci 2008; 27:559-71; PMID:18279309; http://dx.doi.org/10.1111/j.1460-9568.2008.06052.x
27. Lefebvre JL, Kostadinov D, Chen WV, Maniatis T, Sanes JR. Protocadherins mediate dendritic self-avoidance in the mammalian nervous system. Nature 2012; 488:517-21; PMID:22842903; http://dx.doi.org/10.1038/nature11305
28. Chen WV, Maniatis T. Clustered protocadherins. Development 2013; 140:3297-302; PMID:23900538; http://dx.doi.org/10.1242/dev.090621
29. Matthews BJ, Kim ME, Flanagan JJ, Hattori D, Clemens JC, Zipursky SL, Grueber WB. Dendrite self-avoidance is controlled by Dscam. Cell 2007; 129:593-604; PMID:17482551; http://dx.doi.org/10.1016/j.cell.2007.04.013
30. Soba P, Zhu S, Emoto K, Younger S, Yang S-J, Yu H-H, Lee T, Jan LY, Jan Y-N. Drosophila sensory neurons require Dscam for dendritic self-avoidance and proper dendritic field organization. Neuron 2007; 54:403-16; PMID:17481394; http://dx.doi.org/10.1016/j.neuron.2007.03.029
31. Fuerst PG, Bruce F, Tian M, Wei W, Elstrott J, Feller MB, Erskine L, Singer JH, Burgess RW. DSCAM and DSCAML1 function in self-avoidance in multiple cell types in the developing mouse retina. Neuron 2009; 64:484-97; PMID:19945391; http://dx.doi.org/10.1016/j.neuron.2009.09.027
32. Hulpiau P, van Roy F. Molecular evolution of the cadherin superfamily. Int J Biochem Cell Biol 2009; 41:349-69; PMID:18848899; http://dx.doi.org/10.1016/j.biocel.2008.09.027
33. Nose A, Tsuji K, Takeichi M. Localization of specificity determining sites in cadherin cell adhesion molecules. Cell 1990; 61:147-55; PMID:2317870; http://dx.doi.org/10.1016/0092-8674(90)90222-Z
34. Shapiro L, Fannon AM, Kwong PD, Thompson A, Lehmann MS, Grübel G, Legrand JF, Als-Nielsen J, Colman DR, Hendrickson WA. Structural basis of cell-cell adhesion by cadherins. Nature 1995; 374:327-37; PMID:7885471; http://dx.doi.org/10.1038/374327a0
35. Gray KA, Daugherty LC, Gordon SM, Seal RL, Wright MW, Bruford EA. Genenames.org: the HGNC resources in 2013. Nucleic Acids... 2012; 41:D545-52; PMID:23161694
36. Takeichi M. The cadherins: cell-cell adhesion molecules controlling animal morphogenesis. Development 1988; 102:639-55; PMID:3048970
37. Ounkomol C, Yarnada S, Heinrich V. Single-cell adhesion tests against functionalized microspheres arrayed on AFM cantilevers confirm heterophilic E- and N-cadherin binding. Biophys J 2010; 99:L100-2; PMID:21156120; http://dx.doi.org/10.1016/j.bpj.2010.11.013
38. Volk T, Cohen O, Geiger B. Formation of heterotypic adherens-type junctions between L-CAM-containing liver cells and A-CAM-containing lens cells. Cell 1987; 50:987-94; PMID:3621349; http://dx.doi.org/10.1016/0092-8674(87)90525-3
39. Patel SD, Ciatto C, Chen CP, Bahna F, Rajebhosale M, Arkus N, Schieren I, Jessell TM, Honig B, Price SR, et al. Type II cadherin ectodomain structures: implications for classical cadherin specificity. Cell 2006; 124:1255-68; PMID:16564015; http://dx.doi.org/10.1016/j.cell.2005.12.046
40. Shimoyama Y, Tsujimoto G, Kitajima M, Natori M. Identification of three human type-II classic cadherins and frequent heterophilic interactions between different subclasses of type-II classic cadherins. Biochem J 2000; 349:159-67; PMID:10861224; http://dx.doi.org/10.1042/0264-6021:3490159
41. Prakasam AK, Maruthamuthu V, Leckband DE. Similarities between heterophilic and homophilic cadherin adhesion. Proc Natl Acad Sci USA 2006; 103:15434-9; PMID:17023539
42. Jontes JD. In vivo trafficking and targeting of N-cadherin to nascent presynaptic terminals. J Neurosci 2004; 24:9027-34; PMID:15483121; http://dx.doi.org/10.1523/JNEUROSCI.5399-04.2004
43. Yamagata M, Herman JP, Sanes JR. Lamina-specific expression of adhesion molecules in developing chick optic tectum. J Neurosci 1995; 15:4556-71; PMID:7790923
44. Uchida N, Honjo Y, Johnson KR, Wheelock MJ, Takeichi M. The catenin/cadherin adhesion system is localized in synaptic junctions bordering transmitter release zones. J Cell Biol 1996; 135:767-79; PMID:8909549; http://dx.doi.org/10.1083/jcb.135.3.767
45. Fannon AM, Colman DR. A model for central synaptic junctional complex formation based on the differential adhesive specificities of the cadherins. Neuron 1996; 17:423-34; PMID:8816706; http://dx.doi.org/10.1016/S0896-6273(00)80175-0
46. Benson DL, Tanaka H. N-cadherin redistribution during synaptogenesis in hippocampal neurons. J Neurosci 1998; 18:6892-904; PMID:9712659
47. Bartelt-Kirbach B, Langer-Fischer K, Golenhofen N. Different regulation of N-cadherin and cadherin-11 in rat hippocampus. Cell Commun Adhes 2010; 17:75-82; PMID:21250828; http://dx.doi.org/10.3109/15419061.2010.549977
48. Suzuki SC, Furue H, Koga K, Jiang N, Nohmi M, Shimazaki Y, Katoh-Fukui Y, Yokoyama M, Yoshimura M, Takeichi M. Cadherin-8 is required for the first relay synapses to receive functional inputs from primary sensory afferents for cold sensation. J Neurosci 2007; 27:3466-76; PMID:17392463; http://dx.doi.org/10.1523/JNEUROSCI.0243-07.2007
49. Bozdagi O, Shan W, Tanaka H, Benson DL, Huntley GW. Increasing numbers of synaptic puncta during late-phase LTP: N-cadherin is synthesized, recruited to synaptic sites, and required for potentiation. Neuron 2000; 28:245-59; PMID:11086998; http://dx.doi.org/10.1016/S0896-6273(00)00100-8
50. Manabe T. Loss of cadherin-11 adhesion receptor enhances plastic changes in hippocampal synapses and modifies behavioral responses. MolCell Neurosci 2000; 15:534-46; PMID:10860580; http://dx.doi.org/10.1006/mcne.2000.0849
51. Williams ME, Wilke SA, Daggett A, Davis E, Otto S, Ravi D, Ripley B, Bushong EA, Ellisman MH, Klein G, et al. Cadherin-9 regulates synapse-specific differentiation in the developing hippocampus. Neuron 2011; 71:640-55; PMID:21867881; http://dx.doi.org/10.1016/j.neuron.2011.06.019
52. Bayés A, van de Lagemaat LN, Collins MO, Croning MDR, Whittle IR, Choudhary JS, Grant SGN. Characterization of the proteome, diseases and evolution of the human postsynaptic density. Nat Neurosci 2011; 14:19-21; PMID:21170055; http://dx.doi.org/10.1038/nn.2719
53. Boggon TJ, Murray J, Chappuis-Flament S, Wong E, Gumbiner BM, Shapiro L. C-cadherin ectodomain structure and implications for cell adhesion mechanisms. Science 2002; 296:1308-13; PMID:11964443; http://dx.doi.org/10.1126/science.1071559
54. Harrison OJ, Jin X, Hong S, Bahna F, Ahlsen G. The extracellular architecture of adherens junctions revealed by crystal structures of type I cadherins. Structure 2011; 19:244-56; PMID:21300292; http://dx.doi.org/10.1016/j.str.2010.11.016
55. Miskevich F, Zhu Y, Ranscht B, Sanes JR. Expression of multiple cadherins and catenins in the chick optic tectum. Mol Cell Neurosci 1998; 12:240-55; PMID:9828089; http://dx.doi.org/10.1006/mcne.1998.0718
56. Hatta K, Takagi S, Fujisawa H, Takeichi M. Spatial and temporal expression pattern of N-cadherin cell adhesion molecules correlated with morphogenetic processes of chicken embryos. Dev Biol 1987; 120:215-27; PMID:3817290; http://dx.doi.org/10.1016/0012-1606(87)90119-9
57. Suzuki S, Sano K, Tanihara H. Diversity of the cadherin family: evidence for eight new cadherins in nervous tissue. Cell Regul 1991; 2:261-70; PMID:2059658
58. Bekirov IH, Needleman LA, Zhang W, Benson DL. Identification and localization of multiple classic cadherins in developing rat limbic system. Neuroscience 2002; 115:213-27; PMID:12401335; http://dx.doi.org/10.1016/S0306-4522(02)00375-5
59. Inoue T, Tanaka T, Suzuki SC, Takeichi M. Cadherin-6 in the developing mouse brain: expression along restricted connection systems and synaptic localization suggest a potential role in neuronal circuitry. Dev Dyn 1998; 211:338-51; PMID:9566953; http://dx.doi.org/10.1002/(SICI)1097-0177(199804)211:4<338::AID-AJA5>3.0.CO;2-I
60. Arndt K, Nakagawa S, Takeichi M, Redies C. Cadherin-defined segments and parasagittal cell ribbons in the developing chicken cerebellum. Mol Cell Neurosci 1998; 10:211-28; PMID:9618214; http://dx.doi.org/10.1006/mcne.1998.0665
61. Yoon MS, Puelles L, Redies C. Formation of cadherin-expressing brain nuclei in diencephalic alar plate divisions. J Comp Neurol 2000; 427:461-80; PMID:11183875; http://dx.doi.org/10.1002/(SICI)1096-9861(20000612)421:4<461::AID-CNE2>3.0.CO;2-M
62. Suzuki SC, Inoue T, Kimura Y, Tanaka T, Takeichi M. Neuronal circuits are subdivided by differential expression of type-II classic cadherins in postnatal mouse brains. Mol Cell Neurosci 1997; 9:433-47; PMID:9361280; http://dx.doi.org/10.1006/mcne.1997.0626
63. Price SR, De Marco Garcia NV, Ranscht B, Jessell TM. Regulation of motor neuron pool sorting by differential expression of type II cadherins. Cell 2002; 109:205-16; PMID:12007407; http://dx.doi.org/10.1016/S0092-8674(02)00695-5
64. Korematsu K, Redies C. Expression of cadherin-8 mRNA in the developing mouse central nervous system. J Comp Neurol 1997; 387:291-306; PMID:9336230; http://dx.doi.org/10.1002/(SICI)1096-9861(19971020)387:2<291::AID-CNE10>3.0.CO;2-Y
65. Togashi H, Abe K, Mizoguchi A, Takaoka K, Chisaka O, Takeichi M. Cadherin regulates dendritic spine morphogenesis. Neuron 2002; 35:77-89; PMID:12123610; http://dx.doi.org/10.1016/S0896-6273(02)00748-1
66. Demireva EY, Shapiro LS, Jessell TM, Zampieri N. Motor neuron position and topographic order imposed by β- and γ-catenin activities. Cell 2011; 147:641-52; PMID:22036570; http://dx.doi.org/10.1016/j.cell.2011.09.037
67. Arikkath J, Peng I-F, Ng YG, Israely I, Liu X, Ullian EM, Reichardt LF. Delta-catenin regulates spine and synapse morphogenesis and function in hippocampal neurons during development. J Neurosci 2009; 29:5435-42; PMID:19403811; http://dx.doi.org/10.1523/JNEUROSCI.0835-09.2009
68. Paradis S, Harrar DB, Lin Y, Koon AC, Hauser JL, Griffith EC, Zhu L, Brass LF, Chen C, Greenberg ME. An RNAi-based approach identifies molecules required for glutamatergic and GABAergic synapse development. Neuron 2007; 53:217-32; PMID:17224404; http://dx.doi.org/10.1016/j.neuron.2006.12.012
69. Bekirov IH, Nagy V, Svoronos A, Huntley GW, Benson DL. Cadherin-8 and N-cadherin differentially

regulate pre- and postsynaptic development of the hippocampal mossy fiber pathway. Hippocampus 2008; 18:349-63; PMID:18064706; http://dx.doi.org/10.1002/hipo.20395

70. Huntley GW, Elste AM, Patil SB, Bozdagi O, Benson DL, Steward O. Synaptic loss and retention of different classic cadherins with LTP-associated synaptic structural remodeling in vivo. Hippocampus 2010; 22:17-28; PMID:20848607; http://dx.doi.org/10.1002/hipo.20859
71. Osterhout JA, Josten N, Yamada J, Pan F, Wu S-W, Nguyen PL, Panagiotakos G, Inoue YU, Egusa SF, Volgyi B, et al. Cadherin-6 mediates axon-target matching in a non-image-forming visual circuit. Neuron 2011; 71:632-9; PMID:21867880; http://dx.doi.org/10.1016/j.neuron.2011.07.006
72. Duan X, Krishnaswamy A, la Huerta De I, Sanes JR. Type II cadherins guide assembly of a direction-selective retinal circuit. Cell 2014; 158:793-807; PMID:25126785; http://dx.doi.org/10.1016/j.cell.2014.06.047
73. Kuwako K-I, Nishimoto Y, Kawase S, Okano HJ, Okano H. Cadherin-7 regulates mossy fiber connectivity in the cerebellum. Cell Rep 2014; 9:311-23; PMID:25284782; http://dx.doi.org/10.1016/j.celrep.2014.08.063
74. Paulson A, Prasad M, Thuringer A, Manzerra P. Regulation of cadherin expression in nervous system development. Cell Adh Migr 2014; 8:19-28; PMID:24526207; http://dx.doi.org/10.4161/cam.27839
75. Sun Y, Aiga M, Yoshida E, Humbert PO, Bamji SX. Scribble interacts with beta-catenin to localize synaptic vesicles to synapses. Mol Biol Cell 2009; 20:3390-400; PMID:19458197; http://dx.doi.org/10.1091/mbc.E08-12-1172
76. Sun Y, Bamji SX. β-Pix modulates actin-mediated recruitment of synaptic vesicles to synapses. J Neurosci 2011; 31:17123-33; PMID:22114281; http://dx.doi.org/10.1523/JNEUROSCI.2359-11.2011
77. Aiga M, Levinson JN, Bamji SX. N-cadherin and neuroligins cooperate to regulate synapse formation in hippocampal cultures. J Biol Chem 2011; 286:851-8; PMID:21056983; http://dx.doi.org/10.1074/jbc.M110.176305
78. Stan A, Pielarski KN, Brigadski T, Wittenmayer N, Fedorchenko O, Gohla A, Lessmann V, Dresbach T, Gottmann K. Essential cooperation of N-cadherin and neuroligin-1 in the transsynaptic control of vesicle accumulation. Proc Nat Acad Sci 2010; 107:11116-21; PMID:20534458; http://dx.doi.org/10.1073/pnas.0914233107
79. Hill E, Broadbent ID, Chothia C, Pettitt J. Cadherin superfamily proteins in Caenorhabditis elegans and Drosophila melanogaster. J Mol Biol 2001; 305:1011-24; PMID:11162110; http://dx.doi.org/10.1006/jmbi.2000.4361
80. Petrovic M, Hummel T. Temporal identity in axonal target layer recognition. Nature 2008; 456:800-3; PMID:18978776; http://dx.doi.org/10.1038/nature07407
81. Bozdagi O, Valcin M, Poskanzer K, Tanaka H, Benson DL. Temporally distinct demands for classic cadherins in synapse formation and maturation. Mol Cell Neurosci 2004; 27:509-21; PMID:15555928; http://dx.doi.org/10.1016/j.mcn.2004.08.008
82. Huntley GW, Benson DL. Neural (N)-cadherin at developing thalamocortical synapses provides an adhesion mechanism for the formation of somatopically organized connections. J Comp Neurol 1999; 407:453-71; PMID:10235639; http://dx.doi.org/10.1002/(SICI)1096-9861(19990517)407:4<453::AID-CNE1>3.0.CO;2-4
83. Fiederling A, Ewert R, Andreyeva A, Jüngling K, Gottmann K. E-cadherin is required at GABAergic synapses in cultured cortical neurons. Neurosci Lett 2011; 501:167-72; PMID:21782891; http://dx.doi.org/10.1016/j.neulet.2011.07.009
84. Dobrosotskaya IY, James GL. MAGI-1 interacts with β-catenin and is associated with cell–cell adhesion structures. Biochem Biophys Res Commun 2000; 270:903-9; PMID:10772923; http://dx.doi.org/10.1006/bbrc.2000.2471
85. Nishimura W, Yao I, Iida J, Tanaka N, Hata Y. Interaction of synaptic scaffolding molecule and Beta -catenin. J Neurosci 2002; 22:757-65; PMID:11826105
86. Bamji SX, Shimazu K, Kimes N, Huelsken J, Birchmeier W, Lu B, Reichardt LF. Role of beta-catenin in synaptic vesicle localization and presynaptic assembly. Neuron 2003; 40:719-31; PMID:14622577; http://dx.doi.org/10.1016/S0896-6273(03)00718-9
87. Tong C, Ohyama T, Tien A-C, Rajan A, Haueter CM, Bellen HJ. Rich regulates target specificity of photoreceptor cells and N-cadherin trafficking in the Drosophilavisual system via Rab6. Neuron 2011; 71:447-59; PMID:21835342; http://dx.doi.org/10.1016/j.neuron.2011.06.040
88. Ting C-Y, Yonekura S, Chung P, Hsu S-N, Robertson HM, Chiba A, Lee C-H. Drosophila N-cadherin functions in the first stage of the two-stage layer-selection process of R7 photoreceptor afferents. Development 2005; 132:953-63; PMID:15673571; http://dx.doi.org/10.1242/dev.01661
89. Nern A, Nguyen L-VT, Herman T, Prakash S, Clandinin TR, Zipursky SL. An isoform-specific allele of Drosophila N-cadherin disrupts a late step of R7 targeting. Proc Natl Acad Sci USA 2005; 102:12944-9.
90. Lein ES, Zhao X, Gage FH. Defining a molecular atlas of the hippocampus using DNA microarrays and high-throughput in situ hybridization. J Neurosci 2004; 24:3879-89; PMID:15084669; http://dx.doi.org/10.1523/JNEUROSCI.4710-03.2004
91. Schwabe T, Neuert H, Clandinin TR. A network of cadherin-mediated interactions polarizes growth cones to determine targeting specificity. Cell 2013; 154:351-64; PMID:23870124; http://dx.doi.org/10.1016/j.cell.2013.06.011
92. Pecot MY, Tadros W, Nern A, Bader M, Chen Y, Zipursky SL. Multiple interactions control synaptic layer specificity in the drosophila visual system. Neuron [Internet] 2013; 77:299-310. Available from: http://pubget.com/site/paper/23352166?institution=
93. Mendez P, De Roo M, Poglia L, Klauser P, Muller D. N-cadherin mediates plasticity-induced long-term spine stabilization. J Cell Biol 2010; 189:589-600; PMID:20440002; http://dx.doi.org/10.1083/jcb.201003007
94. Scheiffele P, Fan J, Choih J, Fetter R, Serafini T. Neuroligin expressed in nonneuronal cells triggers presynaptic development in contacting axons. Cell 2000; 101:657-69; PMID:10892652; http://dx.doi.org/10.1016/S0092-8674(00)80877-6
95. Saglietti L, Dequidt C, Kamieniarz K, Rousset M-C, Valnegri P, Thoumine O, Beretta F, Fagni L, Choquet D, Sala C, et al. Extracellular interactions between GluR2 and N-cadherin in spine regulation. Neuron 2007; 54:461-77; PMID:17481398; http://dx.doi.org/10.1016/j.neuron.2007.04.012
96. Kwon H-B, Kozorovitskiy Y, Oh W-J, Peixoto RT, Akhtar N, Saulnier JL, Gu C, Sabatini BL. Neuroligin-1–dependent competition regulates cortical synaptogenesis and synapse number. Nat Neurosci 2012; 15:1667-74; PMID:23143522; http://dx.doi.org/10.1038/nn.3256
97. Pagnamenta AT, Khan H, Walker S, Gerrelli D, Wing K, Bonaglia MC, Giorda R, Berney T, Mani E, Molteni M, et al. Rare familial 16q21 microdeletions under a linkage peak implicate cadherin 8 (CDH8) in susceptibility to autism and learning disability. J Med Genet 2011; 48:48-54; PMID:20972252; http://dx.doi.org/10.1136/jmg.2010.079426
98. Sanders SJ, Ercan-Sencicek AG, Hus V, Luo R, Murtha MT, Moreno-De-Luca D, Chu SH, Moreau MP, Gupta AR, Thomson SA, et al. Multiple recurrent de novo CNVs, including duplications of the 7q11.23 Williams syndrome region, are strongly associated with autism. Neuron 2011; 70:863-85; PMID:21658581; http://dx.doi.org/10.1016/j.neuron.2011.05.002
99. Treutlein J, Cichon S, Ridinger M, Wodarz N, Soyka M, Zill P, Maier W, Moessner R, Gaebel W, Dahmen N, et al. Genome-wide association study of alcohol dependence. Arch Gen Psychiatry 2009; 66:773-84; PMID:19581569; http://dx.doi.org/10.1001/archgenpsychiatry.2009.83
100. Franke B, Neale BM, Faraone SV. Genome-wide association studies in ADHD. Hum Genet 2009; 126:13-50; PMID:19384554; http://dx.doi.org/10.1007/s00439-009-0663-4
101. Wang K, Zhang H, Ma D, Bucan M, Glessner JT, Abrahams BS, Salyakina D, Imielinski M, Bradfield JP, Sleiman PMA, et al. Common genetic variants on 5p14.1 associate with autism spectrum disorders. Nature 2009; 459:528-33; PMID:19404256; http://dx.doi.org/10.1038/nature07999
102. Gilling M, Lind-Thomsen A, Mang Y, Bak M, Møller M, Ullmann R, Kristoffersson U, Kalscheuer VM, Henriksen KF, Bugge M, et al. Biparental inheritance of chromosomal abnormalities in male twins with non-syndromic mental retardation. Eur J Med Genet 2011; 54:e383-8; PMID:21426945; http://dx.doi.org/10.1016/j.ejmg.2011.03.008
103. Singh SM, Castellani C, O'Reilly R. Autism meets schizophrenia via cadherin pathway. Schizophr Res 2010; 116:293-4; PMID:19861233; http://dx.doi.org/10.1016/j.schres.2009.09.031
104. St Pourcain B, Wang K, Glessner JT, Golding J, Steer C, Ring SM, Skuse DH, Grant SFA, Hakonarson H, Smith GD, et al. Association between a high-risk autism locus on 5p14 and social communication spectrum phenotypes in the general population. Am J Psychiatry 2010; 167:1364-72; PMID:20634369; http://dx.doi.org/10.1176/appi.ajp.2010.09121789
105. McCarroll SA, Hyman SE. Perspective. Neuron 2013; 80:578-87; PMID:24183011; http://dx.doi.org/10.1016/j.neuron.2013.10.046
106. Arias-Vásquez A, Altink ME, Rommelse NNJ, Slaats-Willemse DIE, Buschgens CJM, Fliers EA, Faraone SV, Sergeant JA, Oosterlaan J, Franke B, et al. CDH13 is associated with working memory performance in attention deficit/hyperactivity disorder. Genes Brain Behav 2011; 10:844-51; PMID:21815997; http://dx.doi.org/10.1111/j.1601-183X.2011.00724.x
107. Coussen F, Normand E, Marchal C, Costet P, Choquet D, Lambert M, Mège R-M, Mulle C. Recruitment of the kainate receptor subunit glutamate receptor 6 by cadherin/catenin complexes. J Neurosci 2002; 22:6426-36; PMID:12151522
108. Gorski JA, Gomez LL, Scott JD, Dell'Acqua ML. Association of an A-Kinase-anchoring protein signaling scaffold with cadherin adhesion molecules in neurons and epithelial cells. 200516:3574-90; PMID:15930126
109. Heisler FF, Lee HK, Gromova KV, Pechmann Y, Schurek B, Ruschkies L, Schroeder M, Schweizer M, Kneussel M. GRIP1 interlinks N-cadherin and AMPA receptors at vesicles to promote combined cargo transport into dendrites. PNAS 2014; 111:5030-5; PMID:24639525; http://dx.doi.org/10.1073/pnas.1304301111
110. Nagaoka T, Ohashi R, Inutsuka A, Sakai S, Fujisawa N. The Wnt/Planar cell polarity pathway component Vangl2 induces synapse formation through direct control of N-cadherin. Cell Rep 2014; 6:916-27; PMID:24582966; http://dx.doi.org/10.1016/j.celrep.2014.01.044
111. Nuriya M, Huganir RL. Regulation of AMPA receptor trafficking by N-cadherin. J Neurochem 2006; 97:652-61; PMID:16515543; http://dx.doi.org/10.1111/j.1471-4159.2006.03740.x

CHAPTER 3

NON-CANONICAL, HETEROPHILIC CADHERIN INTERACTIONS REGULATE LAYER-SPECIFIC SYNAPTIC POTENTIATION IN THE HIPPOCAMPUS

Co-authored by: Xin Duan[2], Shruti Muralidhar[1], Matthew R. Taylor[1], E. Anne Martin[1], Yueqi Wang[1], Luke Gangi-Wellman[1], Masahito Yamagata[2], Peter J. West[3], Joshua R. Sanes[2], and Megan E. Williams[1]

1 – Department of Neurobiology and Anatomy, University of Utah School of Medicine, Salt Lake City, UT 84112

2 – Center for Brain Science and Department of Molecular and Cellular Biology, Harvard University, Cambridge, MA 02138

3 – Department of Pharmacology and Toxicology, University of Utah School of Medicine, Salt Lake City, UT 84112

Summary

Neurons often integrate information by building specialized synapses with different inputs in distinct layers. Hippocampal CA1 neurons form synapses with CA3 neurons in two layers, stratum oriens (SO) and stratum radiatum (SR), and each layer develops unique synaptic properties. We demonstrate SO synapses have more mushroom spines and significantly enhanced long-term potentiation (LTP) than SR synapses and we discovered these differences require cadherins-6, 9, and 10. Though cadherins typically function via trans-cellular homophilic binding, our results suggest presynaptic cadherin-9 binds postsynaptic cadherins-6 and 10 to regulate enhanced SO LTP. Finally, we show cadherin-6, 9, 10 heterophilic binding is highly sensitive to changes in external calcium, providing a potential mechanism whereby calcium depletion during enhanced SO LTP loosens cadherin-6, 9, 10 adhesion to allow synapse rearrangements. These data are the first to demonstrate heterophilic cadherin interactions regulate circuit function in vivo by contributing to layer-specific synaptic potentiation.

Introduction

Complex neural circuits in the mammalian brain often intersect to allow the integration of information during higher-order cognitive tasks such as learning and memory. As a result, individual neurons constantly process synaptic input from multiple sources. Neurons accomplish this, in part, by forming synapses with structural and functional properties unique to each input (Nicholson et al., 2006; Nicoll and Schmitz, 2005). Input-specific synapses are often spatially segregated onto distinct domains of the postsynaptic neuron (Ango et al., 2004; Förster et al., 2006; Petreanu et al., 2009). Thus,

building input-specific synapses on distinct neuronal domains requires two important steps. First, axons must be guided to the correct dendritic region. Second, the appropriate type of synapse must be constructed after axo-dendritic contact. Much progress has been made in understanding how axons are guided to correct dendritic regions (Ango et al., 2004; Duan et al., 2014; Sanes and Yamagata, 2009; Suto et al., 2007). Thus, our research focuses on the second step: identifying the molecules and mechanisms responsible for building different types of synapses on individual neurons.

The classic cadherins are a family of calcium-dependent, homophilic cell adhesion molecules thought to contribute to synaptic specificity in several ways. Mammals have 20 classic cadherins and many are expressed in a cell type-specific manner in the brain. Thus, there is potential for differential matching of cadherins to provide an adhesive code driving specific synapse formation (Redies and Takeichi, 1996). This idea is supported by several studies (Duan et al., 2014; Kuwako et al., 2014; Osterhout et al., 2011; Poskanzer et al., 2003; Suzuki et al., 1997; Williams et al., 2011). Moreover, cadherins localize at synapses and are implicated in regulating many synaptic functions, including synaptic vesicle clustering, short-term plasticity, dendritic spine stabilization, glutamate receptor recruitment, and LTP (Aiga et al., 2010; Bozdagi et al., 2010; Fièvre et al., 2016; Hirano and Takeichi, 2012; Jungling et al., 2006; Mendez et al., 2010; Saglietti et al., 2007; Tang et al., 1998; Togashi et al., 2002; Vitureira et al., 2011). However, the majority of these functional studies only investigated the role of cadherin-2 (also known as N-cadherin). Cadherin-2 is broadly expressed by neurons and likely affects generic properties common to most synapses rather than conferring input-specific properties. Thus, it remains untested whether other differentially expressed classic cadherins confer functionally

unique properties to specific synapses without affecting other synapses on the same neuron.

We showed previously that cadherin-9 is expressed in hippocampal DG and CA3 neurons and is required for DG-CA3 synapse formation in vitro and in vivo (Williams et al., 2011). Here, we turned to the CA3-CA1 synapse to ask whether differentially expressed cadherins confer input-specific functional properties to synapses. CA1 neurons receive different types of excitatory inputs in three distinct synaptic layers. In the distal stratum lacunosum-moleculare (SLM) layer, CA1 neurons receive synapses from entorhinal cortex layer III (ECIII) axons while in the stratum oriens (SO) and stratum radiatum (SR) layers, CA1 neurons receive synapses from CA3 axons (Figure 3.1A). In addition, about 20% of CA1 SO inputs originate from hippocampal CA2 axons (Dudek et al., 2016).

Although the major inputs to CA1 SO and SR layers both come from CA3 axons, the two layers have distinct synaptic properties. Notably, the magnitude of LTP is significantly higher in SO compared to SR (Arai et al., 1994). We confirmed this dramatic layer-specific difference in LTP and our new results identify a corresponding morphological correlate as we show mushroom spine density is also significantly higher in SO. We then identified three classic cadherins, cadherins-6, 9, and 10, that are selectively required for enhanced LTP magnitude and mushroom spine density in the CA1 SO layer. Our results suggest they function via trans-synaptic heterophilic interactions with cadherin-9 acting at the CA3 presynapse and cadherins-6 and 10 at the CA1 postsynapse. These results are the first to directly implicate non-canonical heterophilic cadherin interactions in circuit formation in vivo. Moreover, our results also

identify new molecules underlying laminar synaptic specificity, providing critical insight toward elucidating the function of specific synapses during learning and memory.

Results

CA1 excitatory synapses have layer-specific properties

Synapses are broadly classified by the neurotransmitter released, but even synapses releasing the same neurotransmitter develop unique structural, molecular, and functional properties (Arai et al., 1994; Nicholson et al., 2006; Nicoll and Schmitz, 2005). Whereas unique features of highly unusual synapses like DG-CA3 mossy fiber synapses are well appreciated (Nicoll and Schmitz, 2005), subtle differences between more closely related types of excitatory synapses remain less explored. Here, we address this issue in CA1 neurons, which receive "typical" glutamatergic excitatory synapses in three distinct layers (Figure 3.1A).

To determine if CA1 excitatory synapses have layer-specific properties, we first examined presynaptic structure by electron microscopy. We analyzed asymmetric synapses in CA1 SO (~50-100 μm from cell body), SR (~50-100 μm from cell body), and SLM (~350 μm from cell body). Synaptic vesicles (SVs) were classified as docked if they were touching the active zone membrane and proximal if they were within 30 nm of active zone (Figure 3.2A). We found that SO and SR presynapses, both of which are composed of primarily CA3 inputs, have similar structures and vesicle distributions (Figure 3.1B and C). In contrast, SLM presynapses are morphologically distinct from SO and SR synapses because they have higher SV densities and bouton area and thinner postsynaptic densities (PSDs) (Figures 3.1B, C, and 3.2A).

Second, we tested for layer-specific postsynaptic differences by conducting spine shape and density analyses. CA1 neurons were microinjected with Lucifer Yellow dye (Figure 3.1D) and oblique dendritic segments from each layer were analyzed. Spines were classified according to their shape, which reflects the maturity and potentiation state of each synapse (Bourne and Harris, 2007; Harris, 1999; Harris et al., 1992). Absolute spine densities and the relative proportions of spine classes identified by our light microscopic analyses are consistent with those previously observed in electron microscopic reconstructions (Figures 3.2B-E) (Harris et al., 1992; Katz et al., 2009).

Our first main finding is that, like the presynapses, SLM postsynapses are distinct from those in SR and SO. Specifically, SLM spine densities are significantly lower and spine lengths significantly longer across most spine classes (Figures 3.1D-F and 3.2B-E). Our second main finding is that we also identified significant differences between SR and SO. SO has significantly higher densities of stubby and mushroom spines compared to SR (Figures 3.1E and 3.2C). Because mushroom and stubby spines represent the most mature and potentiated spine states (Harris et al., 1992; Holtmaat et al., 2005; Matsuzaki et al., 2004; Roberts et al., 2010; Tønnesen et al., 2014; Xu et al., 2009), we reasoned higher mushroom and stubby spines in SO may reflect the prior observation that the magnitude of LTP in SO is significantly higher than SR (Arai et al., 1994). We tested this in our system and found that LTP magnitude induced by theta burst stimulation (TBS) of CA3 axons in acute hippocampal slices is significantly higher in SO compared to SR (Figures 3.1G-J). Thus, our results indicate CA1 SO and SR synapses differ at both electrophysiological and morphological levels. This is particularly interesting because both SO and SR are primarily composed of CA3-CA1 synapses that have been largely

assumed to develop the same properties. Thus, here we focused on elucidating molecular mechanisms selectively required for enhanced SO potentiation.

Cadherin-9 specifically regulates synaptic potentiation in the CA1 SO layer

We previously showed cadherin-9 regulates DG-CA3 synapse formation, functioning both presynaptically in DG neurons and postsynaptically in CA3 neurons (Williams et al., 2011). Because cadherin-9 mRNA is expressed by CA3 neurons (Figure 3.3A) (Williams et al., 2011) and cadherins generally localize to both pre- and postsynaptic sites, we tested if cadherin-9 also localizes to CA3 axons. A plasmid encoding cadherin-9 fused to the high-performance epitope tag $smFP^{FLAG}$ (Viswanathan et al., 2015) was expressed in mouse embryos by in utero electroporation. Immunostaining at P21 revealed that cdh9-$smFP^{FLAG}$ is found in distinct puncta along CA3 axons (Figure 3.3B), suggesting cadherin-9 localizes to CA3 presynaptic boutons.

Next, we used cadherin-9 knockout mice (Duan et al., 2014) to test whether cadherin-9 is required for synapse form or function in CA3-CA1 synapses located in SR or SO. EC-CA1 synapses in SLM were also examined as a negative control because cadherin-9 is not expressed by either ECIII or CA1 neurons. We confirmed knockout mice lack cadherin-9 protein in hippocampal lysates (Figure 3.4A) and then analyzed dendritic spines in all excitatory synaptic layers of CA1 neurons in $Cdh9^{+/+}$ and $Cdh9^{-/-}$ mice. All spine analyses were conducted blind to genotype. No changes in total spine densities were detected in any layer, but we observed a specific and significant reduction of mushroom spine density in the SO layer of $Cdh9^{-/-}$ animals (17% average reduction

compared to $Cdh9^{+/+}$ animals) (Figures 3.3C-H and 3.4B-D).

We then tested if the reduction of SO mushroom spines in $Cdh9^{-/-}$ animals correlates with impaired synaptic potentiation specifically in SO by measuring LTP in the SO and SR layers of $Cdh9^{+/+}$ and $Cdh9^{-/-}$ hippocampal slices. In support, LTP is significantly lower in the SO but not the SR of $Cdh9^{-/-}$ mice compared to $Cdh9^{+/+}$ mice (Figure 3.5). Interestingly, LTP levels in $Cdh9^{-/-}$ SO are similar to $Cdh9^{+/+}$ SR (Figure 3.6A). This suggests cadherin-9 is not required for baseline LTP but is required for the enhanced LTP specific to the SO layer. Moreover, analysis of total spine density (Figure 3.3), input-output curves from field recordings (Figures 3.6B and C), and spontaneous miniature excitatory postsynaptic currents (mEPSCs) (Figures 3.6D-F) suggests the LTP defect in $Cdh9^{-/-}$ mice is not due to impaired basal synaptic transmission. In sum, our results indicate cadherin-9 is required for normal mushroom spine density and enhanced LTP in the SO layer of CA1 neurons.

Cadherin-6, 9, and 10 heterophilic interactions mediate trans-cellular adhesion

Cadherins typically function via homophilic interaction. However, at CA3-CA1 SO synapses, cadherin-9 is expressed by CA3 but not CA1 neurons (Figure 3.3A). We therefore reasoned presynaptic cadherin-9 may bind other cadherins expressed in CA1 neurons to carry out the layer-specific functions described above. Heterophilic cadherin interactions have been observed in cultured cell lines (Katsamba et al., 2009; Shan et al., 2000; Shimoyama et al., 2000), but have not yet been shown to have functional relevance in the brain.

To test if cadherin-9 functions trans-synaptically via other classic cadherins expressed in CA1, we identified all classic cadherins expressed in the hippocampus using the Allen Brain Atlas (Lein et al., 2007) and confirmed expression patterns by in situ hybridization. Cadherins-2, 8, and 11 are broadly expressed in all principal hippocampal neurons (Figure 3.7A). In contrast, cadherin-24 is expressed primarily in CA3 neurons and cadherins-6 and 10 are expressed in CA1 neurons (Figure 3.7A). We also examined the expression pattern of cadherin-10 by genetic labeling. Cadherin-10 knockout mice ($Cdh10^{-/-}$) were generated by inserting CreER in the first exon of the *cdh10* gene. These mice were crossed to the Cre-dependent Ai3 YFP reporter line to generate heterozygous *cdh10-CreER*$^{+/-}$;$Ai3^{+/-}$ mice, which were injected with tamoxifen and immunostained for YFP. Our results indicate cadherin-10 expression is highly restricted to glutamatergic spiny CA1 pyramidal neurons (Figures 3.7B and 3.8A).

To determine if cadherin-9 in CA3 neurons can bind in trans to other cadherins expressed in CA1 neurons, we tested for interactions among hippocampally-expressed cadherins using a cell aggregation assay (Takeichi and Nakagawa, 2001). CHO cells, which express no endogenous cadherins (Figure 3.8B) (Ginsberg et al., 1991), were transfected with cadherins fused to GFP or mCherry and cell suspensions were mixed together. If the two cadherins interact in trans, mixed red and green aggregates result (Figure 3.7C, middle). If the two cadherins do not interact heterophilically, separate red and green aggregates form because all cadherins undergo homophilic binding (Figure 3.7C, right). An aggregation index was calculated for each cadherin pair tested (see Supplemental Experimental Procedures). Consistent with a previous report (Shimoyama et al., 2000), we identified 4 heterophilic cadherin pairs; cadherins-6/9, 9/10, 10/6, and

8/11 (Figures 3.7C-E). As expected, all cadherins tested showed homophilic binding while cells expressing GFP and mCherry alone showed no binding (Figures 3.7C-E) and all binding is calcium dependent as it is completely prevented in the presence of EDTA (Figure 3.7C).

Cadherins-6, 9, and 10 accumulate at cell-cell junctions and synapses

We next investigated whether the heterophilic cadherins-6, 9, and 10 are co-recruited to cell-cell junctions in CHO cells and to axo-dendritic contact points in cultured neurons. To mimic hippocampal expression, we expressed cdh9-smFP^{FLAG} in one set of cells to simulate CA3 neurons and plated them with a second set of cells expressing cdh6-smFP^{HA} and cdh10-smFP^{MYC} to simulate CA1 neurons. Immunostaining shows that all three cadherins are preferentially localized at the interaction interfaces of the two cell types in both CHO cells (Figure 3.7F) and neurons (Figure 3.8C). To rule out the possibility that co-localization is an over-expression artifact, we repeated the experiment by mixing neurons expressing cdh9-smFP^{FLAG} with neurons expressing cadherins that do not bind cadherin-9, namely cadherin-2 and cadherin-11. In this case, we did not observe co-localization at axo-dendritic contact points (Figure 3.8D).

For cadherin-6, 9, 10 heterophilic interactions to be biologically relevant, the binding partners need to be expressed at the same place and time in hippocampal synapses. To test this, we purified hippocampal synaptosomes from P7, P14, and P21 mice and immunoblotted for cadherins and synaptic markers (Figure 3.7G). All cadherins tested were enriched in the synaptosome fraction relative to lysates by P21 (Figure 3.7H).

Interestingly, we also observed a sharp and consistent age dependent increase in the levels of cadherins-9 and 10 in the synaptosome fraction while synaptic levels of the broadly expressed cadherins-2 and 8 remained relatively level over time (Figure 3.7I). This suggests different cadherins are recruited to synapses at different times and that cadherins-9 and 10 may play a more specific role in synapse maturation, which is consistent with our finding that cadherin-9 is required for enhanced SO LTP. In sum, our results indicate cadherins-9 and 10 are selectively enriched at cell junctions and maturing synapses.

Cadherins-6 and 10 are required for potentiated synapses in the CA1 SO layer

Our results strongly suggest cadherins-6 and 10 are likely postsynaptic binding partners of cadherin-9 at CA3-CA1 synapses. If so, then mice lacking these cadherins should have reduced mushroom spines and SO LTP similar to $Cdh9^{-/-}$ mice. We first examined the $Cdh10^{-/-}$ mouse line. We confirmed $Cdh10^{-/-}$ mice lack cadherin-10 protein in hippocampal lysates and synaptosomes while expressing normal levels of cadherins-9 (Figure 3.10A).

Spine analysis indicates $Cdh10^{-/-}$ mice have significantly reduced densities of stubby and mushroom spines compared to $Cdh10^{+/+}$ mice specifically in the SO layer (Figures 3.9 and 3.10B-D), resembling the spine phenotype observed in $Cdh9^{-/-}$ mice (Figures 3.3 and 3.4). Correspondingly, $Cdh10^{-/-}$ mice also have reduced SO LTP and normal SR LTP (Figures 3.11A-F) compared to $Cdh10^{+/+}$ mice. However, the reduction of LTP in $Cdh10^{-/-}$ mice did not quite reach statistical significance, likely because of the continued

presence of cadherin-6 in CA1 neurons. To test this, we generated double knockout mice that lack expression of both cadherins-6 and 10 (Figures 3.12A and B). Consistent with our hypothesis, $Cdh6^{-/-}$;$Cdh10^{-/-}$ double knockout mice have significantly reduced SO LTP (Figures 3.11G-I). mEPSC analysis, total spine density, and input/output curves suggest baseline synaptic transmission is normal in the cadherin-10 knockout and $Cdh6^{-/-}$;$Cdh10^{-/-}$ double knockout lines (Figures 3.12C-G). Though reduced, there is still some SO potentiation observed in cadherin-10 knockout and $Cdh6^{-/-}$;$Cdh10^{-/-}$ double knockout mice. This supports our previous data and indicates cadherins-6, 9, and 10 are not required for baseline LTP but are required for the enhanced LTP specific to the SO layer. Taken together, results from binding assays, spine analyses, and LTP recordings strongly suggest presynaptic cadherin-9 interacts with postsynaptic cadherins-6 and 10 to regulate layer-specific spine potentiation and enhanced LTP in CA1 SO.

Unique binding properties of cadherins-6, 9, and 10 may contribute to their specific role in CA1 SO potentiation

Why might cadherins-6, 9, and 10 affect synaptic potentiation specifically in CA1 SO but not SR? First, we tested if these cadherins specifically localize in the SO but not SR layer. We immunoblotted tissue from CA1 SO and SR layers and find cadherins-9 and 10 are expressed at similar levels in SO and SR (Figure 3.13A). We verified our dissection technique using myelin, which is high in SO and low in SR (Gil et al., 2010) (Figure 3.13A). It is still possible these cadherins and/or cadherin-6 are preferentially enriched at active synaptic sites in SO compared to SR but overall layer-specific localization of cadherins-9 and 10 does not explain their specific role in SO.

Second, because CA2 neurons project preferentially to CA1 SO compared to SR (Hitti and Siegelbaum, 2014), we considered the possibility that reduced SO LTP in cadherin knockout animals could reflect disruption of CA2-CA1 synapses instead of CA3-CA1 synapses. However, we find that neither cadherins-6, 9, nor 10 are expressed in CA2 neurons. Using a CA2-specific marker on sections from *Cdh10-CreER*;Ai3 mice, we demonstrate cadherin-10 expression is limited to CA1 neurons (Figure 3.7B). Moreover, double in situ hybridization of cadherins-9/10 and cadherins-9/6 indicates there is consistently a gap in the signal for these probes in the CA2 region (Figure 3.14A and B). Thus, it is unlikely CA2-CA1 synapses are primarily affected in these knockout mice.

Finally, we reasoned that cadherin-6, 9, 10 interactions may display specific properties such that they function preferentially at synapses undergoing enhanced LTP. Elevated synaptic activity is thought to cause a temporary reduction of Ca^{2+} from the synaptic cleft (Egelman and Montague, 1999; Rusakov and Fine, 2003). This Ca^{2+} depletion may cause cadherin-6, 9, and 10 to lose trans-synaptic binding and thereby allow synaptic growth and restructuring (Tai et al., 2008). Thus, we tested whether extracellular Ca^{2+} reduction specifically inhibits binding of cadherins-6, 9, and 10 using the previously described CHO cell aggregation assay. Our results indicate that cadherin-6, 9, 10 binding is highly sensitive to calcium reduction and they significantly differ from other cadherins (Figures 3.13B and C). Specifically, cadherin-2/2 aggregation is robust, reaching near saturation levels at the lowest Ca^{2+} concentration tested (0.5mM) while cadherin-8/11 aggregation shows intermediate Ca^{2+} dependence (Figures 3.13B and C). In contrast, cadherin-9/10 and cadherin-9/6 interactions are weaker and more sensitive to changes in Ca^{2+} concentration. Cadherin-9/10 aggregates could only be detected in this in vitro assay at 5

mM Ca^{2+} (Figures 3.13B and C) and cadherin-9/6 aggregates started to form at 2mM Ca^{2+} (Figure 3.13C). Note that at 1mM Ca^{2+} mixtures of cadherin-9 and cadherin-6 cells results in largely homophilic cadherin-6 aggregates (Figure 3.13C), indicating cadherin-6/6 homophilic binding is stronger than cadherin-9/6 heterophilic binding especially at lower Ca^{2+} concentration. Though this in vitro assay using free-floating cells does not precisely replicate in vivo binding conditions for juxtaposed membranes, it provides a useful estimate of comparative binding strength among different cadherins.

To investigate the calcium-dependent dynamic properties of cadherins in juxtaposed membranes of adherent cells, we performed fluorescence recovery after photobleaching (FRAP) experiments on fluorescently tagged cadherins. CHO cells were separately transfected with a single GFP or mCherry tagged cadherin, then GFP and mCherry transfected cells were mixed, and plated to adherent coverslips for live imaging. Under these conditions, when two cells that express interacting cadherins contact one another, the cadherins readily accumulate at the cell-cell junctions (Figures 3.7F and 3.13D,E). We then performed FRAP on cadherins at the cell junctions to determine if different cadherins have different stabilities or dynamics at cell junctions. Cadherins at cell junctions were photobleached and then imaged every 15 seconds to determine recovery time constants (see Supplemental Experimental Procedures). We determined that presence of the GFP or mCherry tag by itself did not differentially alter recovery time by imaging cell junctions in which the same cadherin (cadherin-2) was tagged with different fluorophores (Figures 3.14C).

Under physiological Ca^{2+} concentrations (2 mM), we observed similar recovery time constants for cadherin-2/2, cadherin-9/6, and cadherin 9/10 junctions (Figures 3.13D and

F). This suggests that turnover rates for different cadherins at physiological Ca^{2+} concentrations are similar. However, under low Ca^{2+} conditions (0.5 mM), cadherin-9/6 and cadherin-9/10 junctions have significantly reduced recovery time constants compared to cadherin-2/2 junctions (Figures 3.13E and G). This indicates cadherins-6, 9, 10 have faster turnover and more dynamic cell junctions compared to cadherin-2 under conditions of limited calcium (Figures 3.13E and G). In summary, we propose cadherin-9 heterophilic interactions would be first and most strongly affected (compared to other cadherins) by Ca^{2+} reduction following synaptic potentiation. This effect is likely to be more pronounced in CA1 SO synapses that undergo enhanced LTP.

Discussion

Principal neurons in the cortex and hippocampus form layer-specific excitatory synapses that are structurally and functionally distinct (Arai et al., 1994; Nicholson et al., 2006; Nicoll and Schmitz, 2005). For example, CA3 neurons provide excitatory input onto CA1 spines in two synaptic layers, each with distinct synaptic potentiation mechanisms. Our new work begins to uncover the mechanisms underlying these differences. Here, we have identified three new molecules, cadherins-6, 9, and 10, required for CA1 layer-specific LTP.

Identifying molecular mechanisms to understand the function of layer-specific LTP

In general, understanding the function of the brain at the cellular level requires 1) identifying specific connections, 2) understanding molecular mechanisms regulating

those connections, and then 3) using that molecular and cellular knowledge to manipulate those specific connections to determine their function. We initially conducted a thorough characterization of the structure of excitatory synapses in three CA1 synaptic layers (Figure 3.1). We used electron microscopy to evaluate presynaptic structures and 3D light microscopy to analyze postsynaptic spine shape and density in each layer. Our results from these analyses support two main conclusions. First, EC-CA1 synapses in the SLM layer have significantly different pre- and postsynaptic structures from CA3-CA1 synapses in SO or SR. This is not entirely surprising given that SLM synapses are located on the thinnest, most distal dendrites and receive inputs from entorhinal cortex, a non-hippocampal cell type. Second, and more surprising because they originate from the same general class of input, we identified subtle but consistent differences between CA3-CA1 SR and SO synapses. Our results indicate the SO has a higher density of mushroom spines than SR and the magnitude of LTP is significantly higher in SO versus SR (Figure 3.1D-J) (Arai et al., 1994).

The consequences of enhanced CA1 SO LTP on brain function are unknown, but relevant differences between CA1 SO and SR synapses have been noted. Spatial exploration tasks in rats cause a specific increase in CA1 SO spine density (Moser et al., 1997), while Alzheimer mouse models have a specific reduction of CA1 SO spines (Perez-Cruz et al., 2011). These findings hint at a uniqueness in CA1 SO synapses and suggest the SO is particularly sensitive to changes in certain behavior or disease states. Further, individual CA3 axons project to both layers but the terminal branching is not equal between the two layers and may vary with the septal-temporal and ipsi-contralateral positions of the CA3 cell body (Li et al., 1994). Thus, though most SO and SR

presynapses originate from CA3 axons, they may represent different subpopulations of CA3 neurons along the hippocampal axis. Regardless, deeper investigation of the role of SO versus SR in hippocampal function requires the ability to molecularly or genetically manipulate SO or SR synapses. Here, we show loss of either cadherin-9 or cadherins-6 and 10 results in specific reduction of CA1 SO mushroom spines and LTP compared to CA1 SR levels. Therefore, the knockout mice analyzed here and other tools targeting cadherins-6, 9, and 10 should provide important access to test enhanced potentiation in CA1 SO impacts hippocampal circuits and behaviors.

Cadherins interact heterophilically to wire the brain in vivo

Thus far, most biological functions of cadherins are attributed to trans-cellular homophilic interactions. However, some cadherins engage in heterophilic interactions in cultured cell lines (Shan et al., 2000; Shimoyama et al., 2000). It was previously suggested that cadherins may use these heterophilic interactions in vivo (Duan et al., 2014), but it had not yet been directly investigated. Our new results provide strong evidence that trans-cellular heterophilic interactions between cadherin-9 and cadherins-6 and 10, expressed in CA3 and CA1 neurons, respectively, are necessary for synaptic potentiation in a subset of CA3-CA1 synapses.

Cadherins interact in cis (laterally) as well as in trans (Wu et al., 2010). Similar to trans interactions, most attention has been paid to homophilic cis interactions (Harrison et al., 2011). However, heterophilic cis interactions may be particularly important in the nervous system where most neurons express multiple cadherins. Here, we show that cadherins-6 and 10 expressed in CA1 neurons co-aggregate in cis when exogenously co-

expressed in CHO cells and cultured neurons (Figure 3.7F, 3.8C). Our results suggest cadherin-6, 9, and 10 likely use heterophilic cis interactions (between cadherins-6 and 10) and heterophilic trans interactions (between cadherins-9 and 6 and cadherins-9 and 10) to form a trimeric complex regulating mushroom spine formation and LTP. Because CA1 neurons also express cadherins-2, 8, and 11 (Figure 3.7A), it will be interesting to determine in future studies how adhesion is affected by even more complex combinations of synaptic cadherins.

A new role for classic cadherins in layer-specific synaptic potentiation

Synapses are not static structures and instead require a complex balance of adhesive stability and flexibility. As a result, adhesion molecules are required for LTP, yet paradoxically, a loss of cell adhesion is likely required for spine restructuring following potentiation (Benson and Huntley, 2012; Tai et al., 2008). Our results suggest that cadherins-6, 9, and 10 are uniquely suited to this role during LTP because their adhesive state and motility are highly regulated.

Our results are not the first to implicate cadherins in LTP. Blocking cadherin-2 function or deleting the gene results in impaired LTP in CA1 SR synapses (Bozdagi et al., 2010; Tang et al., 1998) and cadherin-2 is necessary for stabilizing potentiated spines (Mendez et al., 2010). However, cadherin-2 forms stable protease resistant dimers after neuronal activation (Tanaka et al., 2000) and our new results indicate that cadherin-2 mediates adhesion in low calcium concentrations. Thus, the stable nature of cadherin-2-mediated adhesion is not ideal for promoting initial synapse rearrangements. In fact, loss

of cadherin-2 does not alter the initial rise of synaptic strength following LTP stimulation but it is required for the sustained persistance of LTP after spines enlarge (Bozdagi et al., 2010; Tang et al., 1998). In contrast, cadherins-6, 9, and 10 are required for the enhanced potentiation observed in CA1 SO layer starting from the initiation of LTP. One model to explain our results is that SO synaptic clefts undergo enhanced calcium depletion following LTP stimulus. This may selectively weaken cadherin-9/6/10 heterophilic interactions, thereby allowing restructuring of these synapses. It is possible that, in the absence of cadherins-6, 9 and 10, other more adhesive cadherins such as cadherin-2 or cadherin-11 are recruited to or dominate adhesion at the synapse. This could reduce the flexibility for synaptic growth and restructuring in cadherin-9 and $Cdh6^{-/-};Cdh10^{-/-}$ double knockout mice and thereby lead to impaired LTP in CA1 SO synapses.

Work from others lends additional support to our model that synapse dynamics depend on the presence of multiple cadherins with different degrees of trans-cellular binding affinities. For example, cadherin-8 but not cadherin-2 levels are reduced following LTP induction in medial perforant path-DG synapses (Huntley et al., 2010). Further, cadherin-11 has increased trans-cellular binding in low pH and Ca^{2+} concentrations (Heupel et al., 2008). This is exactly opposite to what we observe for cadherins-6, 9, and 10 but accordingly, deletion of cadherin-11 causes increased CA1 SR LTP (Manabe et al., 2000), suggesting the high stability of cadherin-11 in low calcium normally acts to restrict synaptic plasticity.

The role of cadherin diversity in the brain

Understanding the true function of the classic cadherins in the brain has been challenging. First, most of the 20 classic cadherins are expressed in the brain. Thus, many likely have overlapping functions that mask defects in single gene gain and loss of function experiments. Second, most classic cadherins are persistently expressed through brain development and maturity. Thus, they likely take on new functions as the animal develops. Consistent with this, cadherins function in diverse processes, including neural tube formation (Hirano and Takeichi, 2012), axon targeting (Duan et al., 2014; Kuwako et al., 2014; Osterhout et al., 2011; Poskanzer et al., 2003), synapse formation (Togashi et al., 2002; Williams et al., 2011), synapse pruning (Bian et al., 2015), and synaptic function (Bozdagi et al., 2010; Fièvre et al., 2016; Jungling et al., 2006; Mendez et al., 2010; Tang et al., 1998; Vitureira et al., 2011). Third, there is an overwhelming focus on the study and function of the broadly expressed cadherin-2. This has led many to assume that all cadherins function in the same manner with little attention on the differences between cadherin family members.

In this study, we have begun to address the roles of cadherin diversity in synapse function. By carefully analyzing input-specific excitatory synapses across the entire CA1 dendritic tree, we show that differential binding affinities may allow distinct sets of cadherins to confer specialized properties in specific synapses. Overall, our results reveal a novel role for non-canonical, heterophilic cadherin interactions between cadherins-6, 9 and 10 in layer-specific synaptic potentiation of CA3-CA1 synapses. Our study suggests different cadherins have complex regulatory roles on synaptic potentiation and the relative levels of diverse cadherins may govern synapse dynamics.

Methods

Plasmids

A mammalian codon optimized cadherin-9 cDNA was synthesized (Genscript) and all other cadherin cDNAs were obtained from Open Biosystems (GE Healthcare) (Williams et al., 2011). All cadherins were subsequently cloned into the mammalian expression vector pCAG or an in vitro transcription compatible vector using standard procedures. Spaghetti monster fluorescent proteins (smFPs) (Viswanathan et al., 2015), GFP, and mCherry tags were inserted at the C-terminus of all cadherin constructs.

In situ hybridization

Antisense mRNA probes labeled with DIG-UTP (Roche) were in vitro transcribed from full length cadherin cDNAs. The probes were hybridized to 20µm thick coronal cryosections of mouse brain tissue, immunolabeled with alkaline phosphatase conjugated anti-DIG antibody (Roche), and detected using NBT/BCIP stock solution (Roche).

Synaptosome preparation

Synaptosomes were purified as described previously (Jones and Matus, 1974). Briefly, hippocampi were dissected from mice aged P7, P14, or P21. Tissue was homogenized with a Dounce homogenizer (20% w/v) in ice-cold 0.32 M sucrose + 20 mM HEPES, pH 7.4 supplemented with protease inhibitors. Homogenates were cleared by spinning at 1000 x g for 10 minutes at 4˚C. The supernatant was spun at 17000 x g for 15 minutes. The pellet containing crude synaptosomes were resuspended in 0.32 M sucrose + 20 mM HEPES and layered at the top of a sucrose gradient (made of 4 mls of 1.2 M, 4 mls of 1

M, and 3 mls of 0.8 M sucrose in 20 mM HEPES) and centrifuged at 41000 x g for 2 hours. Purified synaptosomes were collected at the interface between 1.2 M and 1 M sucrose. 5µg of protein per lane was loaded for immunoblotting.

Mouse lines

The cadherin-9 knockout mouse line was described previously (Duan et al., 2014). To generate a cadherin-10 knockout mouse line, CreER was inserted into the first coding exon of the *cdh10* gene by homologous recombination in mouse embryonic stem (ES) cells (strategy described in (Krishnaswamy et al., 2015)). The *cdh10*-targeting vector was obtained via lambda phage-mediated recombination. Multiple chimeric mice with the targeted embryonic stem cells were generated and two lines with germ line transmissions were mated to produce stable knockout lines. The Cadherin-6 knockout mouse line was obtained using the same strategy and was described previously (Kay et al., 2011). To obtain $Cdh6^{-/-}$;$Cdh10^{-/-}$ double knockout mice, first *cdh6-cdh10* trans-heterozygotes were made by breeding the single knockouts. Subsequently, the trans-heterozygotes were mated to obtain cis *cdh6-cdh10* trans-heterozygotes. These cis-heterozygotes were mated to obtain homozygous $Cdh6^{-/-}$;$Cdh10^{-/-}$ double knockout mice. All animals and experiments were maintained and conducted in accordance with the NIH guidelines on the care and use of animals and approved by the University of Utah and Harvard University IACUC committees.

Transmission electron microscopy

Mice aged P21-P23 were transcardially perfused with cold phosphate buffered saline pH 7.4 (PBS) for 1 minute followed by cold fixative (1% paraformaldehyde (PFA) and 2.5 % glutaraldehyde in 0.1 M sodium cachodylate buffer pH 7.2) for 7 minutes. Brains were removed, soaked in fixative for two days, and sectioned into 150 μm thick coronal sections. The CA1 region was cut out, washed with 0.1 M sodium cachodylate buffer, fixed with 1% osmium tetroxide and 1.5% potassium ferrocyanide for 1 hour, and stained with 1% uranyl acetate for 1 hour. The tissue was subsequently dehydrated in increasing concentrations of ethanol, embedded in epon resin, and cured at 60°C for 48 hours. Next, 40nm sections were cut using a Leica UC6 ultramicrotome and stained using lead citrate. Images were acquired using a JEM-1400Plus TEM (JEOL) at 10000X magnification.

Microiontophoresis and spine analysis

Lucifer yellow microiontophoresis was performed as described previously (Dumitriu et al., 2011). Neurons were filled until the tips of distal dendrites appeared bright. Slices were post-fixed in the fixative for 15 minutes and dendrites were imaged using a Zeiss LSM 710 confocal microscope. Images were deconvolved using AutoQuant X3 (Bitplane) and spines were modeled using Imaris software (Bitplane). Spine paramaters like head width (H), mean neck width (N), and length (L) were calculated and used for further classification. Spines were classified into thin ($H > 1.2*N$ and $0.15\ \mu m < H < 0.3\ \mu m$), mushroom ($H > 1.2*N$ and $H > 0.3\ \mu m$), stubby ($H < 1.2*N$ and $L < 0.5$), and filopodia ($H < 0.15\ \mu m$ and $N < 0.15\ \mu m$). The rare spine not satisfying any of these conditions was deemed unclassified. The spine head width cutoff of 0.3 μm resulted in a

mushroom to thin spine ratio of 0.3, which is close to the value defined previously (Harris et al., 1992).

Cell aggregation assay

Cells transfected with cadherins fused to GFP or mCherry were washed with HEPES-based calcium and magnesium-free buffer (HCMF, 137 mM NaCl, 5.4 mM KCl, 1 mM $CaCl_2$, 0.34 mM Na_2HPO_4, 10 mM HEPES, 5.55 mM Glucose) and dissociated with 0.01% Trypsin in HCMF + 1 mM $CaCl_2$. Cells were subsequently spun down and resuspended in HCMF. 50,000 cells expressing a GFP tagged cadherin were mixed with 50,000 cells expressing a mCherry tagged cadherin. The cell mixture was supplemented to obtain final concentrations of 4 mM $CaCl_2$, 20 µg/ml DNAse I, and 1 mM $MgCl_2$. To test for calcium dependence of aggregation (Figure 7B), cell mixtures were supplemented with 2mM EDTA or 0, 0.5, 1, 2, and 5 mM $CaCl_2$ (final concentration). Aggregation was performed for 90 minutes in a nutating shaker at 37°C. Post-aggregation cells were fixed with 4% PFA in PBS. Cells were transferred to 96 well glass bottom dishes and imaged using a Zeiss LSM 710 confocal microscope. To calculate the aggregation index (AI), the entire well was imaged and cellular clusters bigger than $900\mu m^2$ were defined as aggregates. For every aggregate, the net GFP (g) and mCherry (m) fluorescence signal was quantified. These values were normalized to the total GFP (G) and mCherry (M) signal in the well to obtain Gn and Mn, respectively (i.e., Gn=g/G, Mn=m/M). Next, a heterophilic score (S) for an aggregate was calculated using the formula $S = (Gn+Mn)*\sin(\pi*Gn/(Gn+Mn))$. This function quantified the 'heterophilicity' of an aggregate. Subsequently, the AI for the entire well was calculated as $AI = \sum S_i /(G+M)$,

where S_i is the heterophilic score of the i^{th} aggregate. Image analysis was done using ImageJ.

Cell culture

Cell culture was carried out as described previously (Martin et al., 2015). For neuron cultures, P2 rat cortical glia were cultured on PDL/collagen-coated coverslips to form a monolayer. One week later, P0 mouse hippocampi were dissected in cold HEPES-buffered saline solution, incubated in papain for 30 minutes, dissociated, and plated to glial monolayers at 10^5 cells/ml. Glia media: DMEM, 10% FBS, 75 mM glucose, and penicillin/streptomycin. Neuron plating media: MEM, 10% horse serum, 50 mM glucose, 0.250 mM sodium pyruvate, 2 mM Glutamax, 100 U/ml Penicillin, 100 g/ml Streptomycin. Neuron feeding media: Neurobasal A, B27, 30 mM glucose, 0.5 mM Glutamax, 20 U/ml Penicillin, 20 g/ml Streptomycin. Neurons were transfected by electroporation using a ECM830 model (BTX, Harvard Apparatus). For CHO cell cultures, cells were maintained in CHO media: F12K media (Corning Inc.), 10% FBS, and penicillin/streptomycin.

Antibodies

The following primary antibodies were used in this study: mouse anti-FLAG M2 1:3000 (Sigma), rabbit anti-Myc 1:1000 (Sigma), rat anti-HA 1:1000 (Roche), goat anti-GFP 1:3000 (Abcam), chicken anti-MAP2 1:5000 (Abcam), rabbit anti-GABA 1:1500 (Sigma), rabbit anti-synaptoporin 1:1000 (Synaptic Systems), mouse anti-PSD95 1:1000 (Neuromab), mouse anti-GFAP 1:1000 (EMD Millipore), rabbit anti-GluR1 1:1000

(Chemicon), guinea pig anti-vGLUT1 1:2000 (Millipore), mouse anti-GAPDH 1:3000 (Millipore), rabbit anti-Myelin basic protein 1:1000 (Abcam), rabbit anti-cadherin-9 1:500 (gift from Dr. Gerd Klein, University of Tuebingen), mouse anti-cadherin-2 1:1000 (BD Biosciences), rabbit anti pan cadherin antibody 1:200 (Sigma), and mouse anti-cadherin-8 1:50 (Developmental studies hybridoma bank). The rabbit anti-cadherin-10 was used at 1:500 and was generated for this study. A peptide corresponding to part of the intracellular domain of cadherin-10 (QNTIHLRVLESSPV) was synthesized (Selleckchem.com) and used for inoculation (Cocalico Biologicals). All secondary antibodies were purchased from Jackson ImmunoResearch.

Immunoblotting

Protein concentrations from synaptosomal preparation were quantified with a BCA assay (Thermo Scientific). 5 μg of synaptosomal or cleared lysate proteins was loaded per lane for Western blot analysis. Proteins were run on Bis-Tris gradient acrylamide gels and transferred to nitrocellulose membranes . Membranes were incubated in blocking solution (50 mM Tris pH7.5, 300 mM NaCl, 3% w/v dry milk powder, and 0.05% tween-20) for 10 minutes, primary antibody overnight at 4˚C, washed, incubated in HRP-conjugated secondary antibodies for 1 hour at room temperature, and detected using the BioRad Clarity ECL kit on a BioRad ChemiDoc XRS+ imaging system. Hippocampal lysates were prepared by homogenizing 100 mg of hippocampal tissue in 1 ml of reducing sample buffer.

Immunostaining

Cultured cells were fixed in 4% PFA for 10 minutes, washed with PBS, and incubated in blocking solution (PBS with 3% bovine albumin and 0.1% Triton-X100) for 30 minutes. Cells were incubated in primary antibodies (diluted in blocking solution) for 1-2 hours. After 3 washes, secondary antibody was added for 45 minutes, washed, and cells were mounted for imaging using Fluoromount-G (Southern Biotech). For tissue sections, mice were transcardially perfused with 4% PFA in PBS. Brains were post-fixed in PFA overnight and 100 μm vibratome sections were cut. Sections were incubated in blocking solution (PBS, 3% BSA, 0.3% triton-x 100) for 2 hours and incubated in primary antibody at 4°C overnight. Secondary antibody incubation was performed at room temperature for 1 hour. Sections were mounted in Fluoromount-G for imaging.

Live-imaging and FRAP

CHO cells transfected with individual GFP or mCherry tagged cadherins were trypsinized, mixed, and plated on coverslips 48 hours before imaging. 15 minutes prior to imaging, cells were equilibrated with live imaging buffer containing 137 mM NaCl, 5 mM KCl, 1mM $MgCl_2$, 20 mM glucose, 10mM HEPES pH 7.4, and supplemented with 2 mM or 0.5 mM $CaCl_2$. A single z-plane covering the maximum dimension of cadherin-mediated cellular junctions was used for imaging. Cells were imaged in a 37°C incubator chamber with live imaging buffer continuously perfused. Images were acquired every 15 seconds for 75 seconds followed by single photobleaching pulse (comprising laser power of 100% and 12.61 μs pixel dwell) followed again by imaging every 15 seconds for 1500 seconds. Imaging was carried out in a Zeiss LSM 710 confocal microscope. For

analyzing the recovery kinetics of cadherins in transcellular junctions, post-bleach fluorescence of the bleached region was measured as a function of time and the data were fit to the exponential recovery curve $I(t)=I_{\infty}-(I_{\infty}-I_0)e^{-t/\tau}$. Here, I(t), I_{∞}, and I_0 denotes the instantaneous fluorescence, saturation fluorescence, and immediate post-bleach fluorescence, respectively. τ represents the recovery time constants reported in Figures 3.13F and G and Figure 3.14C.

Data analysis and statistics

Whenever possible, data were collected and analyzed blind to the genotype of the animals. Sample sizes were chosen based on previous studies or power analysis. All statistical analyses were done using Prism (GraphPad).

Whole cell recordings

17–21- day-old mice were rapidly decapitated and their brains carefully removed and kept in iced, artificial cerebrospinal fluid (aCSF) with sucrose (200 mM Sucrose, 3 mM KCl, 1.4 mM Na_2PO_4, 3mM $MgSO_4$, 26 mM $NaHCO_3$, 10 mM Glucose, and 0.5 mM $CaCl_2$). 300 μm thick transverse slices were cut on a Leica vibratome (Leica VT1200) and left at room temperature in the holding chamber until recording. Cells were visualized by oblique illumination using a bright light source (Olympus BX51WI microscope, Hitachi color CCD camera KP-D20BU). Slices kept in the patching chamber were continuously superfused with aCSF containing 126 mM NaCl, 26 mM $NaHCO_3$, 3 mM KCl, 1.4 mM NaH_2PO_4, 2 mM $CaCl_2$, 1.5 mM $MgSO_4$, and 10 mM D-glucose, bubbled with 95% O_2–5% CO_2. The intracellular pipette solution contained 80 mM

Cesium methylsulfonate, 60 mM CsCl, 10 mM HEPES, 1mM EGTA (adjusted with CsOH), 0.5 mM $CaCl_2$, 10 mM Glucose, and 5 mM QX-314, adjusted to 290–300 mOsm/Lt at pH 7.3. Tetrodotoxin (Ttx) (Tocris Biosciences) was used at working concentration of 0.5 μM, diluted from a 1 mM stock. Somatic whole cell recordings were performed with Axon Multiclamp 700B amplifies (Molecular Devices) in voltage clamp mode at 34 ± 1°C bath temperature for mEPSC experiments. Data acquisition was performed via an Axon Digidata 1550 (Molecular Devices), connected to a Windows 7 computer, running pClamp (Version 10, Molecular Devices). Current signals were sampled at 1 kHz and filtered with a 2 kHz Bessel filter. Patch pipettes with a tip resistance of 6 - 8 MΩ were pulled with a Flaming/Brown micropipette puller P-97 (Sutter Instruments and Co.) using borosilicate glass capillaries with filaments (1B150F-4, World Precision Instruments). All cells patched were held in voltage clamp at -70mV. Acquired traces were analyzed with pClamp (Version 10, Molecular Devices). mEPSC event detection was performed with a template match search.

Field recordings

Adult (3-5 months old) mice were anesthetized with sodium pentobarbital (60 mg/kg, i.p.), and brains rapidly removed and placed in ice-cold (4°C) oxygenated sucrose-based artificial cerebral spinal fluid (aCSF) solution (bubbled with 95% O_2/5% CO_2) containing 200 mM Sucrose, 3 mM KCl, 1.4 mM Na_2HPO_4, 3 mM $MgSO_4$, 26 mM $NaHCO_3$, 10 mM glucose, and 0.5 mM $CaCl_2$. Subsequently, the brain was sectioned horizontally into 350 μm thick sections using a vibratome. Slices were then incubated (for 2 hours) in a chamber containing oxygenated aCSF containing 126 mM NaCl, 3 mM KCl, 1.4 mM

Na_2HPO_4, 1 mM $MgSO_4$, 26 mM $NaHCO_3$, 10 mM glucose, and 2.5 mM $CaCl_2$. The pH (7.30–7.40) and osmolarity (290–300) mOsm of the ACSF were verified prior to each experiment. Extracellular field excitatory postsynaptic potentials (fEPSPs) were recorded using a Slicemaster high-throughput brain slice recording system (Scientifica). Slices were continuously perfused with oxygenated aCSF (2.5 ml/minute). Recordings were performed at 30–31°C. Concentric bipolar stimulating electrodes (MCE-100; Rhodes Medical Instrument) were placed in either the stratum oriens or stratum radiatum of the CA2-CA1 junction region. Recording microelectrodes (2-3 MΩ resistance) were filled with aCSF and placed within 250–500 μm of the stimulating electrodes. Data were acquired using pClamp 10 interfaced to a Digidata 1440A data acquisition board at a sampling rate of 10 kHz, low-pass filtered at 1 kHz, and high-pass filtered at 3 Hz. 100 μs stimuli ranging from 1 to 40 V were used to evoke fEPSPs. Input-output curves were generated and the stimulation strength was set so that the fEPSP amplitude was half that of the smallest fEPSP accompanied by a population spike. Slices were then stimulated every 30 sec for a 30-minute baseline period. LTP was induced using theta burst stimulation (TBS, five trains of four pulses at 100 Hz separated by 200 msec and repeated once with a 20 sec interval). Low frequency stimulation was resumed for 60 minutes post TBS at which point LTP was quantified relative to baseline. fEPSP slope was calculated from 25%-85% of the rising phase of the fEPSP

Figure 3.1: CA1 excitatory synapses have layer-specific properties.

(A) Schematic of excitatory inputs to CA1 neurons. **(B)** Representative ultrastructural images of asymmetric synapses in each CA1 layer. **(C)** Quantification of ultrastructural analysis. Average SV density per bouton area, docked SV density per active zone length, proximal SV density per active zone length, bouton area, PSD width, and synaptic cleft width. All values are normalized to mean SR values. Sample sizes: 181 (SR), 149 (SO), and 134 (SLM) synapses evenly sampled from 3 mice aged P23. **(D)** Representative confocal images of Lucifer Yellow filled CA1 dendrites (top) and corresponding 3D models (bottom). **(E and F)** Average spine density **(E)** and spine length **(F)** of indicated spine classes. All values are normalized to mean SR values. Sample sizes: 61 (SO), 62 (SR), and 51 (SLM) dendrites from 6 wildtype mice aged P21-P23. Statistical differences between SO, SR, and SLM for EM and spine analyses were calculated using one-way ANOVA followed by pairwise p-value calculation using Holm-Šidák multiple comparison test. **(G and H)** Representative LTP traces from CA1 SO **(G)** and CA1 SR **(H)** layer. **(I)** Mean LTP time course induced in CA1 SO (brown) and SR (green) layers. Arrow indicates TBS. **(J)** Mean LTP amplitudes defined as average percentage of fEPSP slope during 58.5-60 minutes after TBS in SO and SR layers. Sample sizes: 24 (SO) and 23 (SR) slices from 10 wildtype mice aged 3-5 months. p-values for LTP quantification were calculated using t-test. $p<0.05$, $p<0.01$, $p<0.001$, and $p<0.0001$ is denoted by *, **, ***, and **** respectively, otherwise $p>0.05$. All data shown as mean ± s.e.m.

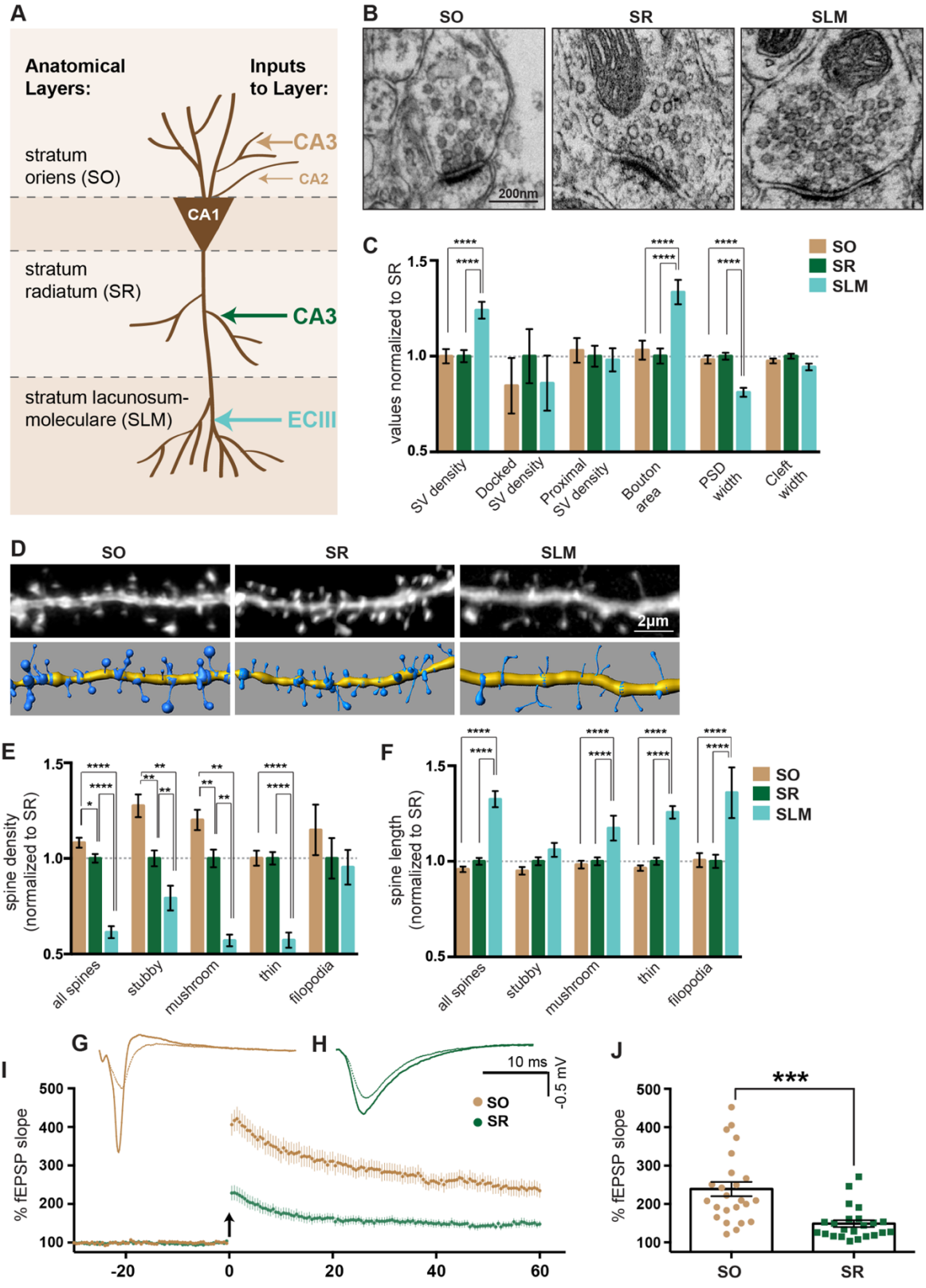
A
Anatomical Layers:
Inputs to Layer:
stratum oriens (SO)
stratum radiatum (SR)
stratum lacunosum-moleculare (SLM)
CA3
CA2
CA1
CA3
ECIII
B
SO
SR
SLM
200nm
C
values normalized to SR
SO
SR
SLM
SV density
Docked SV density
Proximal SV density
Bouton area
PSD width
Cleft width
D
SO
SR
SLM
2µm
E
spine density (normalized to SR)
all spines
stubby
mushroom
thin
filopodia
F
spine length (normalized to SR)
G
H
10 ms
-0.5 mV
I
% fEPSP slope
J
% fEPSP slope
***
SO
SR

Figure 3.2: CA1 excitatory synapses have differences in spine properties.

(A) Schematic of EM analysis parameters. **(B-E)** CA1 spine density and length analyses for each layer as indicated. These graphs show absolute values for the same data that are normalized to SR in main figures 1E and 1F. Sample sizes: 61 (SO), 62 (SR), and 51 (SLM) dendrites from 6 wildtype animals aged P21-P23. Significant differences between SO, SR, and SLM parameters were calculated using one-way ANOVA followed by pair wise p-value calculation using Holm-Šidák multiple comparison test. $p<0.05$, $p<0.01$, $p<0.001$, and $p<0.0001$ is denoted by *, **, ***, and **** respectively, otherwise $p>0.05$. All data shown as mean ± s.e.m.

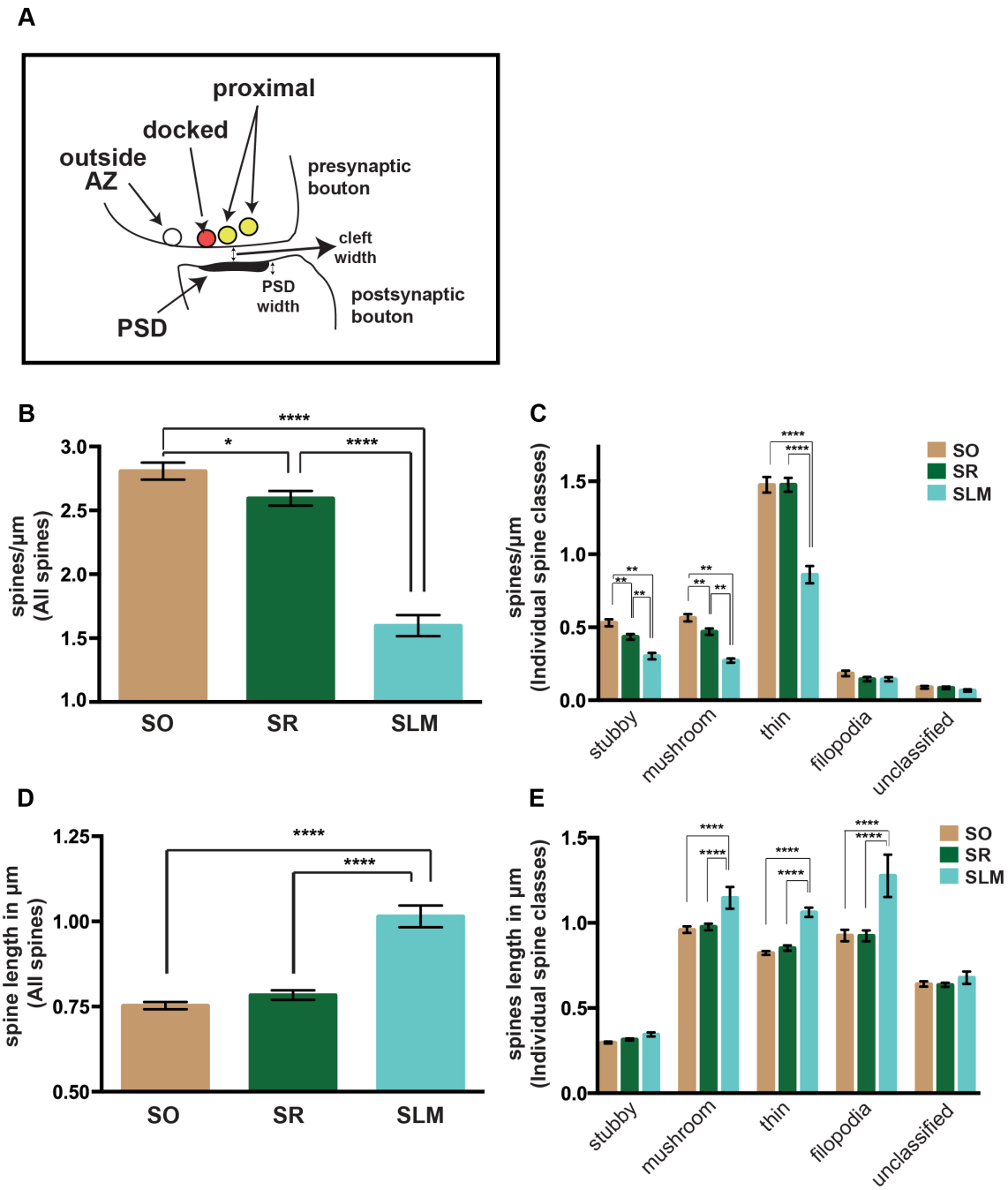
A
proximal
docked
outside AZ
presynaptic bouton
cleft width
PSD width
postsynaptic bouton
PSD
B
spines/µm (All spines)
SO
SR
SLM
C
spines/µm (Individual spine classes)
SO
SR
SLM
stubby
mushroom
thin
filopodia
unclassified
D
spine length in µm (All spines)
SO
SR
SLM
E
spines length in µm (Individual spine classes)
SO
SR
SLM
stubby
mushroom
thin
filopodia
unclassified

Figure 3.3: Cadherin-9 selectively regulates mushroom spines in the CA1 SO layer.

(A) In situ hybridization shows cadherin-9 mRNA is expressed in DG and CA3 neurons with little to no expression in CA1 neurons. **(B)** Immunostaining of a P14 CA3 axon in utero electroporated with cdh9-smFP^{FLAG} and smFP^{MYC} at embryonic age 14.5 days. smFP^{MYC} was used to fill the axon. **(C,E,G)** Representative images of SO **(C)**, SR **(E)**, and SLM **(G)** dendrites analyzed in Cdh9$^{+/+}$ and Cdh9$^{-/-}$ mice (top) and corresponding 3D model (bottom). **(D,F,H)** Quantification of average spine density and indicated spine classes. All data are normalized to wildtype. Absolute values are shown in Figure 3.4. Sample sizes: SO= 28 Cdh9$^{+/+}$ and 25 Cdh9$^{-/-}$ dendrites, SR= 33 Cdh9$^{+/+}$ and 31 Cdh9$^{-/-}$ dendrites, SLM= 15 Cdh9$^{+/+}$ and 18 Cdh9$^{-/-}$ dendrites. All conditions evenly sampled from 3 mice aged P21-P23 and all analyses were done blind to genotype. p-values calculated using students t-test and $p<0.05$ is represented by *, otherwise $p>0.05$.

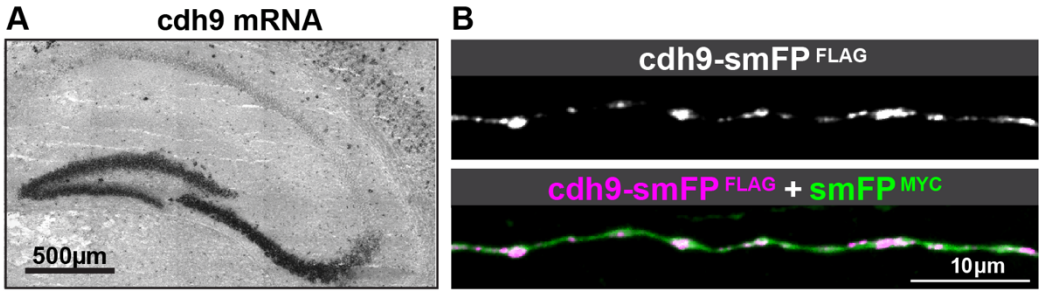
A
cdh9 mRNA
500µm
B
cdh9-smFP FLAG
cdh9-smFP FLAG + smFP MYC
10µm

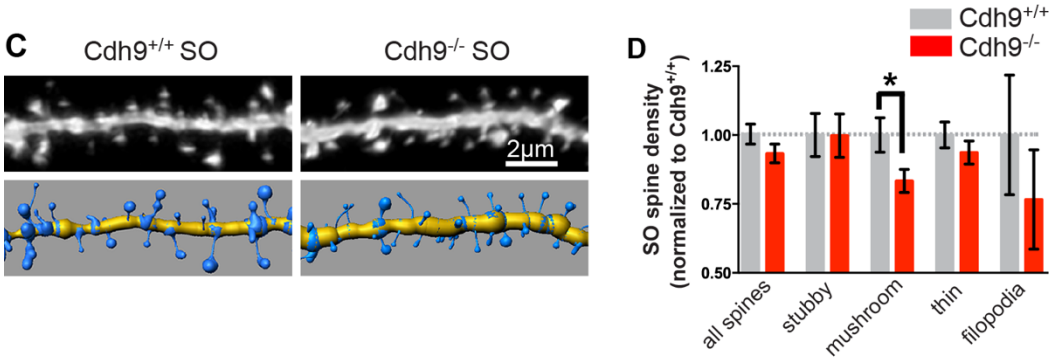
C
Cdh9+/+ SO
Cdh9-/- SO
2µm
D
Cdh9+/+
Cdh9-/-
SO spine density (normalized to Cdh9+/+)
1.25
1.00
0.75
0.50
*
all spines
stubby
mushroom
thin
filopodia

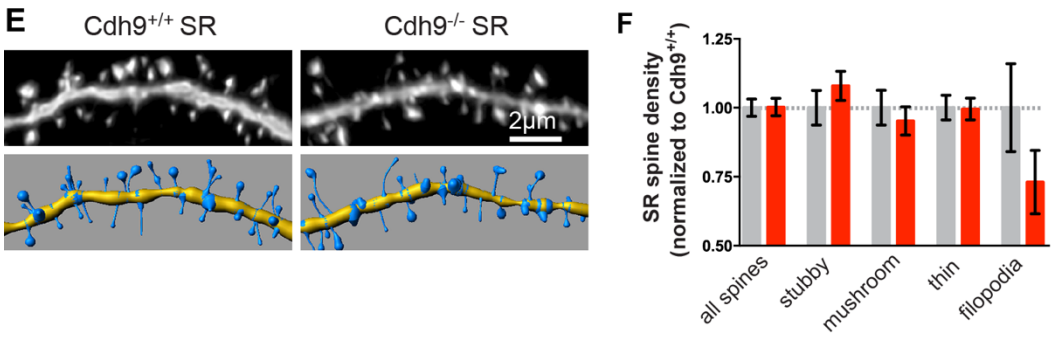
E
Cdh9+/+ SR
Cdh9-/- SR
2µm
F
SR spine density (normalized to Cdh9+/+)
1.25
1.00
0.75
0.50
all spines
stubby
mushroom
thin
filopodia

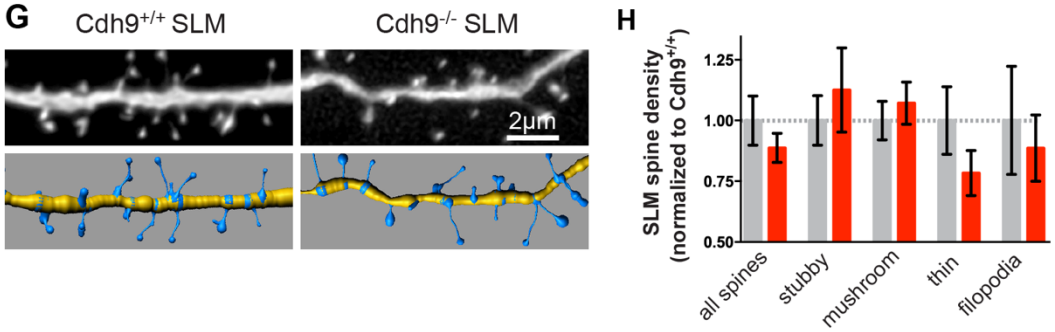
G
Cdh9+/+ SLM
Cdh9-/- SLM
2µm
H
SLM spine density (normalized to Cdh9+/+)
1.25
1.00
0.75
0.50
all spines
stubby
mushroom
thin
filopodia

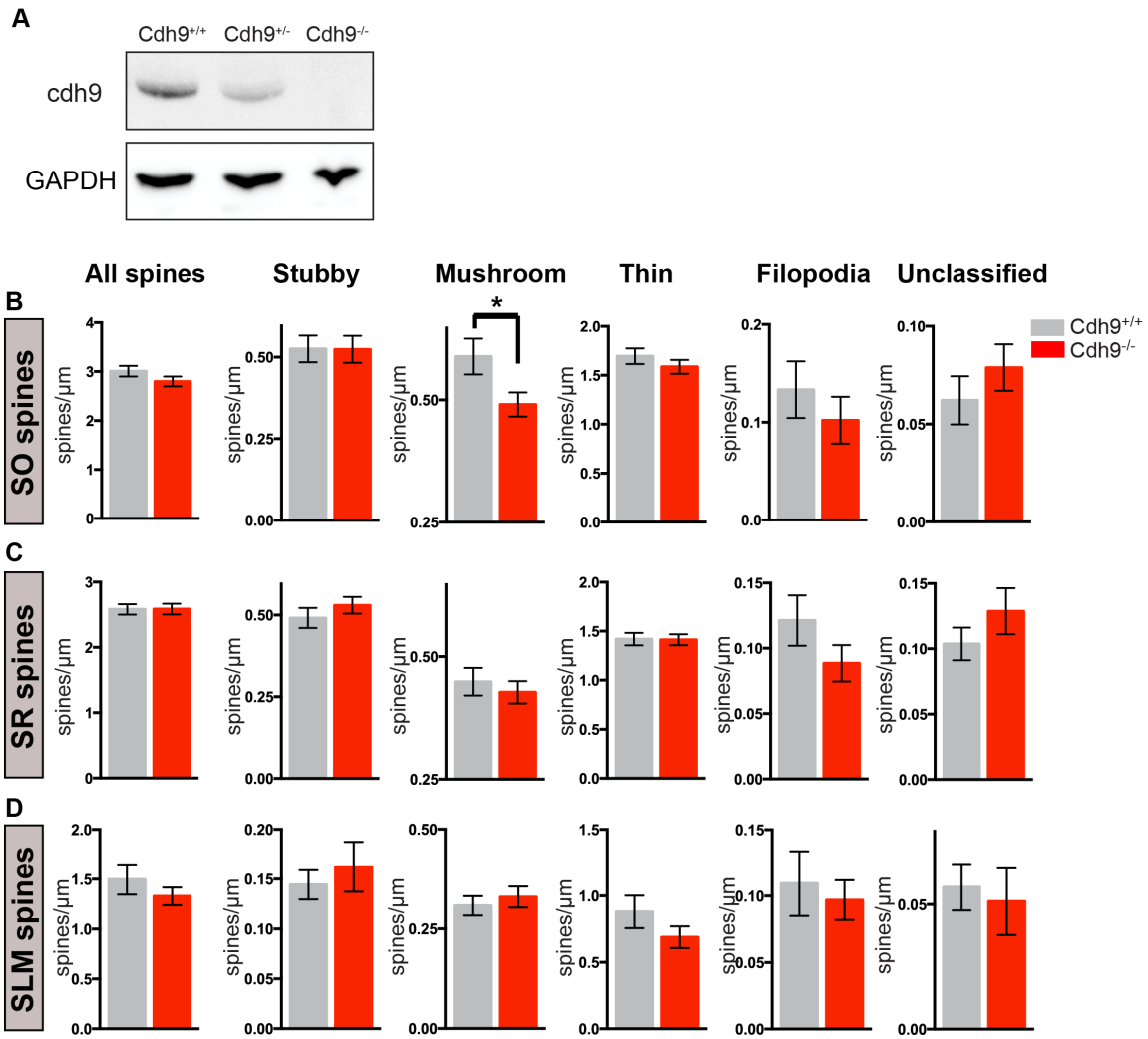

Figure 3.4: Absence of cadherin-9 reduces mushroom spine density specifically in CA1 SO layer.

(A) Western blot of cadherin-9 from hippocampal lysates from $Cdh9^{+/+}$, $Cdh9^{+/-}$, and $Cdh9^{-/-}$ mice. GAPDH is shown as a loading control. **(B-D)** Quantification of average spine density of overall spines and individual spine classes in CA1 SO **(B)**, SR **(C)**, and SLM **(D)** layers from $Cdh9^{+/+}$ and $Cdh9^{-/-}$ animals. These graphs show absolute values for the same data that are normalized to $Cdh9^{+/+}$ in main figures 2D, 2F, and 2H. Sample sizes: SO= 28 $Cdh9^{+/+}$ and 25 $Cdh9^{-/-}$ dendrites, SR= 33 $Cdh9^{+/+}$ and 31 $Cdh9^{-/-}$ dendrites, and SLM= 15 $Cdh9^{+/+}$ and 18 $Cdh9^{-/-}$ dendrites. All conditions were evenly sampled from 3 mice aged P21-P23 and all analyses were blind to genotype. p-values calculated using students t-test and $p<0.05$ is represented by *, otherwise $p>0.05$. All data shown as mean ± s.e.m.

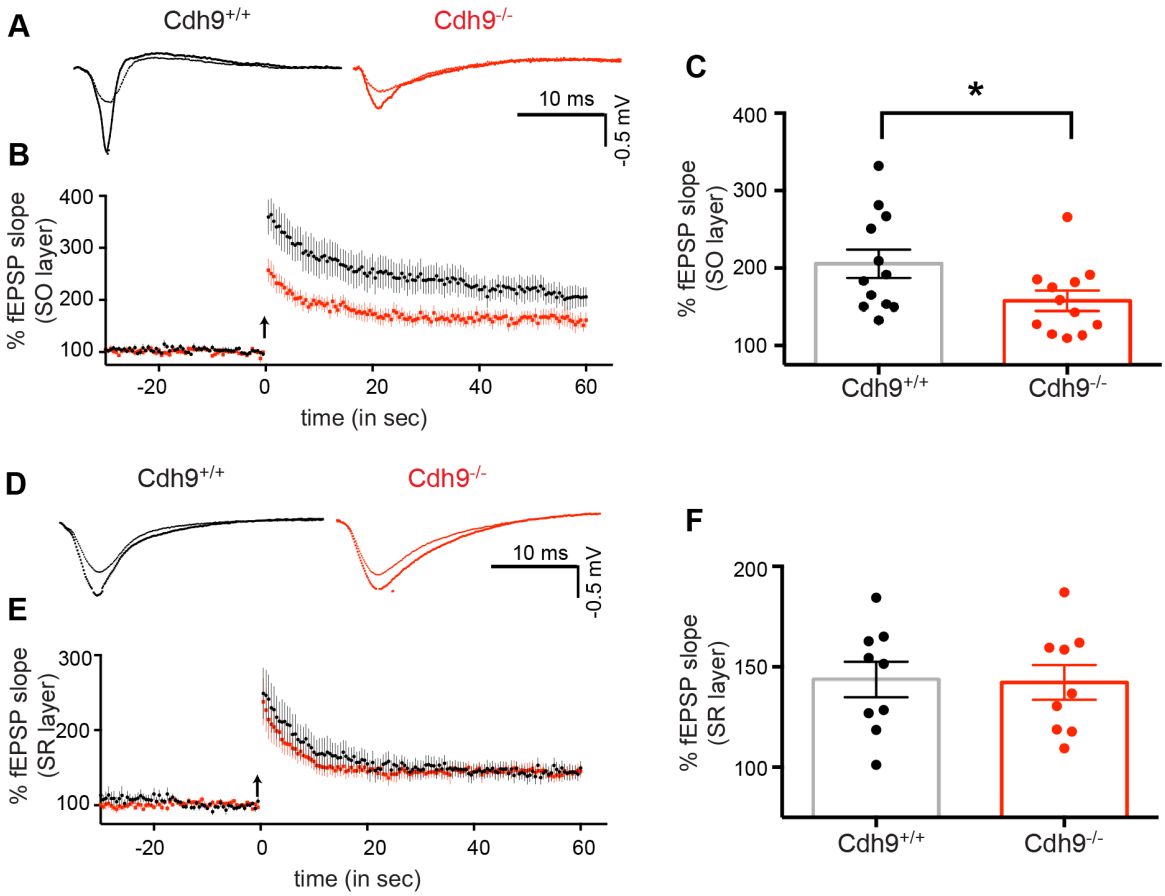

Figure 3.5: Cadherin-9 regulates synaptic potentiation in CA1 SO.

(A) Representative traces of LTP induced in CA1 SO of $Cdh9^{+/+}$ and $Cdh9^{-/-}$ hippocampal slices. **(B-C)** mean LTP time course **(B)** and amplitudes **(C)** recorded in CA1 SO layer of $Cdh9^{+/+}$ and $Cdh9^{-/-}$ hippocampal slices. **(D-F)** Same as Figures 3.5A-C except data from SR layer are shown. Sample sizes: SO= 12 $Cdh9^{+/+}$ and 12 $Cdh9^{-/-}$ slices, and SR= 10 $Cdh9^{+/+}$ and 10 $Cdh9^{-/-}$ slices. Data collected from 4 animals per genotype aged 3-5 months. p-values calculated using students t-test. $p<0.05$ is represented by *, otherwise $p>0.05$. All data shown as mean ± s.e.m.

Figure 3.6: Basal synaptic transmission is normal in $Cdh9^{-/-}$ mice.

(A) Side-by-side comparison of mean LTP amplitudes recorded from CA1 SO and SR layers from $Cdh9^{+/+}$ and $Cdh9^{-/-}$ hippocampal slices as shown in Figure 3.5. Dotted line represents the mean SR LTP amplitude from $Cdh9^{+/+}$ hippocampal slices. **(B,C)** Input-output (I/O) curves representing fEPSP slope versus the corresponding fiber volley amplitude for SO **(B)** and SR **(C)** in $Cdh9^{+/+}$ and $Cdh9^{-/-}$ hippocampal slices. Sample sizes: SO= 12 $Cdh9^{+/+}$ and 12 $Cdh9^{-/-}$ slices, and SR= 10 $Cdh9^{+/+}$ and 10 $Cdh9^{-/-}$ slices. Data collected from 4 animals per genotype aged 3-5 months. p-values calculated using Holm-Šidák multiple comparison test. $p<0.05$ is represented by *, otherwise $p>0.05$. All data shown as mean ± s.e.m. **(D)** Representative traces of mini EPSCs (mEPSCs) from $Cdh9^{+/+}$ and $Cdh9^{-/-}$ CA1 neurons. **(E,F)** Average mEPSC frequency **(E)** and amplitude **(F)** in $Cdh9^{+/+}$ and $Cdh9^{-/-}$ CA1 neurons. For each genotype n=15 cells from 3 animals aged P17-21. Student's t-test indicates no significant differences. All data shown as mean ± s.e.m.

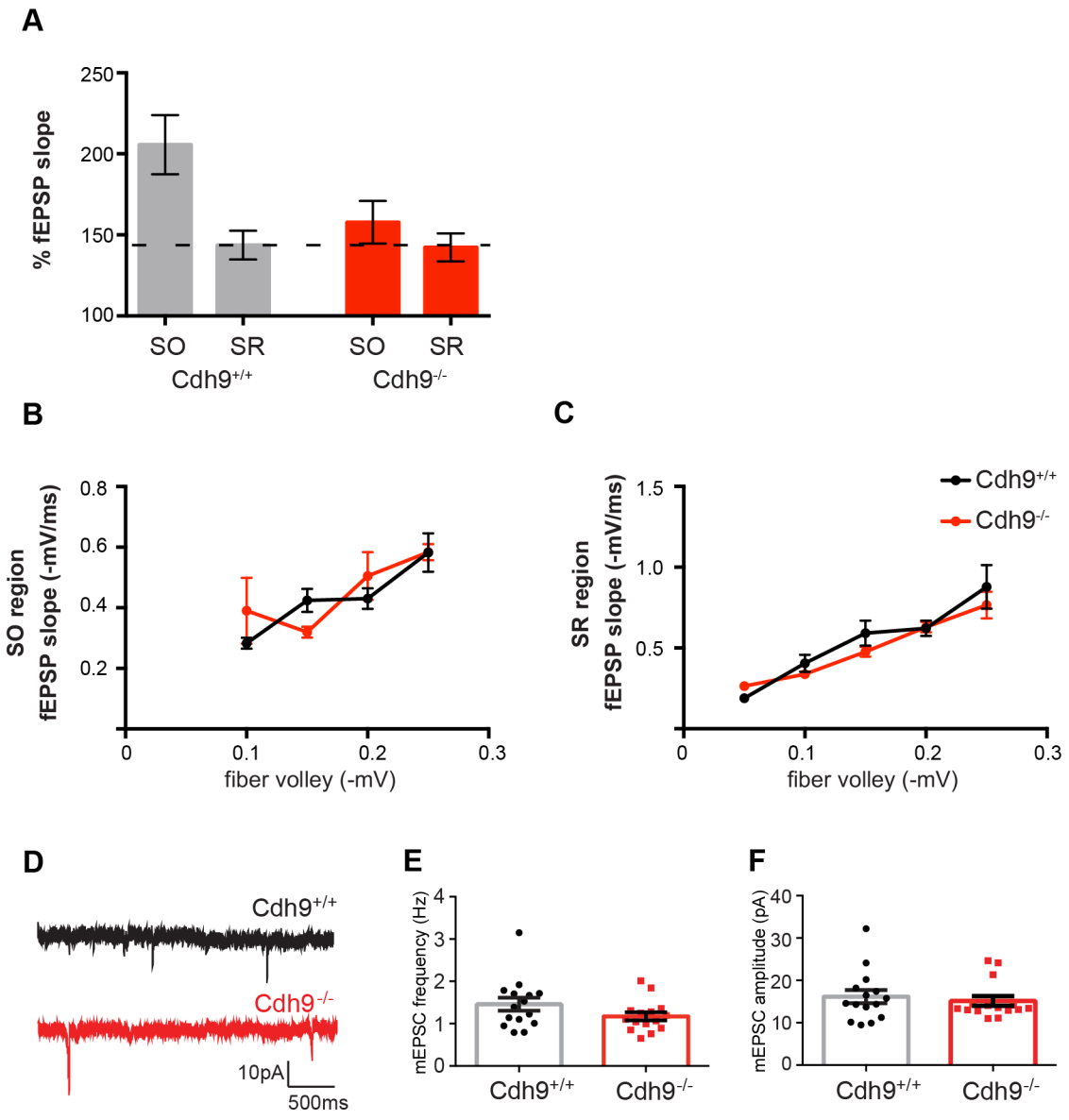
A
% fEPSP slope
250
200
150
100
SO
SR
SO
SR
Cdh9+/+
Cdh9-/-
B
SO region
fEPSP slope (-mV/ms)
0.8
0.6
0.4
0.2
0
0.1
0.2
0.3
fiber volley (-mV)
C
SR region
fEPSP slope (-mV/ms)
1.5
1.0
0.5
0
0.1
0.2
0.3
fiber volley (-mV)
Cdh9+/+
Cdh9-/-
D
Cdh9+/+
Cdh9-/-
10pA
500ms
E
mEPSC frequency (Hz)
4
3
2
1
0
Cdh9+/+
Cdh9-/-
F
mEPSC amplitude (pA)
40
30
20
10
0
Cdh9+/+
Cdh9-/-

Figure 3.7: Cadherin-9 mediates trans-cellular adhesion via cadherins-6 and 10.

(A) In situ hybridizations of hippocampal cadherins. **(B)** Immunostaining against YFP (green) and CA2 marker RGS14 (red) in hippocampus from Cdh10-CreER$^{+/-}$;Ai3$^{+/-}$ mice injected with tamoxifen. Hoechst (blue) labels all cell nuclei. **(C)** Representative images of CHO cell aggregation assays in presence of 4 mM calcium (top) and with the addition of 2 mM EDTA (bottom). The left panel shows no cell aggregation when control GFP cells (green) are mixed with mCherry cells (magenta). The middle panel shows mixed red/green aggregates when cadherin-9 cells (green) are mixed with cadherin-10 cells (magenta) indicating heterophilic trans-cellular interactions. The right panel shows separate red and green aggregates when cadherin-6 cells (green) are mixed with cadherin-2 cells (magenta) indicating only homophilic trans-cellular interactions. All interactions are abolished in the presence of EDTA. **(D)** Summary of all interactions tested. A check mark indicates binding and an X indicates no binding. For space, cadherin is abbreviated "C" (a convention also used in Figure 3.7E). **(E)** Quantification of aggregation index (see Supplemental Experimental Procedures) of pair-wise combinations of hippocampal cadherins. **(F)** CHO cells expressing cdh9-smFP^{FLAG} (green) were mixed with cells co-expressing cdh6-smFP^{HA} (red) and cdh10-smFP^{MYC} (blue). Note that cadherins-6, 9, and 10 co-cluster at the interaction interfaces (white arrows in the merged image). **(G)** Immunoblots show cadherins- 9 and 10 are enriched in hippocampal synaptosomes over time from P7, P14, and P21 mice. Samples were also probed for cadherins-2 and 8, a presynaptic marker synaptoporin (SPO), the postsynaptic markers PSD95 and GluA1, and a non-neuronal marker GFAP. **(H)** Quantification of synaptic enrichment of each indicated cadherin relative to their levels in lysate at each time point. **(I)** Quantification of cadherin levels in synaptosomes over time. Each protein is normalized to its level in synaptosomes at P7. For **H** and **I**, 3 independent experiments were done for each age with hippocampi from 3-4 animals pooled per experiment.

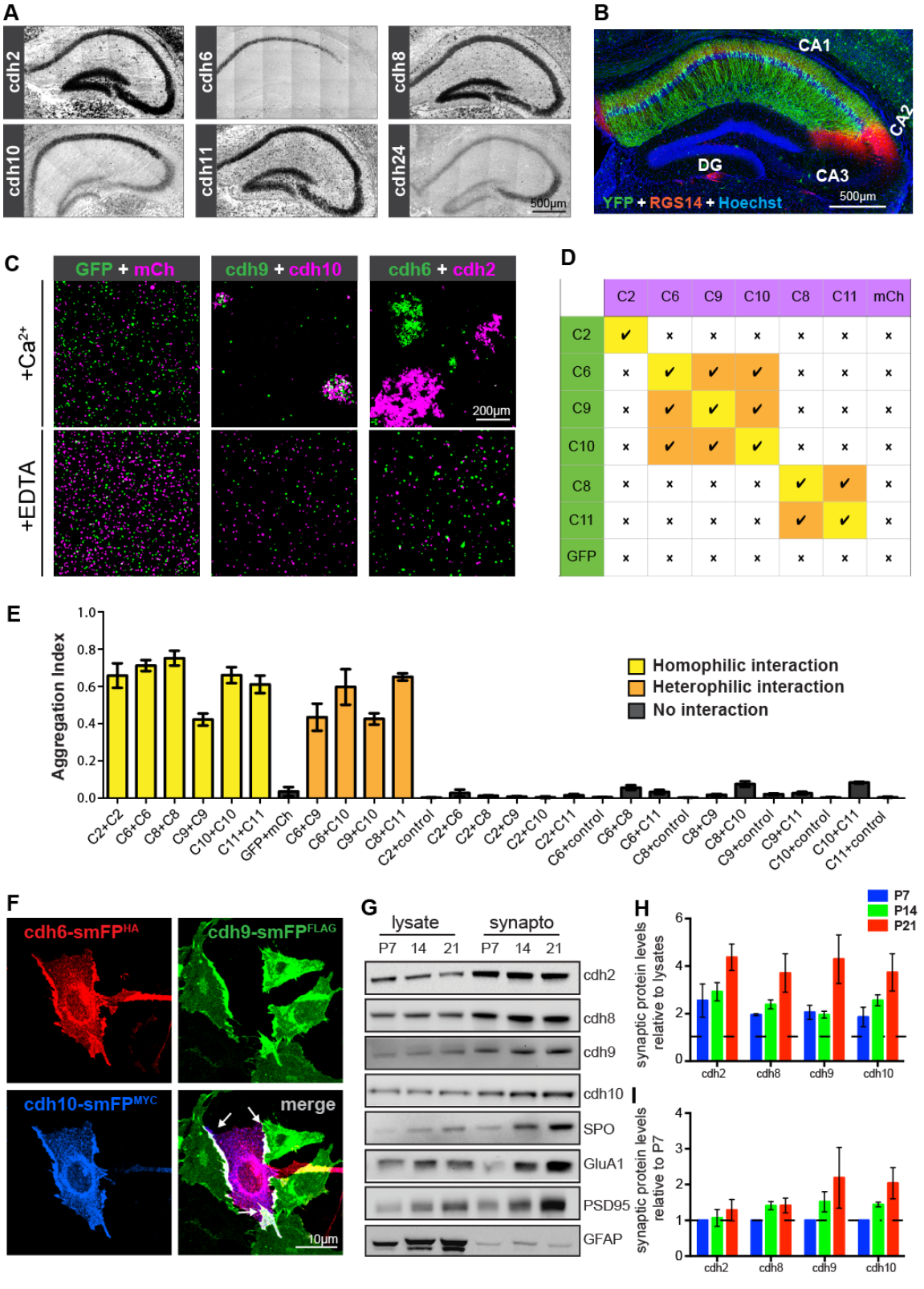
A
cdh2
cdh6
cdh8
cdh10
cdh11
cdh24
500μm
B
CA1
CA2
DG
CA3
YFP + RGS14 + Hoechst
500μm
C
GFP + mCh
cdh9 + cdh10
cdh6 + cdh2
+Ca2+
+EDTA
200μm
D
C2 C6 C9 C10 C8 C11 mCh
C2 ✔ × × × × × ×
C6 × ✔ ✔ ✔ × × ×
C9 × ✔ ✔ ✔ × × ×
C10 × ✔ ✔ ✔ × × ×
C8 × × × × ✔ ✔ ×
C11 × × × × ✔ ✔ ×
GFP × × × × × × ×
E
Aggregation Index
1.0
0.8
0.6
0.4
0.2
0.0
Homophilic interaction
Heterophilic interaction
No interaction
C2+C2
C6+C6
C8+C8
C9+C9
C10+C10
C11+C11
GFP+mCh
C6+C9
C6+C10
C9+C10
C8+C11
C2+control
C2+C6
C2+C8
C2+C9
C2+C10
C2+C11
C6+control
C6+C8
C6+C11
C8+control
C8+C9
C8+C10
C9+control
C9+C11
C10+control
C10+C11
C11+control
F
cdh6-smFPHA
cdh9-smFPFLAG
cdh10-smFPMYC
merge
10μm
G
lysate
synapto
P7 14 21 P7 14 21
cdh2
cdh8
cdh9
cdh10
SPO
GluA1
PSD95
GFAP
H
P7
P14
P21
synaptic protein levels relative to lysates
6
4
2
0
cdh2
cdh8
cdh9
cdh10
I
synaptic protein levels relative to P7
4
3
2
1
0
cdh2
cdh8
cdh9
cdh10

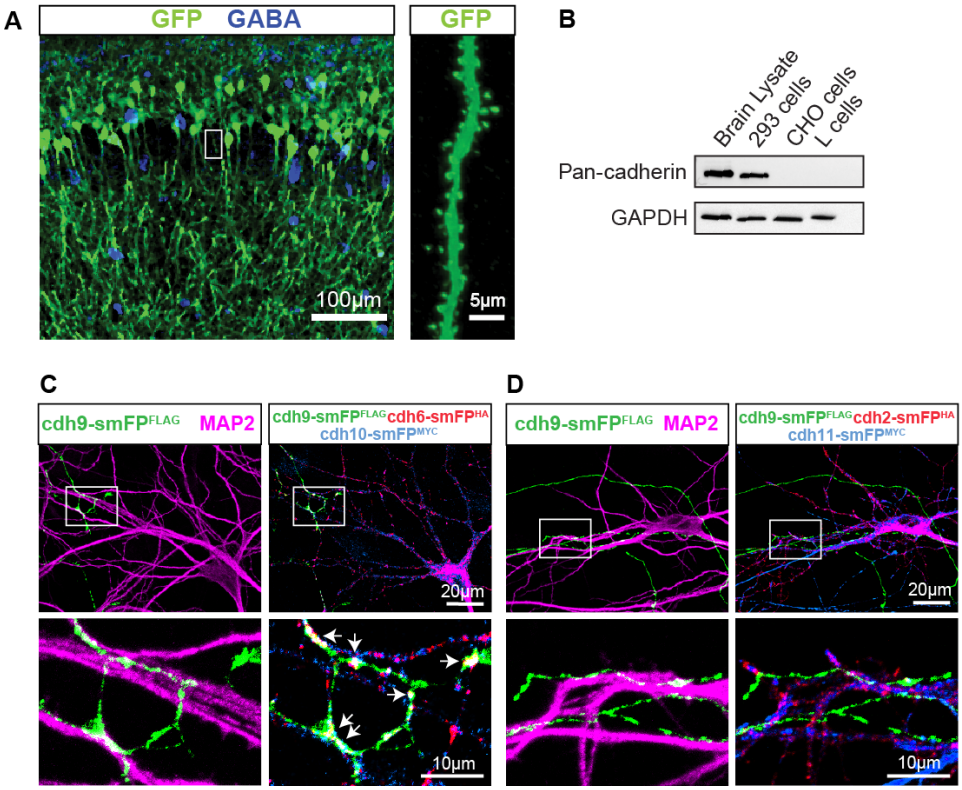

Figure 3.8: Cadherin-9 co-clusters in trans with cadherins-6 and 10 but not other cadherins in neurons.

(A) Immunostaining of CA1 region from Cdh10-CreER$^{+/-}$;Ai3$^{+/-}$ mice (as in Figure 3.7B) with anti-YFP (green) and anti-GABA (blue) antibodies indicates cadherin-10 is expressed by CA1 pyramidal neurons and not GABAergic neurons. The boxed region is magnified on right to show cadherin-10 expressing neurons have spines. **(B)** Immunoblot showing the absence of cadherin expression in CHO cells. GAPDH served as the loading control. **(C)** Cultured neurons expressing cdh9-smFP^{FLAG} (green) were plated with neurons co-expressing cdh6-smFP^{HA} (red) and cdh10-smFP^{MYC} (blue). Shown is a cdh9-smFP^{FLAG} expressing axon contacting cdh6-smFP^{HA} and cdh10-smFP^{MYC} expressing dendrites labeled by MAP2 (magenta). All three cadherins co-localize (white pixels in bottom right panel) at axon-dendrite contact points as indicated by arrows. **(D)** Similar to Figure S4C but neurons expressing cdh9-smFP^{FLAG} were plated with neurons co-expressing cdh2-smFP^{HA} and cdh11-smFP^{MYC}. Note that although the cdh9-smFP^{FLAG} expressing axon contacts the cdh2-smFP^{HA} and cdh11-smFP^{MYC} expressing dendrite, little to no triple co-localization among the cadherins is observed.

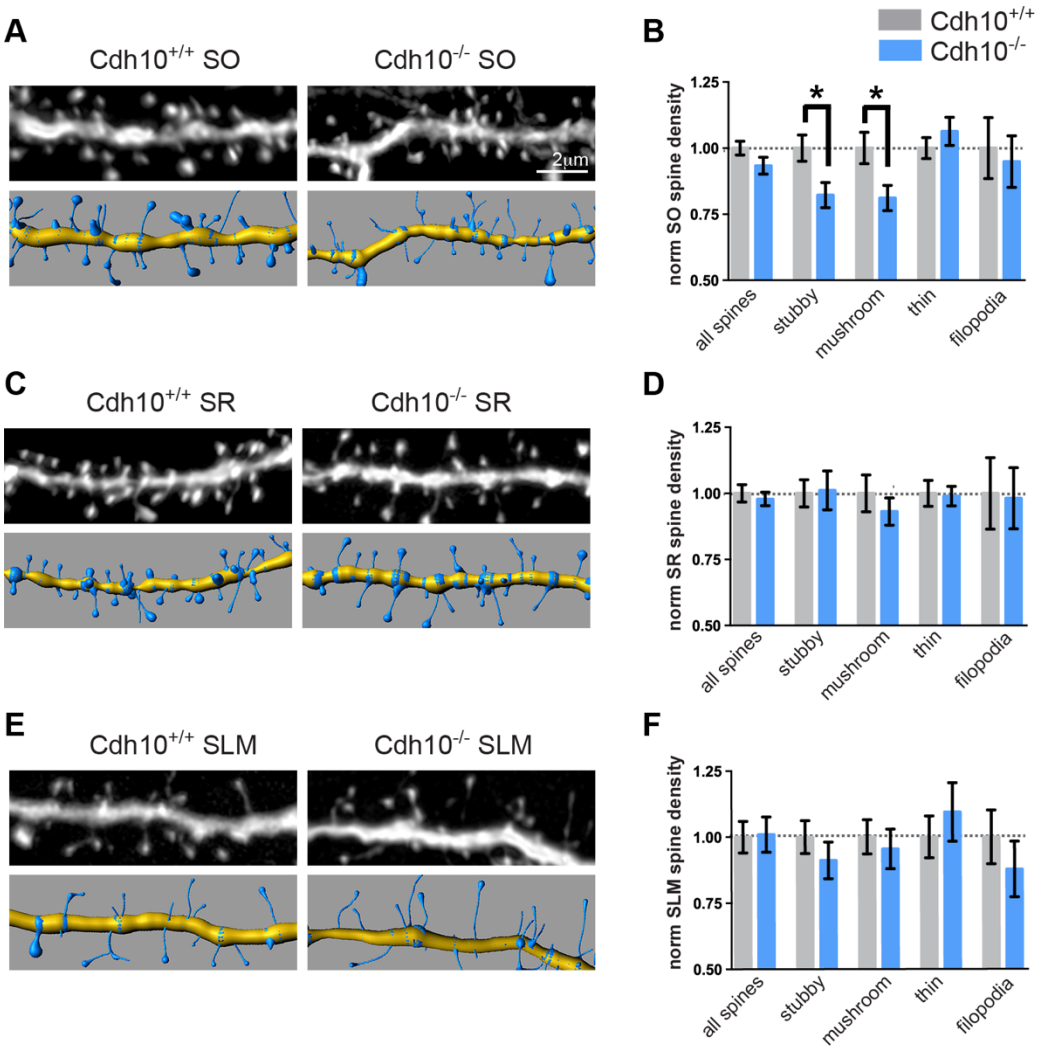

Figure 3.9: Cadherin-10 regulates mushroom spine formation in CA1 SO.

(A,C,E) Representative images of SO **(A)**, SR **(C)**, and SLM **(E)** dendrites analyzed in $Cdh10^{+/+}$ and $Cdh10^{-/-}$ mice (top), and their 3D models (bottom). **(B,D,F)** Quantification of average spine density of indicated spine classes. All measurements are normalized to mean $Cdh10^{+/+}$ values. Sample sizes: SO= 32 $Cdh10^{+/+}$ and 31 $Cdh10^{-/-}$ dendrites, SR= 27 $Cdh10^{+/+}$ and 30 $Cdh10^{-/-}$ dendrites, SLM= 35 $Cdh10^{+/+}$ and 18 $Cdh10^{-/-}$ dendrites. All conditions were evenly sampled from 3 mice aged P21-P23 and all analyses was done blind to genotype. p-values were calculated using students t-test. $p<0.05$ is represented by *, otherwise $p>0.05$. All data shown as mean ± s.e.m.

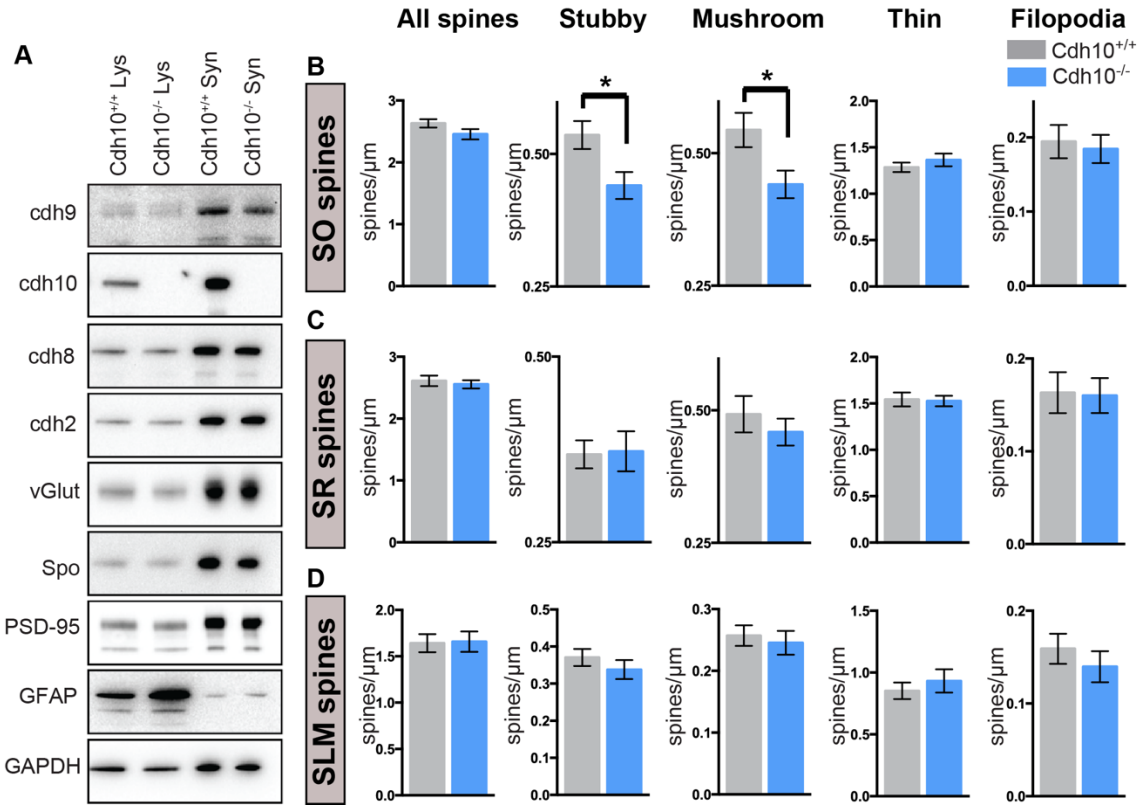

Figure 3.10: Absence of cadherin-10 reduces mushroom spine density specifically in CA1 SO layer.

(A) Immunoblots of hippocampal lysates (Lys) and synaptosomes (Syn) from P21 $Cdh10^{+/+}$ and $Cdh10^{-/-}$ animals. Proteins are as indicated including cadherins, the presynaptic markers vesicular glutamate transporter-1 (vGlut) and synaptoporin (SPO), the postsynaptic marker PSD95, the non-neuronal marker GFAP, and a loading control GAPDH. **(B-D)** Quantification of raw average spine density of overall spines and individual spine classes in CA1 SO **(B)**, SR **(C)**, and SLM **(D)** layers from $Cdh10^{+/+}$ and $Cdh10^{-/-}$ animals. These graphs show absolute values for the same data that are normalized to $Cdh10^{+/+}$ in main Figures 3.9B, 3.9D, and 3.9F. Sample sizes: SO= 32 $Cdh10^{+/+}$ and 31 $Cdh10^{-/-}$ dendrites, SR= 27 $Cdh10^{+/+}$ and 30 $Cdh10^{-/-}$ dendrites, SLM= 35 $Cdh10^{+/+}$ and 18 $Cdh10^{-/-}$ dendrites. All conditions were evenly sampled from 3 independent mice aged P21-P23 and all analyses were blind to genotype. p-values calculated using students t-test. $p<0.05$ is represented by *, otherwise $p>0.05$. All data shown as mean ± s.e.m.

Figure 3.11: Cadherins-6 and 10 regulate LTP in CA1 SO.

(A) Representative traces of LTP induced in CA1 SR of $Cdh10^{+/+}$ (left) and $Cdh10^{-/-}$ (right) hippocampal slices. **(B-C)** mean LTP time course **(B)** and mean LTP amplitudes **(C)** recorded in CA1 SR layer of $Cdh10^{+/+}$ and $Cdh10^{-/-}$ hippocampal slices. Sample sizes: data collected from 11 $Cdh10^{+/+}$ and 13 $Cdh10^{-/-}$ slices from 6 animals per genotype aged 3-5 months. p-values were calculated using students t-test. **(D-F)** Same as in **(A-C)** except recordings performed in CA1 SO layer. Sample sizes: data collected from 12 $Cdh10^{+/+}$ and 11 $Cdh10^{-/-}$ slices from 6 animals per genotype aged 3-5 months. **(G)** Representative traces of LTP induced in CA1 SO of $Cdh6^{+/+}$;$Cdh10^{+/+}$ and $Cdh6^{-/-}$;$Cdh10^{-/-}$ hippocampal slices. **(H-I)** mean LTP time course **(H)** and mean LTP amplitudes **(I)** recorded in CA1 SO layer of $Cdh6^{+/+}$;$Cdh10^{+/+}$ (wildtype) and $Cdh6^{-/-}$;$Cdh10^{-/-}$ mice. Sample sizes: data collected from 12 $Cdh6^{+/+}$;$Cdh10^{+/+}$ and 14 $Cdh6^{-/-}$;$Cdh10^{-/-}$ slices from 4 animals per genotype aged 3-5 months. p-values were calculated using students t-test. All data shown as mean ± s.e.m.

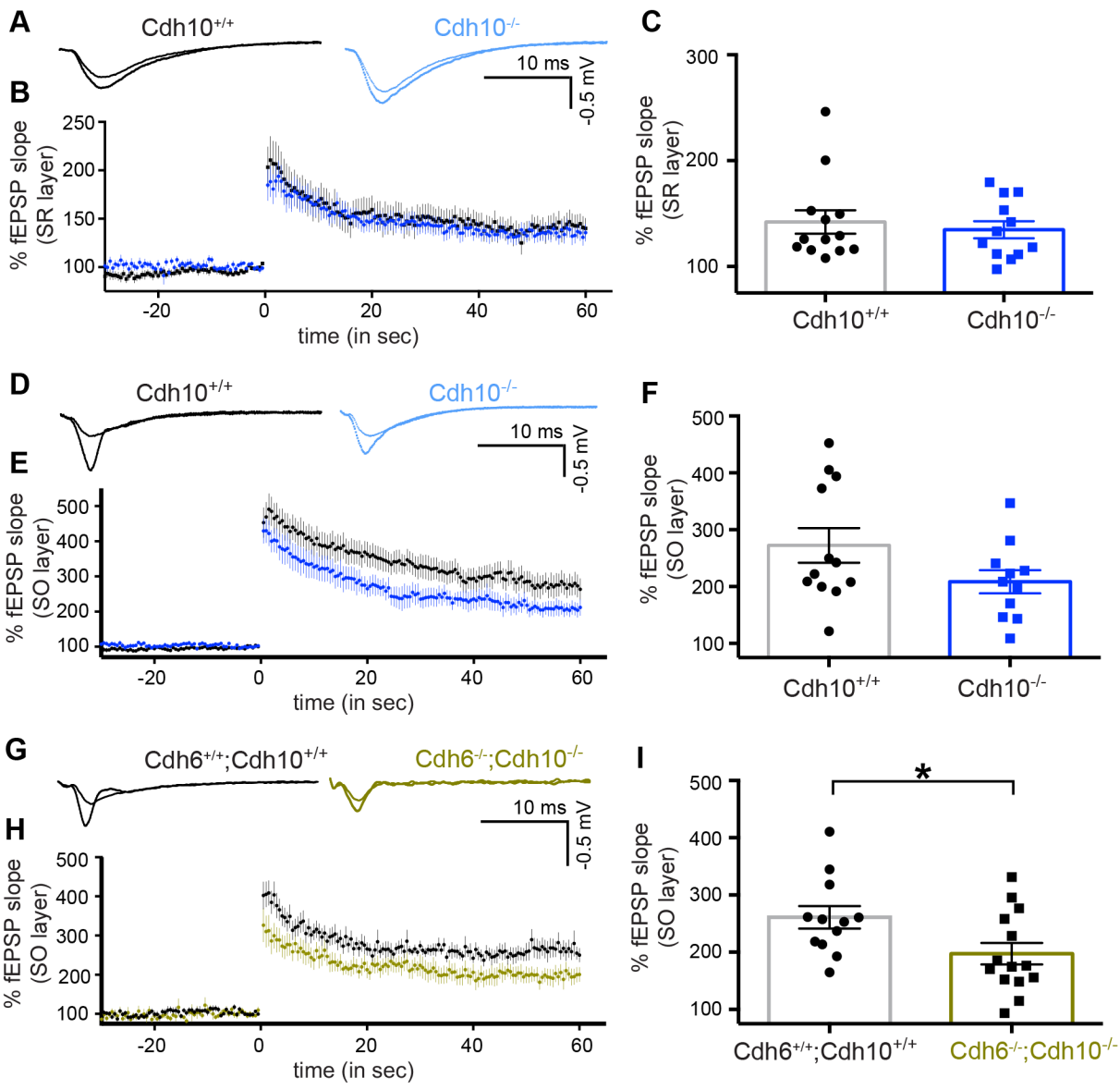
A
Cdh10+/+
Cdh10-/-
10 ms
-0.5 mV
B
% fEPSP slope (SR layer)
250
200
150
100
-20
0
20
40
60
time (in sec)
C
% fEPSP slope (SR layer)
300
200
100
Cdh10+/+
Cdh10-/-
D
Cdh10+/+
Cdh10-/-
10 ms
-0.5 mV
E
% fEPSP slope (SO layer)
500
400
300
200
100
-20
0
20
40
60
time (in sec)
F
% fEPSP slope (SO layer)
500
400
300
200
100
Cdh10+/+
Cdh10-/-
G
Cdh6+/+;Cdh10+/+
Cdh6-/-;Cdh10-/-
10 ms
-0.5 mV
H
% fEPSP slope (SO layer)
500
400
300
200
100
-20
0
20
40
60
time (in sec)
I
*
% fEPSP slope (SO layer)
500
400
300
200
100
Cdh6+/+;Cdh10+/+
Cdh6-/-;Cdh10-/-

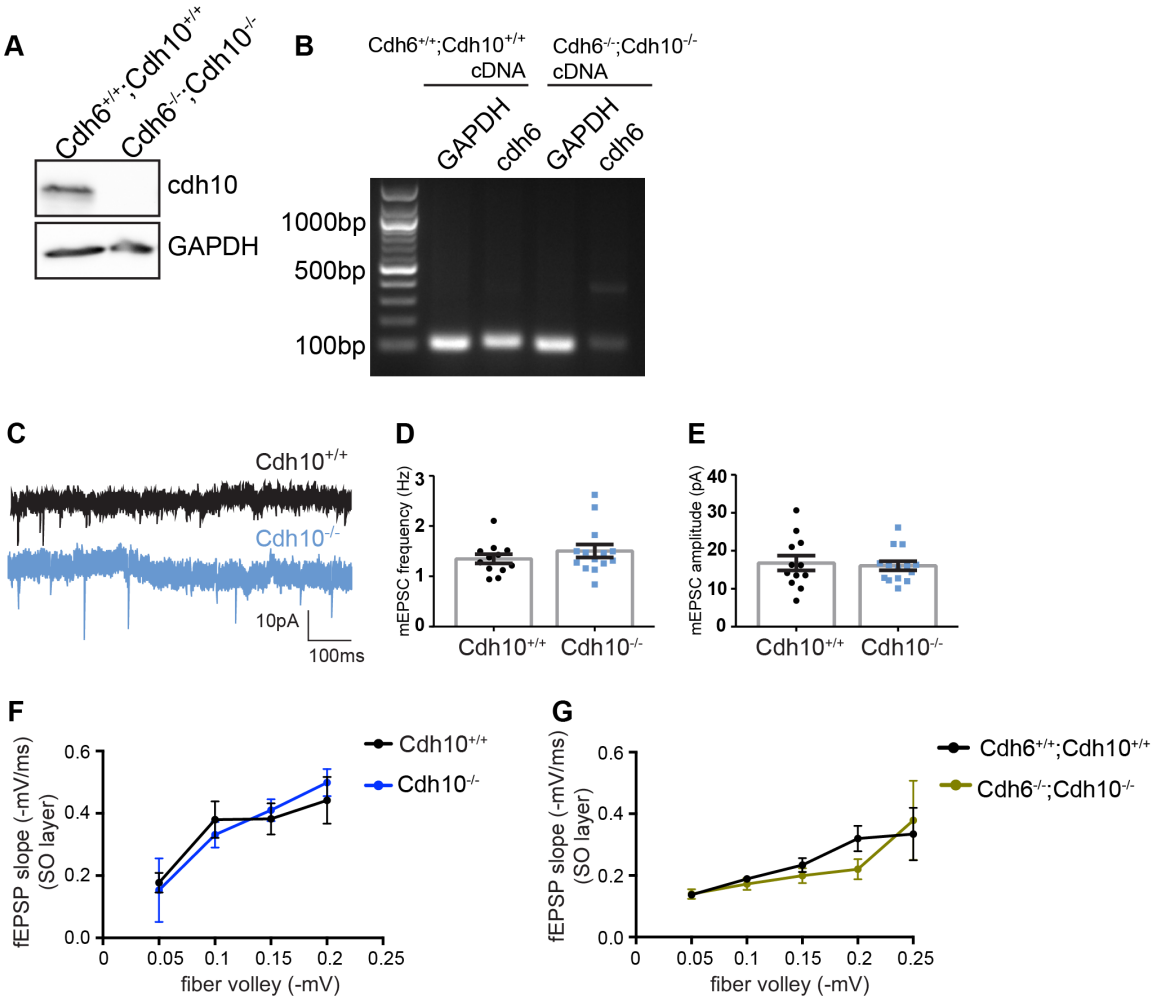

Figure 3.12: Absence of cadherins-6 and 10 does not impair basal transmission in CA1 SO.

(A) Immunoblot showing absence of cadherin-10 expression in hippocampal lysates of Cdh6$^{-/-}$;Cdh10$^{-/-}$ mice. **(B)** Reverse transcription PCR analysis of cDNA obtained from Cdh6$^{+/+}$;Cdh10$^{+/+}$ and Cdh6$^{-/-}$;Cdh10$^{-/-}$ hippocampi showing significant reduction of cadherin-6 transcript levels in double knockout mice. **(C)** Representative traces of mini EPSCs (mEPSCs) from Cdh10$^{+/+}$ and Cdh10$^{-/-}$ CA1 neurons**. (D-E)** Average mEPSC frequency **(D)** and amplitude **(E)** in Cdh10$^{+/+}$ and Cdh10$^{-/-}$ CA1 neurons. Sample sizes: 12 cells from 3 Cdh10$^{+/+}$ mice and 14 cells from 3 Cdh10$^{-/-}$ mice. All animals aged P17-21. **(F-G)** Input-output (I/O) curves representing fEPSP slope versus the corresponding fiber volley amplitude in SO layer of Cdh10$^{+/+}$ and Cdh10$^{-/-}$ slices **(F)** and WT and Cdh6$^{-/-}$;Cdh10$^{-/-}$ slices **(G)**. Sample sizes: 12 Cdh10$^{+/+}$ and 11 Cdh10$^{-/-}$ slices from 6 animals per genotype aged 3-5 months. and 12 Cdh6$^{+/+}$;Cdh10$^{+/+}$ and 14 Cdh6$^{-/-}$;Cdh10$^{-/-}$ slices from 4 animals per genotype aged 3-5 months. p-values calculated using Holm-Šidák multiple comparison test. All data shown as mean ± s.e.m.

Figure 3.13: Ca^{2+} dependence of cadherin-9 heterophilic interactions.

(A) Immunoblots showing expression of cadherins- 9 and 10 in CA1 SO and SR layers. Myelin expression, specifically in the CA1 SO but not SR layer, confirms minimal tissue contamination across layers. PSD95 and GAPDH staining are used as loading controls. **(B-C)** Representative images **(B)** and quantification **(C)** of CHO cell aggregation assays with indicated cadherins ("C") under varying Ca^{2+} concentrations. Sample size: 3 independent experiments per cadherin pair for every Ca^{2+} concentration. **(D)** Representative images of FRAP experiments between CHO cells expressing indicated GFP and mCherry tagged cadherins in the presence of 2 mM extracellular Ca^{2+}. Each row shows the contacting GFP and mCherry expressing cells (with both cells outlined in yellow) on the left, followed by time lapse images of the individual channels of the boxed region in right. Time point of 0 seconds indicates time immediately after photobleaching while negative and positive time points represent baseline and recovery fluorescence respectively. **(E)** Same as **(D)** but with 0.5 mM extracellular Ca^{2+}. **(F-G)** Recovery time constants (see Supplemental Experimental Procedures) for cadherins at 2 mM **(F)** and 0.5 mM **(G)** extracellular Ca^{2+}. Sample size: For 2mM Ca^{2+}: 8, 9, and 10 cell pairs were analyzed for cadherin-2/2, cadherin-9/6, and cadherin-9/10 junctions, respectively. For 0.5 mM Ca^{2+}: 8, 6, and 6 cell pairs were analyzed for cadherin-2/2, cadherin-9/6, and cadherin-9/10 junctions, respectively. Cells were evenly sampled from three independent experiments. Statistical differences were calculated using one-way ANOVA followed by pairwise p-value calculation using Holm-Šidák multiple comparison test. $p<0.05$, and $p<0.01$ is denoted by *, and ** respectively, otherwise $p>0.05$. All data shown as mean ± s.e.m.

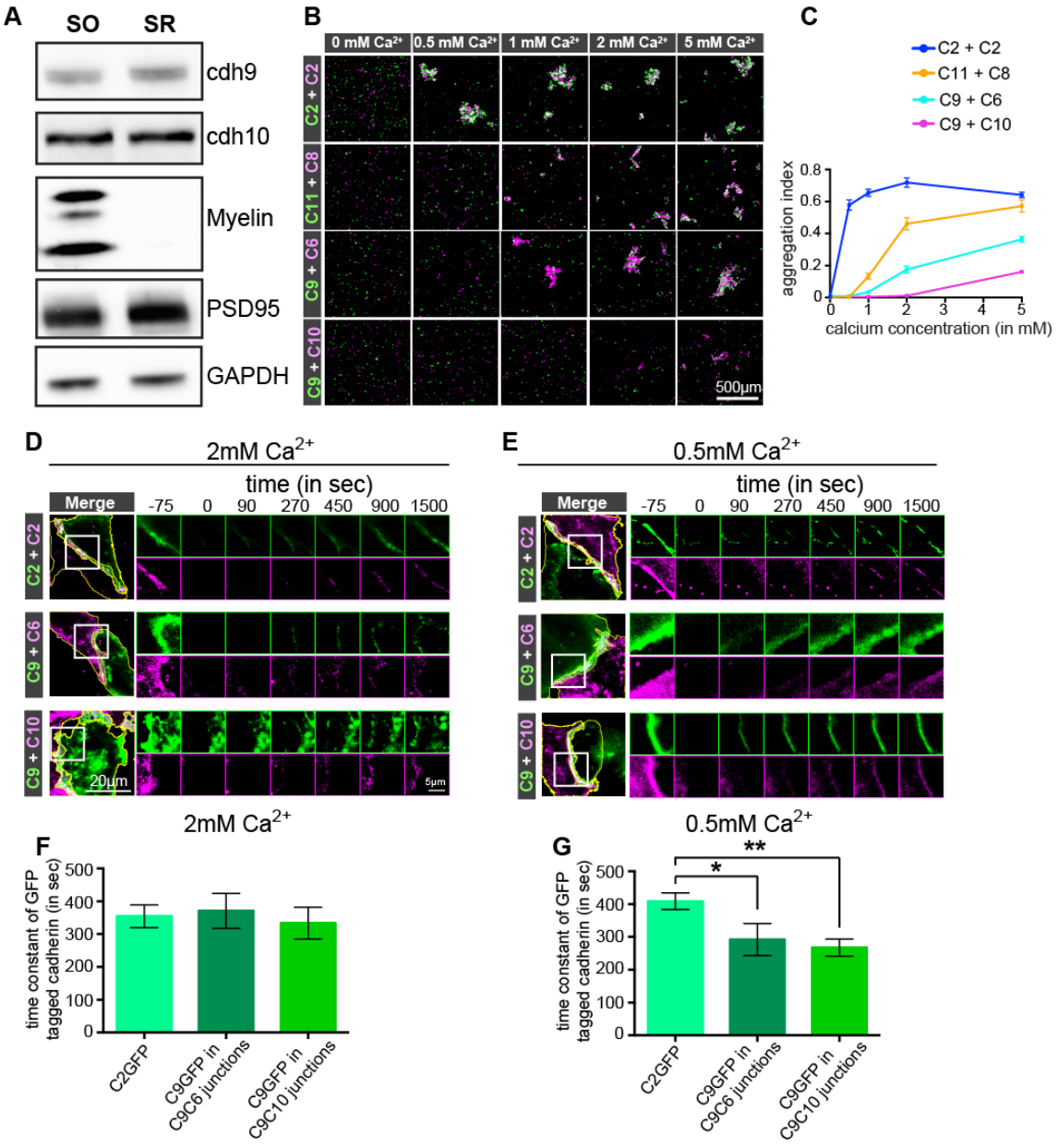
A
SO
SR
cdh9
cdh10
Myelin
PSD95
GAPDH
B
0 mM Ca2+
0.5 mM Ca2+
1 mM Ca2+
2 mM Ca2+
5 mM Ca2+
C2 + C2
C11 + C8
C9 + C6
C9 + C10
500µm
C
C2 + C2
C11 + C8
C9 + C6
C9 + C10
aggregation index
calcium concentration (in mM)
D
2mM Ca2+
time (in sec)
Merge
-75 0 90 270 450 900 1500
20µm
5µm
E
0.5mM Ca2+
F
2mM Ca2+
time constant of GFP tagged cadherin (in sec)
C2GFP
C9GFP in C9C6 junctions
C9GFP in C9C10 junctions
G
0.5mM Ca2+
**
*

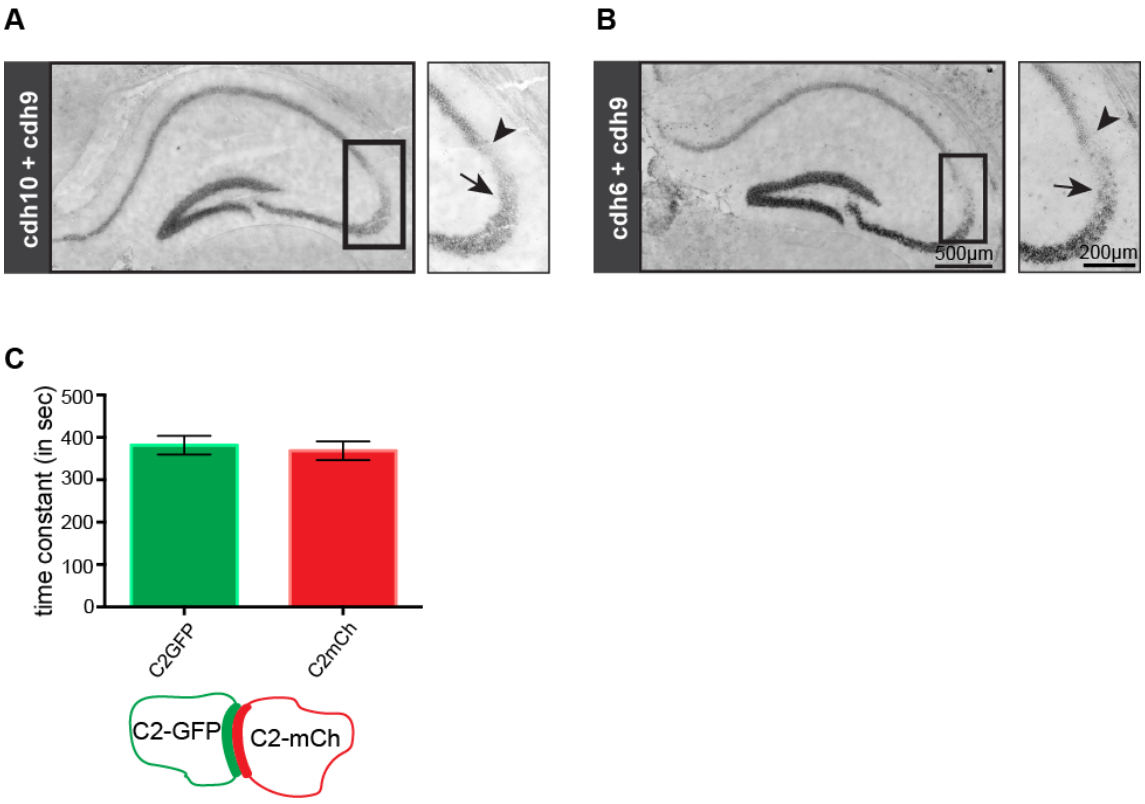

Figure 3.14: Cadherins-6 and 9 are not expressed in CA2.

(A-B) Double in situ hybridization against cadherin-9 and cadherin-10 mRNA **(A)** and cadherin-9 and cadherin-6 mRNA **(B)**. The boxed regions with area CA2 are magnified on right. Arrows indicate the boundary of cadherin-9 expression. Arrow heads indicate the boundaries of cadherin-10 **(A)** and cadherin-6 **(B)** expression. **(C)** Average recovery time constants of GFP and mCherry tagged cadherin-2 (top) at junctions formed by CHO cells expressing GFP and mCherry tagged cadherin-2 (bottom schematic). Sample sizes: 16 cadherin-2 cell pairs. Cells from 2 mM and 0.5 mM extracellular Ca^{2+} (shown in Figures7F and G) were pooled together. No significant differences by student's t-test. Data shown as mean ± s.e.m.

References

Aiga, M., Levinson, J.N., and Bamji, S.X. (2010). N-cadherin and neuroligins cooperate to regulate synapse formation in hippocampal cultures. J. Biol. Chem. *286*, 851–858.

Ango, F., di Cristo, G., Higashiyama, H., Bennett, V., Wu, P., and Huang, Z.J. (2004). Ankyrin-based subcellular gradient of neurofascin, an immunoglobulin family protein, directs GABAergic innervation at purkinje axon initial segment. Cell *119*, 257–272.

Arai, A., Black, J., and Lynch, G. (1994). Origins of the variations in long-term potentiation between synapses in the basal versus apical dendrites of hippocampal neurons. Hippocampus *4*, 1–9.

Benson, D.L., and Huntley, G.W. (2012). Synapse adhesion: a dynamic equilibrium conferring stability and flexibility. Curr. Opin. Neurobiol. *22*, 397–404.

Bian, W.-J., Miao, W.-Y., He, S.-J., Qiu, Z., and Yu, X. (2015). Coordinated spine pruning and maturation mediated by inter-spine competition for cadherin/catenin complexes. Cell 1–39.

Bourne, J., and Harris, K.M. (2007). Do thin spines learn to be mushroom spines that remember? Curr. Opin. Neurobiol. *17*, 381–386.

Bozdagi, O., Wang, X.B., Nikitczuk, J.S., Anderson, T.R., Bloss, E.B., Radice, G.L., Zhou, Q., Benson, D.L., and Huntley, G.W. (2010). Persistence of coordinated long-term potentiation and dendritic spine enlargement at mature hippocampal CA1 synapses requires N-cadherin. J. Neurosci. *30*, 9984–9989.

Duan, X., Krishnaswamy, A., la Huerta, De, I., and Sanes, J.R. (2014). Type II cadherins guide assembly of a direction-selective retinal circuit. Cell *158*, 793–807.

Dudek, S.M., Alexander, G.M., and Farris, S. (2016). Rediscovering area CA2: unique properties and functions. Nat. Rev. Neurosci. *17*, 89–102.

Dumitriu, D., Rodriguez, A., and Morrison, J.H. (2011). High-throughput, detailed, cell-specific neuroanatomy of dendritic spines using microinjection and confocal microscopy. Nat. Protoc. *6*, 1391–1411.

Egelman, D.M., and Montague, P.R. (1999). Calcium dynamics in the extracellular space of mammalian neural tissue. Biophys. J. *76*, 1856–1867.

Fièvre, S., Carta, M., Chamma, I., Labrousse, V., Thoumine, O., and Mulle, C. (2016). Molecular determinants for the strictly compartmentalized expression of kainate receptors in CA3 pyramidal cells. Nat. Commun. *7*, 12738.

Förster, E., Zhao, S., and Frotscher, M. (2006). Laminating the hippocampus. Nat. Rev. Neurosci. *7*, 259–268.

Gil, V., Bichler, Z., Lee, J.K., Seira, O., Llorens, F., Bribian, A., Morales, R., Claverol-Tinture, E., Soriano, E., Sumoy, L., et al. (2010). Developmental expression of the oligodendrocyte myelin glycoprotein in the mouse telencephalon. Cereb. Cortex *20*, 1769–1779.

Ginsberg, D., DeSIMONE, D., and Geiger, B. (1991). Expression of a novel cadherin (EP-cadherin) in unfertilized eggs and early Xenopus embryos. Development *111*, 315–325.

Harris, K.M. (1999). Structure, development, and plasticity of dendritic spines. Curr. Opin. Neurobiol. *9*, 343–348.

Harris, K.M., Jensen, F.E., and Tsao, B. (1992). Three-dimensional structure of dendritic spines and synapses in rat hippocampus (CA1) at postnatal day 15 and adult ages: implications for the maturation of synaptic physiology and long-term potentiation. J. Neurosci. *12*, 2685–2705.

Harrison, O.J., Jin, X., Hong, S., Bahna, F., Ahlsen, G., Brasch, J., Wu, Y., Vendome, J., Felsovalyi, K., Hampton, C.M., et al. (2011). The extracellular architecture of adherens junctions revealed by crystal structures of Type I cadherins. Structure *19*, 244–256.

Heupel, W.M., Baumgartner, W., Laymann, B., Drenckhahn, D., and Golenhofen, N. (2008). Different Ca2+ affinities and functional implications of the two synaptic adhesion molecules cadherin-11 and N-cadherin. Mol. Cell. Neurosci. *37*, 548–558.

Hirano, S., and Takeichi, M. (2012). Cadherins in brain morphogenesis and wiring. Physiol. Rev. *92*, 597–634.

Hitti, F.L., and Siegelbaum, S.A. (2014). The hippocampal CA2 region is essential for social memory. Nature *508*, 88–92.

Holtmaat, A.J.G.D., Trachtenberg, J.T., Wilbrecht, L., Shepherd, G.M., Zhang, X., Knott, G.W., and Svoboda, K. (2005). Transient and persistent dendritic spines in the neocortex in vivo. Neuron *45*, 279–291.

Huntley, G.W., Elste, A.M., Patil, S.B., Bozdagi, O., Benson, D.L., and Steward, O. (2010). Synaptic loss and retention of different classic cadherins with LTP-associated synaptic structural remodeling in vivo. Hippocampus *22*, 17–28.

Jungling, K., Eulenburg, V., Moore, R., Kemler, R., Lessmann, V., and Gottmann, K. (2006). N-cadherin transsynaptically regulates short-term plasticity at glutamatergic synapses in embryonic stem cell-derived neurons. J. Neurosci. *26*, 6968–6978.

Katsamba, P., Carroll, K., Ahlsen, G., Bahna, F., Vendome, J., Posy, S., Rajebhosale, M., Price, S., Jessell, T.M., Ben-Shaul, A., et al. (2009). Linking molecular affinity and cellular specificity in cadherin-mediated adhesion. Proc. Natl. Acad. Sci. USA *106*, 11594–11599.

Katz, Y., Menon, V., Nicholson, D.A., Geinisman, Y., Kath, W.L., and Spruston, N. (2009). Synapse distribution suggests a two-stage model of dendritic integration in CA1 pyramidal neurons. Neuron *63*, 171–177.

Kay, J.N., la Huerta, De, I., Kim, I.J., Zhang, Y., Yamagata, M., Chu, M.W., Meister, M., and Sanes, J.R. (2011). Retinal ganglion cells with distinct directional preferences differ in molecular identity, structure, and central projections. J. Neurosci. *31*, 7753–7762.

Krishnaswamy, A., Yamagata, M., Duan, X., Hong, Y.K., and Sanes, J.R. (2015). Sidekick 2 directs formation of a retinal circuit that detects differential motion. Nature *524*, 466–470.

Kuwako, K.-I., Nishimoto, Y., Kawase, S., Okano, H.J., and Okano, H. (2014). Cadherin-7 regulates mossy fiber connectivity in the cerebellum. Cell Rep. 1–35.

Lein, E.S., Hawrylycz, M.J., Ao, N., Ayres, M., Bensinger, A., Bernard, A., Boe, A.F., Boguski, M.S., Brockway, K.S., Byrnes, E.J., et al. (2007). Genome-wide atlas of gene expression in the adult mouse brain. Nature *445*, 168–176.

Li, X.G., Somogyi, P., Ylinen, A., and Buzsáki, G. (1994). The hippocampal CA3 network: an in vivo intracellular labeling study. J. Comp. Neurol. *339*, 181–208.

Manabe, T., Togashi, H., Uchida, N., Suzuki, S.C., Hayakawa, Y., Yamamoto, M., Yoda, H., Miyakawa, T., Takeichi, M., and Chisaka, O. (2000). Loss of cadherin-11 adhesion receptor enhances plastic changes in hippocampal synapses and modifies behavioral responses. Mol. Cell. Neurosci. *15*, 534–546.

Martin, E.A., Muralidhar, S., Wang, Z., Cervantes, D.C., Basu, R., Taylor, M.R., Hunter, J., Cutforth, T., Wilke, S.A., Ghosh, A., et al. (2015). The intellectual disability gene Kirrel3 regulates target-specific mossy fiber synapse development in the hippocampus. Elife *4*, e09395.

Matsuzaki, M., Honkura, N., Ellis-Davies, G.C.R., and Kasai, H. (2004). Structural basis of long-term potentiation in single dendritic spines. Nature *429*, 761–766.

Mendez, P., De Roo, M., Poglia, L., Klauser, P., and Muller, D. (2010). N-cadherin mediates plasticity-induced long-term spine stabilization. J. Cell Biol. *189*, 589–600.

Moser, M.B., Trommald, M., Egeland, T., and Andersen, P. (1997). Spatial training in a complex environment and isolation alter the spine distribution differently in rat CA1 pyramidal cells. J. Comp. Neurol. *380*, 373–381.

Nicholson, D.A., Trana, R., Katz, Y., Kath, W.L., Spruston, N., and Geinisman, Y. (2006). Distance-dependent differences in synapse number and AMPA receptor expression in hippocampal CA1 pyramidal neurons. Neuron *50*, 431–442.

Nicoll, R.A., and Schmitz, D. (2005). Synaptic plasticity at hippocampal mossy fibre synapses. Nat. Rev. Neurosci. *6*, 863–876.

Osterhout, J.A., Josten, N., Yamada, J., Pan, F., Wu, S.-W., Nguyen, P.L., Panagiotakos, G., Inoue, Y.U., Egusa, S.F., Volgyi, B., et al. (2011). Cadherin-6 mediates axon-target matching in a non-image-forming visual circuit. Neuron *71*, 632–639.

Perez-Cruz, C., Nolte, M.W., van Gaalen, M.M., Rustay, N.R., Termont, A., Tanghe, A., Kirchhoff, F., and Ebert, U. (2011). Reduced spine density in specific regions of CA1 pyramidal neurons in two transgenic mouse models of Alzheimer's disease. J. Neurosci. *31*, 3926–3934.

Petreanu, L., Mao, T., Sternson, S.M., and Svoboda, K. (2009). The subcellular organization of neocortical excitatory connections. Nature *457*, 1142–1145.

Poskanzer, K., Needleman, L.A., Bozdagi, O., and Huntley, G.W. (2003). N-cadherin regulates ingrowth and laminar targeting of thalamocortical axons. J. Neurosci. *23*, 2294–2305.

Redies, C., and Takeichi, M. (1996). Cadherins in the developing central nervous system: an adhesive code for segmental and functional subdivisions. Dev. Biol. *180*, 413–423.

Roberts, T.F., Tschida, K.A., Klein, M.E., and Mooney, R. (2010). Rapid spine stabilization and synaptic enhancement at the onset of behavioural learning. Nature *463*, 948–952.

Rusakov, D.A., and Fine, A. (2003). Extracellular Ca2+ depletion contributes to fast activity-dependent modulation of synaptic transmission in the brain. Neuron *37*, 287–297.

Saglietti, L., Dequidt, C., Kamieniarz, K., Rousset, M.-C., Valnegri, P., Thoumine, O., Beretta, F., Fagni, L., Choquet, D., Sala, C., et al. (2007). Extracellular interactions between GluR2 and N-Cadherin in spine regulation. Neuron *54*, 461–477.

Sanes, J.R., and Yamagata, M. (2009). Many paths to synaptic specificity. Annu. Rev. Cell Dev. Biol. *25*, 161–195.

Shan, W.S., Tanaka, H., Phillips, G.R., Arndt, K., Yoshida, M., Colman, D.R., and Shapiro, L. (2000). Functional cis-heterodimers of N- and R-cadherins. J. Cell Biol. *148*, 579–590.

Shimoyama, Y., Tsujimoto, G., Kitajima, M., and Natori, M. (2000). Identification of three human type-II classic cadherins and frequent heterophilic interactions between different subclasses of type-II classic cadherins. Biochem. J. *349*, 159–167.

Suto, F., Tsuboi, M., Kamiya, H., Mizuno, H., Kiyama, Y., Komai, S., Shimizu, M., Sanbo, M., Yagi, T., Hiromi, Y., et al. (2007). Interactions between Plexin-A2, Plexin-A4, and Semaphorin 6A control lamina-restricted projection of hippocampal mossy fibers. Neuron *53*, 535–547.

Suzuki, S.C., Inoue, T., Kimura, Y., Tanaka, T., and Takeichi, M. (1997). Neuronal

circuits are subdivided by differential expression of type-II classic cadherins in postnatal mouse brains. Mol. Cell. Neurosci. *9*, 433–447.

Tai, C.-Y., Kim, S.A., and Schuman, E.M. (2008). Cadherins and synaptic plasticity. Curr. Opin. Cell Biol. *20*, 567–575.

Takeichi, M., and Nakagawa, S. (2001). Cadherin-dependent cell-cell adhesion. Curr. Protoc. Cell Biol. *Chapter 9*, Unit9.3–9.3.15.

Tanaka, H., Shan, W., Phillips, G.R., Arndt, K., Bozdagi, O., Shapiro, L., Huntley, G.W., Benson, D.L., and Colman, D.R. (2000). Molecular modification of N-cadherin in response to synaptic activity. Neuron *25*, 93–107.

Tang, L., Hung, C.P., and Schuman, E.M. (1998). A role for the cadherin family of cell adhesion molecules in hippocampal long-term potentiation. Neuron *20*, 1165–1175.

Togashi, H., Abe, K., Mizoguchi, A., Takaoka, K., Chisaka, O., and Takeichi, M. (2002). Cadherin regulates dendritic spine morphogenesis. Neuron *35*, 77–89.

Tønnesen, J., Katona, G., Rózsa, B., and Nägerl, U.V. (2014). Spine neck plasticity regulates compartmentalization of synapses. Nat. Neurosci. *17*, 678–685.

Viswanathan, S., Williams, M.E., Bloss, E.B., Stasevich, T.J., Speer, C.M., Nern, A., Pfeiffer, B.D., Hooks, B.M., Li, W.-P., English, B.P., et al. (2015). High-performance probes for light and electron microscopy. Nat. Meth. *12*, 568–576.

Vitureira, N., Letellier, M., White, I.J., and Goda, Y. (2011). Differential control of presynaptic efficacy by postsynaptic N-cadherin and β-catenin. Nat. Neurosci. *15*, 81–89.

West, P.J., Saunders, G.W., Remigio, G.J., Wilcox, K.S., and White, H.S. (2014). Antiseizure drugs differentially modulate theta-burst induced long-term potentiation in C57BL/6 mice. Epilepsia *55*, 214–223.

Williams, M.E., Wilke, S.A., Daggett, A., Davis, E., Otto, S., Ravi, D., Ripley, B., Bushong, E.A., Ellisman, M.H., Klein, G., et al. (2011). Cadherin-9 regulates synapse-specific differentiation in the developing hippocampus. Neuron *71*, 640–655.

Wu, Y., Jin, X., Harrison, O., and Shapiro, L. (2010). Cooperativity between trans and cis interactions in cadherin-mediated junction formation. Proc. Natl Acad. Sci. USA 107, 17592–17597 (2010).

Xu, T., Yu, X., Perlik, A.J., Tobin, W.F., Zweig, J.A., Tennant, K., Jones, T., and Zuo, Y. (2009). Rapid formation and selective stabilization of synapses for enduring motor memories. Nature *462*, 915–919.

CHAPTER 4

THE ROLE OF CADHERINS-6, 9, AND 10 IN PRESYNAPTIC VESICLE ORGANIZATION OF CA3-CA1 SYNAPSES

Introduction

In the previous chapter, I demonstrated how interactions between cadherins-6, 9, and 10 mediate synaptic plasticity specifically in the CA1 SO layer. LTP in CA1 excitatory synapses occur predominantly through postsynaptic mechanisms (Herring and Nicoll, 2016). However, synaptic adhesion proteins can function in both pre- and postsynaptic compartments even if they are expressed only on one side of the synapse. For example, Neurexins, predominantly expressed in the presynaptic terminals, are known to have both pre- and postsynaptic functions (Anderson et al., 2015; Aoto et al., 2013). In another example of bidirectional regulation of synaptic properties, postsynaptic cadherin-2 has been shown to regulate both pre- and postsynaptic properties (Jungling et al., 2006; Mendez et al., 2010; Saglietti et al., 2007; Togashi et al., 2002; Vitureira et al., 2011). Hence, I subsequently tested if cadherins-6, 9, and 10 have any role on the structural organization of presynaptic terminals of excitatory synapses in CA1 SO and SR layers.

Results

First, I analyzed asymmetric synapses in CA1 SO and SR synaptic layers of $Cdh9^{+/+}$ and $Cdh9^{-/-}$ mice aged P21 using transmission electron microcopy (TEM). For every presynaptic bouton, I counted the number of total vesicles, vesicles docked on to the active zone (AZ) membrane, and vesicles within 30 nm of AZ termed proximal vesicles (Watanabe et al., 2013) (Schematic in Figure 3.2A). In contrast to our postsynaptic phenotypes, $Cdh9^{-/-}$ mice had significant reduction in overall and proximal vesicle density and also had a trend towards increased docked vesicle density in CA1 SR but not SO layer (Figure 4.1). I also confirmed that the difference in vesicle densities was not due

to difference in synaptic dimensions like bouton area or active zone length. Measurements from $Cdh9^{+/+}$ and $Cdh9^{-/-}$ synapses revealed no significant differences in bouton area and active zone length among the two genotypes.

Subsequently, I analyzed CA1 SO and SR synapses in $Cdh10^{+/+}$, $Cdh10^{-/-}$, and $Cdh6^{-/-}$;$Cdh10^{-/-}$ mice to test if absence of postsynaptic cadherins have similar phenotypes as $Cdh9^{-/-}$ mice. In the SO layer, I did not observe any major difference in the presynaptic architecture among the genotypes except $Cdh10^{-/-}$ mice had slight but significant increase in overall synaptic vesicle density compared to $Cdh10^{+/+}$ or $Cdh6^{-/-}$;$Cdh10^{-/-}$ mice (Figure 4.2). However, in the SR layer, the phenotypes observed in $Cdh6^{-/-}$;$Cdh10^{-/-}$ mice were opposite of that observed in $Cdh9^{-/-}$ mice. $Cdh6^{-/-}$;$Cdh10^{-/-}$ mice have significantly reduced docked vesicles and increased proximal vesicles compared to $Cdh10^{+/+}$ mice (Figure 4.2).

Discussion

Absence of cadherin-9 results in increased docked vesicles and reduced proximal vesicles specifically in the CA1 SR layer. Hence, I predict that cadherin-9 acts as a restriction factor preventing proximal to docked vesicle transition. However, given the synaptic role of cadherin9 specifically in SO synapses (Chapter 3), results in Figure 4.1 showing a presynaptic role of cadherin-9 specifically in CA1 SR synapses are surprising. Below I will provide two possible explanations for this discrepancy.

Cadherin-9 may have differential subsynaptic localization in the SO and SR synapses. Cadherins are typically believed to localize in a subsynaptic region called adherens junction, which is a major site of adhesion between the pre- and postsynaptic terminals

(Fannon and Colman, 1996; Uchida et al., 1996). The adherens junction is generally situated at a distance from the active zone. However, recent studies have shown that several cadherins, including cadherins-8, 9, and 10, can localize even in the active zone (Friedman et al., 2015; Loh et al., 2016). These studies, however, do not describe what fraction of cadherins are localized to the adherens junction versus the active zone. Hence, it is possible that there is substantial localization of cadherin-9 in the active zone of SR synapses. This may explain how it can affect the dynamics between proximal and docked vesicles in these synapses. In contrast, cadherin-9 may be localized more in the adherens junction of SO synapses, thereby exerting a bigger effect on spine stability in these synapses. Loss of both cadherins-6 and 10 resulted in reduced docked vesicles and increased proximal vesicles specifically in the CA1 SR layer, which is completely opposite to that observed for $Cdh9^{-/-}$ mice. This gives rise to the possibility that the heterophilic interaction of cadherin-9 with cadherins-6 and 10 probably impairs cadherin-9 from performing its presynaptic role. Hence, in the $Cdh6^{-/-}$;$Cdh10^{-/-}$ mice, cadherin-9 is unbound from its transsynaptic interactions, which results in its hyperactivity in the CA1 SR presynapses, thereby resulting in reduced docked vesicles and increased proximal vesicles.

Another explanation for the layer-specific pre- and postsynaptic roles of cadherin-9 may be that docked vesicles are difficult to identify using the chemical fixation method used here (see methods section). Recent studies have shown that the commonly used aldehyde-based brain fixation methods result in significantly less docked vesicles compared to the newer methods that better preserve the native ultrastructure of synapses (Korogod et al., 2015). Further, unambiguous identification of docked vesicles requires

well-preserved lipid bilayers both in the synaptic vesicles and the active zone. Such clarity can be best obtained using high-pressure freezing followed by freeze substitution methods of tissue fixation and staining (Korogod et al., 2015; Watanabe et al., 2013). In line with this argument, the total number of docked and proximal vesicles remain unchanged in both SO and SR layers in all the knockout mice when compared to their corresponding wildtype counterparts (Figure 4.3). Hence, it is likely that the differences observed in docked and proximal vesicles may be an artifact of stochastic variance resulting from chemical fixation and the inability to accurately classify "true" docked vesicles. This issue can be resolved by either analyzing synapses from more mice to gain statistical power or by performing analyses on tissues processed by high-pressure freezing.

Methods

Mice aged P21-P23 were transcardially perfused with cold phosphate buffered saline pH 7.4 (PBS) for 1 minute followed by cold fixative (1% paraformaldehyde (PFA) and 2.5 % glutaraldehyde in 0.1 M sodium cachodylate buffer pH 7.2) for 7 minutes. Brains were removed, soaked in fixative for two days, and sectioned into 150 μm thick coronal sections. The CA1 region was cut out, washed with 0.1 M sodium cachodylate buffer, fixed with 1% osmium tetroxide and 1.5% potassium ferrocyanide for 1 hour, and stained with 1% uranyl acetate for 1 hour. The tissue was subsequently dehydrated in increasing concentrations of ethanol, embedded in epon resin, and cured at 60°C for 48 hours. Next, 40nm sections were cut using a Leica UC6 ultramicrotome and stained using lead citrate. Images were acquired using a JEM-1400Plus TEM (JEOL) at 10000X magnification.

Both SO and SR synapses were imaged at a distance of 100 μm from the cell body. Excitatory synapses were identified from the presence of a visible PSD. Image analyses were done using ImageJ. The various parameters analyzed are outlined in a schematic presented in Figure 3.2A.

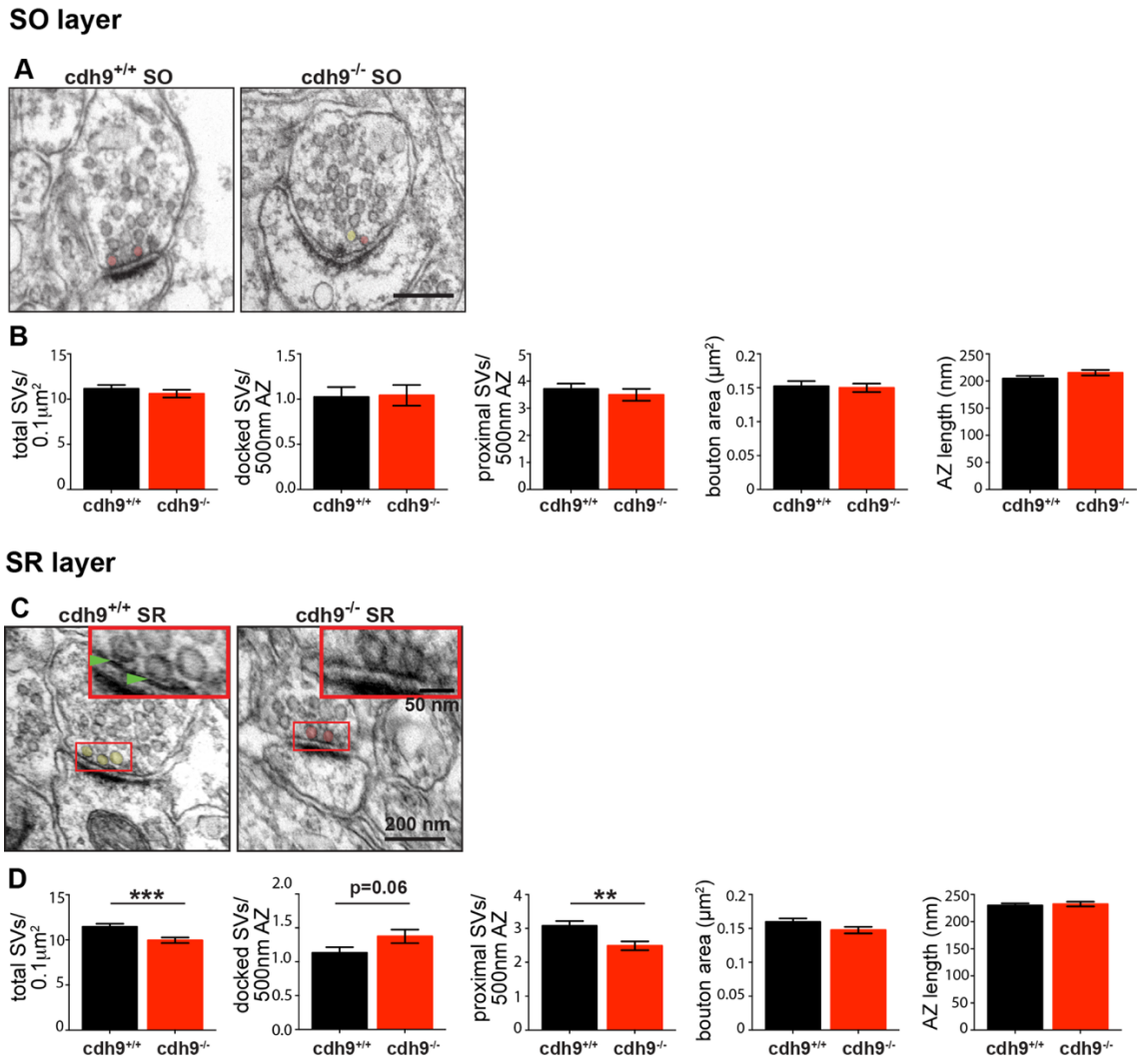

Figure 4.1: Cadherin-9 regulates synaptic vesicle distribution in SR synapses.

Ultrastructural analysis of asymmetric synapses in each CA1 layer as indicated. **(A,C)** Representative electron microscopic images of $Cdh9^{+/+}$ and $Cdh9^{-/-}$ asymmetric synapses. **(B,D)** Quantification of average SV density/0.1 μm^2 synaptic bouton volume, average docked SVs/500 nm active zone (AZ), average tethered SVs/500 nm AZ, average bouton area (in μm^2), and average AZ length (in nm). Inserts in panel **(C)** represent zoomed view of corresponding boxed regions. Tethered SVs are shown in yellow whereas docked SVs are shown in red. Visible gaps between tethered SV and AZ membrane are highlighted by green arrow heads. Sample sizes: SO = 190 WT synapses and 170 KO synapses. SR = 317 WT synapses and 316 KO synapses. All conditions were evenly sampled from 3 independent mice aged P21 and all analysis was done blind to genotype. p-values indicate unpaired t-test and $p<0.05$, $p<0.01$, and $p<0.001$ is denoted by *, **, and *** respectively. All data represented as mean ± s.e.m.

Figure 4.2: Cadherins-6 and 10 regulates synaptic vesicle distribution in SR synapses.

Ultrastructural analysis of asymmetric synapses in each CA1 layer as indicated. **(A,C)** Representative electron microscopic images of $Cdh10^{+/+}$,$Cdh10^{-/-}$, and $Cdh6^{-/-}$;$Cdh10^{-/-}$ asymmetric synapses. **(B,D)** Quantification of average SV density/0.1 μm^2 synaptic bouton volume, average docked SVs/500 nm active zone (AZ), average tethered SVs/500 nm AZ, average bouton area (in μm^2), and average AZ length (in nm). Sample sizes: SO = 149 ($Cdh10^{+/+}$), 177 ($Cdh10^{-/-}$), and 147 ($Cdh6^{-/-}$;$Cdh10^{-/-}$) synapses. SR = 181 ($Cdh10^{+/+}$), 173 ($Cdh10^{-/-}$), and 139 ($Cdh6^{-/-}$;$Cdh10^{-/-}$) synapses. All conditions were evenly sampled from 3 independent mice aged P21 and all analysis was done blind to genotype. Statistical differences were calculated using one-way ANOVA followed by pairwise p-value calculation using Holm-Šidák multiple comparison test. $p<0.05$, $p<0.01$, and $p<0.001$ is denoted by *, **, and *** respectively. All data represented as mean ± s.e.m.

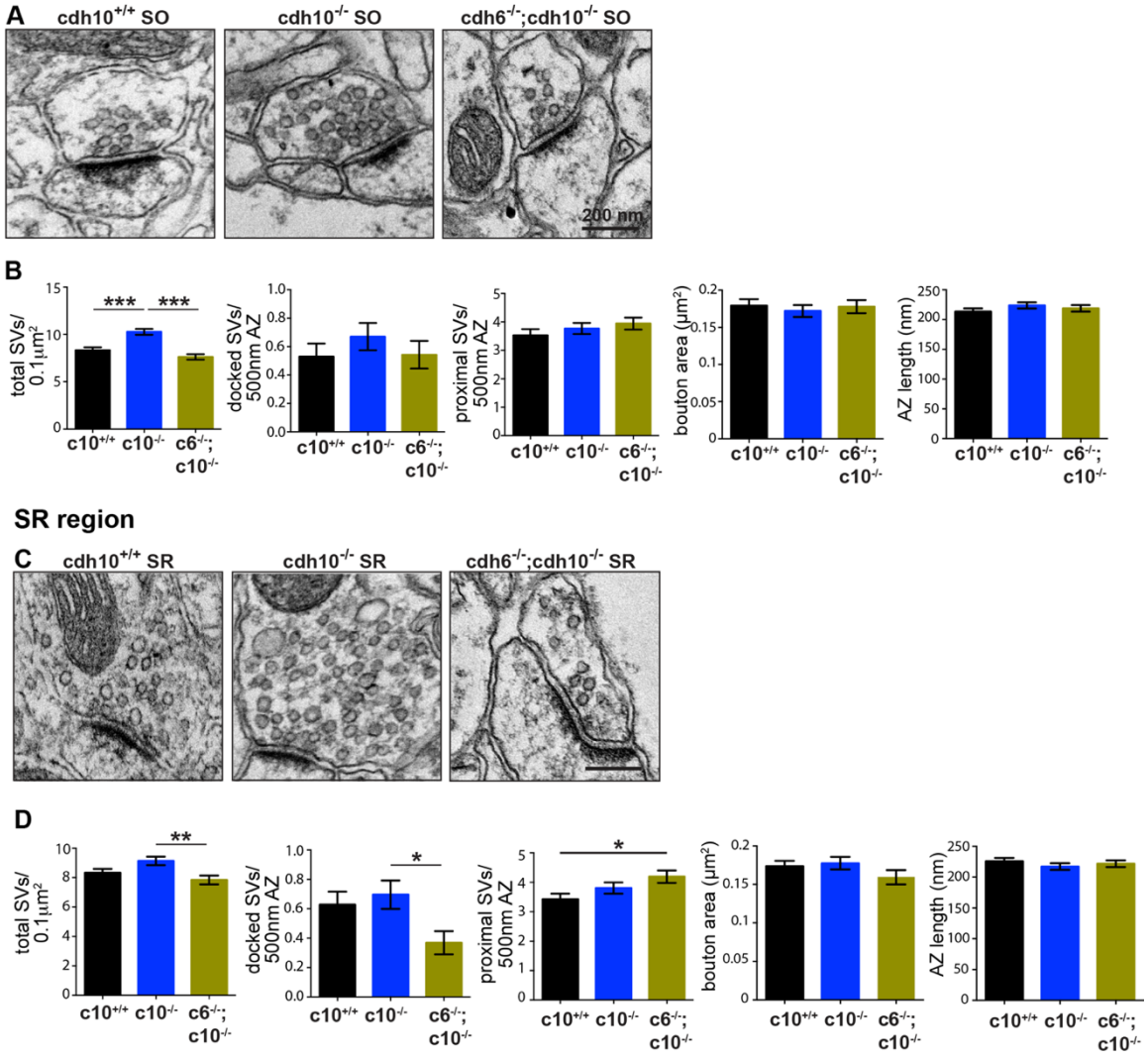
SO region
A
cdh10+/+ SO
cdh10-/- SO
cdh6-/-;cdh10-/- SO
200 nm
B
total SVs/ 0.1μm2
***
***
docked SVs/ 500nm AZ
proximal SVs/ 500nm AZ
bouton area (μm2)
AZ length (nm)
c10+/+
c10-/-
c6-/-; c10-/-
SR region
C
cdh10+/+ SR
cdh10-/- SR
cdh6-/-;cdh10-/- SR
D
**
*
*

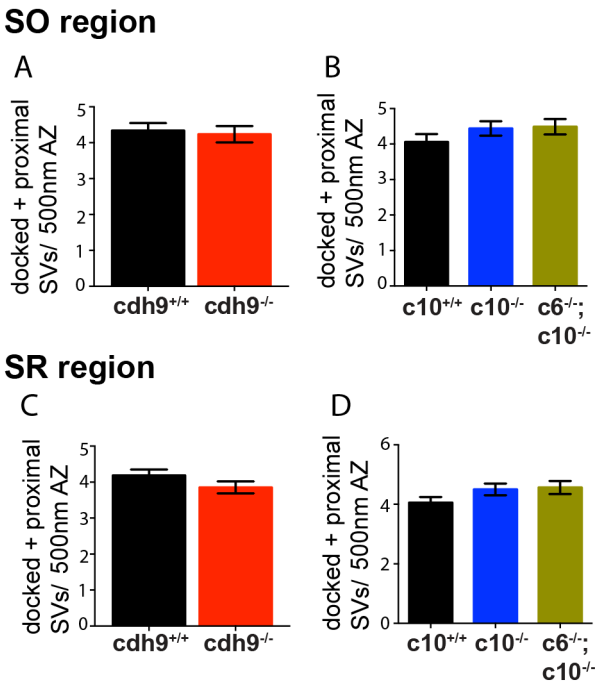

Figure 4.3: Sum of docked and proximal vesicles remain unchanged in the knockout animals.

(A,B) Quantification of average sum of docked and proximal vesicles in the CA1 SR synapses of $Cdh9^{+/+}$ and $Cdh9^{-/-}$ animals **(A)** and $Cdh10^{+/+}$,$Cdh10^{-/-}$, and $Cdh6^{-/-}$;$Cdh10^{-/-}$ animals **(B)**. **(C,D)** Quantification of average sum of docked and proximal vesicles in the CA1 SO synapses of $Cdh9^{+/+}$ and $Cdh9^{-/-}$ animals **(C)** and $Cdh10^{+/+}$,$Cdh10^{-/-}$, and $Cdh6^{-/-}$;$Cdh10^{-/-}$ animals **(D)**. Quantification done from the same images analyzed in figures 4.1 and 4.2. Statistical analyses were performed using students t-test for $Cdh9^{+/+}$ and $Cdh9^{-/-}$ animals. Statistical analyses for $Cdh10^{+/+}$,$Cdh10^{-/-}$, and $Cdh6^{-/-}$;$Cdh10^{-/-}$ animals were calculated using one-way ANOVA followed by pairwise p-value calculation using Holm-Šidák multiple comparison test. No statistically significant differences were observed.

References

Anderson, G.R., Aoto, J., Tabuchi, K., Földy, C., Covy, J., Yee, A.X., Wu, D., Lee, S.-J., Chen, L., Malenka, R.C., et al. (2015). β-Neurexins control neural circuits by regulating synaptic endocannabinoid signaling. Cell *162*, 593–606.

Aoto, J., Martinelli, D.C., Malenka, R.C., Tabuchi, K., and Südhof, T.C. (2013). Presynaptic neurexin-3 alternative splicing trans-synaptically controls postsynaptic AMPA receptor trafficking. Cell *154*, 75–88.

Fannon, A.M., and Colman, D.R. (1996). A model for central synaptic junctional complex formation based on the differential adhesive specificities of the cadherins. Neuron *17*, 423–434.

Friedman, L.G., Riemslagh, F.W., Sullivan, J.M., Mesias, R., Williams, F.M., Huntley, G.W., and Benson, D.L. (2015). Cadherin-8 expression, synaptic localization, and molecular control of neuronal form in prefrontal corticostriatal circuits. J. Comp. Neurol. *523*, 75–92.

Herring, B.E., and Nicoll, R.A. (2016). Long-Term Potentiation: From CaMKII to AMPA receptor trafficking. Annu. Rev. Physiol. *78*, 351–365.

Jungling, K., Eulenburg, V., Moore, R., Kemler, R., Lessmann, V., and Gottmann, K. (2006). N-cadherin transsynaptically regulates short-term plasticity at glutamatergic synapses in embryonic stem cell-derived neurons. J. Neurosci. *26*, 6968–6978.

Korogod, N., Petersen, C., and Knott, G.W. (2015). Ultrastructural analysis of adult mouse neocortex comparing aldehyde perfusion with cryo fixation. Elife. 4:e05793

Loh, K.H., Stawski, P.S., Draycott, A.S., Udeshi, N.D., Lehrman, E.K., Wilton, D.K., Svinkina, T., Deerinck, T.J., Ellisman, M.H., Stevens, B., et al. (2016). Proteomic analysis of unbounded cellular compartments: synaptic clefts. Cell *166*, 1295–1307.e21.

Mendez, P., De Roo, M., Poglia, L., Klauser, P., and Muller, D. (2010). N-cadherin mediates plasticity-induced long-term spine stabilization. J. Cell Biol. *189*, 589–600.

Saglietti, L., Dequidt, C., Kamieniarz, K., Rousset, M.-C., Valnegri, P., Thoumine, O., Beretta, F., Fagni, L., Choquet, D., Sala, C., et al. (2007). Extracellular interactions between GluR2 and N-cadherin in spine regulation. Neuron *54*, 461–477.

Togashi, H., Abe, K., Mizoguchi, A., Takaoka, K., Chisaka, O., and Takeichi, M. (2002). Cadherin regulates dendritic spine morphogenesis. Neuron *35*, 77–89.

Uchida, N., Honjo, Y., and Johnson, K.R. (1996). The catenin/cadherin adhesion system is localized in synaptic junctions bordering transmitter release zones. J. Cell Biol. *135*, 767-779.

Vitureira, N., Letellier, M., White, I.J., and Goda, Y. (2011). Differential control of

presynaptic efficacy by postsynaptic N-cadherin and β-catenin. Nat. Neurosci. *15*, 81–89.

Watanabe, S., Rost, B.R., Camacho-Pérez, M., Davis, M.W., Söhl-Kielczynski, B., Rosenmund, C., and Jorgensen, E.M. (2013). Ultrafast endocytosis at mouse hippocampal synapses. Nature *504*, 242–247.

CHAPTER 5

DISCUSSION

Overview

In Chapter 3, I described how deleting cadherin-9 or cadherins-6 and 10 reduces the enhanced synaptic potentiation and mushroom spine density in CA1 SO synapses. However, Western blot analysis from both CA1 SO and SR layers revealed equal expression of these cadherins in both CA1 layers (Figure 3.13A). These observations raise the question "how can heterophilic interactions between these three cadherins regulate LTP and mushroom spines specifically in the CA1 SO layer?"

In this chapter, I will first address whether cadherins-6, 9, and 10 function specifically at the SO layer or whether they function specifically at synapses with high LTP. Along these lines, I will present preliminary data that support the hypothesis that cadherins-6, 9, and 10 functions specifically at synapses with high LTP. Next, I will discuss possible mechanisms through which cadherins-6, 9, and 10 function specifically in high LTP synapses. More specifically, I will describe the sequence of events leading to LTP expression followed by the description of several models through which the CA1 SO layer can exhibit higher LTP than SR. I will further propose detailed anatomical and functional experiments to test each model, and discuss how the model may explain the specific role of cadherins-6, 9, and 10 in high LTP synapses.

Do cadherins-6, 9, and 10 selectively function in high magnitude LTP synapses or do they selectively function in LTP at SO but not SR synapses?

The role of cadherins-6, 9, and 10 specifically in CA1 SO LTP but not in SR LTP can result from two distinct possibilities. First, cadherins-6, 9, and 10 may specifically

localize to the CA1 SO layer or may function through a downstream signaling molecule that specifically localizes to SO synapses. Second, the role of heterophilic interactions among cadherins-6, 9, and 10 may not be layer specific but rather LTP level specific. In other words, cadherins-6, 9, and 10 may function specifically during high levels of LTP. This hypothesis would further imply that if the LTP levels of CA1 SR synapses were enhanced, these cadherins would be functional even in SR.

To test the first possibility, in Chapter 3, I performed layer-specific Western blots and demonstrated cadherins-6, 9 and 10 are expressed in equal amounts in CA1 SO and SR layers. In addition, using electron microscopic analysis of knockout synapses, I showed cadherins-6, 9 and 10 may also have a presynaptic role in synaptic vesicle organization in CA1 SR synapses (discussed in Chapter 4). These results suggest these cadherins may localize to both SO and SR synapses. Although less likely, it is still possible that these cadherins have different synaptic localization patterns within the SO and SR layers or functions through an unknown SO specific downstream molecule.

To test if cadherins-6, 9, and 10 function specifically at high LTP, I performed a preliminary experiment where I artificially increased the levels of SR LTP. I reasoned if postsynaptic depolarization is required for LTP (explained later), then its levels can be further enhanced by blocking feed forward inhibition. Hence, I carried out LTP studies in SR layer of wildtype, and $Cdh9^{-/-}$, slices in the presence of 20 μM Picrotoxin, a $GABA_A$ receptor antagonist. Introduction of picrotoxin for 10 minutes before and during the theta burst stimulation (TBS) caused a significant increase in SR LTP in wildtype slices (Figure 5.1). Interestingly, $Cdh9^{-/-}$ slices did not exhibit any increase in SR LTP following picrotoxin treatment (Figure 5.1). This result suggests cadherin-9 also

functions in SR LTP if the magnitude of LTP is high. Hence, cadherin-9 regulates high levels of LTP, which is normally observed in the SO synapses. Future experiments on $Cdh6^{-/-}$;$Cdh10^{-/-}$ slices will test if the heterophilic interaction between cadherins-6, 9, and 10 specifically regulate high levels of LTP. In the subsequent sections, I will discuss the possible synapse level manifestation of the high-magnitude LTP observed in CA1 SO and how cadherins- 6, 9, and 10 may have a role specifically in such high LTP synapses.

Dissecting the specific role of cadherins-6, 9, and 10 in high LTP expression

To better understand how cadherins-6, 9, and 10 specifically regulate high levels of LTP, it is necessary to first understand the sequence of events that lead to typical/low LTP expression. Postsynaptic NMDAR-mediated LTP in an excitatory spine synapse (like the ones in CA1 neurons) is a multistep process that ultimately increases the number of GluR1 containing AMPARs in the postsynapse. LTP is induced by either high-frequency synaptic stimulation or by low-frequency stimulation while the cell is injected with a constant depolarizing current or by spike timing-dependent plasticity protocols where synaptic stimulation is followed by an action potential in the postsynaptic neuron (Chen et al., 1999; Markram et al., 1997). Essentially, all of these techniques result in depolarization of the spine. Sufficient depolarization relieves the Mg^{2+} block in NMDARs, resulting in calcium influx. The calcium binds and activates an enzyme Ca^{2+}/calmodulin-dependent protein kinase (CamKII). Activated CamKII performs many functions, including synaptic recruitment of AMPARs and activation of Rho family of GTPases, which promote actin polymerization and spine enlargement (Herring and Nicoll, 2016). Hence, expression of LTP entails building a structurally enlarged and

stable spine that harbors increased numbers of AMPARs (Matsuzaki et al., 2004). Studies also show that silent synapses that express only NMDARs and no AMPARs can also undergo activation or "unsilencing" post LTP induction by AMPAR insertion (Isaac et al., 1995; Liao et al., 1995). As silent synapses do not conduct any current during basal activity, their sudden activation post LTP induction causes disproportionate increase of overall synaptic transmission. Hence, further AMPAR insertion and stabilization in AMPAR containing synapses and silent synapses together causes an increase in overall synaptic response to afferent stimulation post LTP induction.

It was previously hypothesized that SO synapses undergo higher LTP due to reduced feed forward inhibition in SO layer compared to SR layer (Arai et al., 1994). Lower inhibition would result in higher depolarization, thereby promoting higher LTP as described in the picrotoxin experiment. However, this study did not perform specific experiments to test the feed forward inhibition in the SO and SR layers. In general, enhanced depolarization in the SO layer can result from either reduced feed forward inhibition or mechanisms intrinsic to SO synapses and dendrites. Such intrinsic mechanisms can include the following pathways:

1) Individual SO spines may harbor higher densities of calcium channels or reduced numbers of potassium leak channels, leading to greater depolarization of the spines following synaptic activation.
2) SO dendrites may have different active properties compared to SR.

Active properties entail the expression of certain voltage gated ion channels that open up to generate a dendritic spike when the dendritic voltage reaches a threshold. Additional depolarization generated from dendritic spikes can trickle into the surrounding

spines, thereby increasing their depolarization and often aiding with LTP as observed in cortical pyramidal and hippocampal CA1 neurons (Golding et al., 2002; Gordon et al., 2006). Higher SO synaptic depolarization can result from higher SO dendritic spikes either due to increased densities of dendritic ion channels or presence of specific ion channels in the SO dendrites.

Enhanced SO depolarization can further manifest as high LTP through three mechanisms,

1) The proportion of non-silent synapses that are further potentiated (by AMPAR insertion) is higher in SO compared to SR.
2) Similar proportion of synapses are potentiated in both layers but the level of potentiation (or the number of extra AMPARs captured) per synapse is significantly higher in SO compared to SR.
3) More activation of silent synapses in SO compared to SR.

These mechanisms are not mutually exclusive and it is likely that a combination of these result in the higher magnitude of LTP in CA1 SO layer. Cadherins-6, 9, and 10 can regulate high LTP through any one of the steps mentioned above. However, results from the picrotoxin experiment (Figure 5.1) indicates cadherin-9 can play a role even in SR LTP. Hence, although higher SO LTP can result from a SO-specific enhanced depolarization pathway, cadherins-6, 9, and 10 are likely to act downstream of that pathway (highlighted above as three possible mechanisms). In the subsequent sections, I will first describe future experiments that can distinguish between mechanisms 1 and 2 followed by experiments that can test silent synapse activation in the two layers. I will also simultaneously discuss how cadherins-6, 9, and 10 can function along these

pathways.

Although less likely, LTP induction may result in similar depolarization in SO and SR synapses while SO synapses may possess some special mechanism via which they can express higher levels of LTP even at similar depolarization. However, if such mechanisms are depolarization independent, it is unlikely that they will be employed in SR synapses during picrotoxin application. Hence, a role of cadherin-9 in artificially enhanced SR LTP argues against its involvement in such mechanisms.

Does high LTP comprise higher proportion of potentiated synapses or similar proportion of highly potentiated synapses?

Higher LTP in CA1 SO indicates that the increase in AMPAR post LTP induction is greater in SO synapses compared to SR synapses. This increase can result either from an increase in AMPAR in more SO synapses or from a massive increase in AMPAR content in similar proportions of SO synapses (when compared to the number of potentiated SR synapses). Further, as increase in spine size (or structural LTP) is in complete coherence with increase in synaptic strength (functional LTP) (Matsuzaki et al., 2004), the above dichotomy can be extended to SO spine size as well (Figure 5.2). The majority of LTP studies are performed using field recordings or voltage clamped neurons. In these systems, a postsynaptic response is an ensemble response from multiple synapses. Hence, the changes in properties of individual synapses are lost in these experiments. TEM reconstruction studies exploring structural LTP using field stimulation could not detect any overall increase in spine size in contrast to 2-photon stimulation of single spines (Bourne and Harris, 2010; Matsuzaki et al., 2004) possibly because they could not

identify the synapses undergoing LTP. Further, the increased SO mushroom spine density discussed in Chapter 3 likely results from behavior-mediated intrinsic potentiation of the animals while they were in their home cages. These data, although corroborative of high SO LTP, is not a direct time-controlled measure of pre- versus post-LTP spine sizes in SO and SR layers. Hence, to resolve the above dichotomy, I will propose experiments that measure spine sizes and electrical strength of single synapses before and after LTP induction in both CA1 SO and SR layer.

As mentioned in the previous section, higher depolarization in SO dendrites may result from a network or dendritic effect. Hence, although 2-photon uncaging near a single spine is ideal to measure spine size differences pre and post LTP induction, it cannot recruit feed forward inhibition or active dendritic mechanisms contributing to dendritic spikes. Hence, structural LTP in SO versus SR needs to be analyzed by stimulating Schaffer collateral axons and identifying spines that respond to the stimulation. One way to achieve this is to patchclamp a CA1 neuron with a calcium indicator and a cell filler in the patch pipette (Gordon et al., 2006). Once the stimulation strength is determined, test stimulations accompanied by high-speed 2-photon imaging of different regions of the dendritic tree can help identify spines responsive to the afferent stimulation. Imaging these spines before and after LTP induction in both SO and SR layer can help resolve the dichotomy in terms of structural LTP. Calculation of the proportion of responsive spines that got potentiated and the mean size of the potentiated spines can identify if SO layer post LTP induction (compared to SR) comprises a) higher proportion of similarly enlarged spines, or b) similar proportions of highly enlarged spines, or c) a combination of both. Further, carrying out this experiment in cadherin

knockout slices can explain precisely why these animals have lower densities of CA1SO mushroom spines. Structural LTP is especially relevant to cadherins as studies on cadherin-2 have led to the hypothesis that cadherins stabilize enlarged spines (Benson and Huntley, 2012; Bozdagi et al., 2000; 2010; Mendez et al., 2010; Tai et al., 2007; Tang et al., 1998). Based on these studies, I speculate that if high SO LTP results from highly enlarged spines, then cadherins-6, 9, and 10 likely affect the stability of these spines through their unique biophysical properties (Patel et al., 2006) or other unknown intracellular signaling properties. On the contrary, if high SO LTP results from higher proportion of similarly enlarged spines and if absence of cadherins-6, 9, and 10 reduces this proportion, then it can be argued that these cadherins function as a second wave of reinforcements while other cadherins (like cadherin-2) get recruited for the regular LTP expression observed in SR.

In addition to spine enlargement data, this experiment can also provide information regarding the calcium transients in the potentiated spines. Experiments on knockout slices can indicate if absence of cadherins cause reduced calcium influx in the spines or if they act downstream of that. However, calcium forms a minor fraction of the total ions entering a postsynapse and hence, to resolve the above dichotomy in terms of functional LTP, synaptic currents from individual potentiated synapses need to be measured.

To understand the effect of potentiation on individual synapses the average current conducted through each synapse, or the average quantal size of a synapse, pre- and post-LTP induction needs to be quantified. Quantal analysis can be performed on a patch clamped postsynaptic neuron that is receiving near minimal stimulation. EPSPs from a single CA1 neuron receiving a low-frequency minimal stimulation in both SO and SR

layer can be graphed into a amplitude frequency histogram. This histogram will have discrete peaks representing release from different numbers of release sites (or synapses) (Bekkers and Stevens, 1990; Larkman et al., 1997; 1991; Liao et al., 1992). The average spacing between these peaks gives an estimate of the quantal size of the synapses that are stimulated. Performing this analysis pre and post LTP induction can indicate the increase in quantal size following LTP (Liao et al., 1992). If the SO contains higher proportion of similarly potentiated synapses, then post-LTP quantal size between SO and SR would be similar (but the relative frequency of the different peaks would be unequal). On the contrary, if the high SO LTP results from equal proportions of highly potentiated synapses, the quantal size of SO synapses would increase compared to SR. These experiments can be further conducted in cadherin knockout slices to understand how the absence of heterophilic cadherin-6,9, and 10 interaction affects the SO quantal size post LTP. One argument against this line of experiments can be that minimal stimulation may stimulate too few synapses to result in the sufficient difference in depolarization among the two layers. Hence, if no difference in SO versus SR LTP is observed by this method, then a special trick can be used to perform quantal analysis in strongly stimulated neurons as described below.

Replacing the extracellular calcium by strontium results in asynchronous release (or aEPSC) from individual synapses for few hundred milliseconds following single stimulation of the pathway (Levy et al., 2015; Xu-Friedman and Regehr, 2000). These release events are almost equivalent to mini EPSC events but with the advantage of selectively arising form the stimulated synapses. Hence, the average amplitude of aEPSCs gives an estimate of the quantal size. As strontium can be easily washed out and

replaced with calcium, this analysis can be performed pre- and post-LTP induction. Post-LTP increase in average aEPSC amplitude in SO versus SR layer can be interpreted as explained in the previous paragraph.

Once the dichotomy is resolved, future experiments can address the exact step(s) where cadherins-6, 9, and 10 function. If post-LTP SO quantal size is higher than that of SR and if the cadherin knockouts affect this high SO quantal size, several interesting possibilities arise. For example, if cadherin knockouts also affect structural LTP of highly enlarged spines as described above, then future experiments need to disentangle if cadherins-6, 9, and 10 are required for stabilizing the large spines or whether they are required for extra AMPAR recruitment/stability or they somehow affect the underlying cytoskeleton changes. It has been proposed that there are slots in the postsynaptic densities that trap AMPARs post LTP induction. These slot have been further argued to be mostly resulting from newly formed actin filaments (Herring and Nicoll, 2016). Hence, the high SO LTP could result from massively increased slots in the potentiated SO synapses caused by some special degree of actin remodeling occurring in these synapses. It is easy to envision that enhanced depolarization by picrotoxin can result in such increased slots even in SR synapses. Cadherins-6, 9, and 10 may be instrumental in orchestrating these special actin dynamics in the SO synapses and thereby, their loss can affect both synapse enlargement and AMPAR recruitment. Or these cadherins may simply be acting as special glues that help stabilize highly enlarged spines by keeping them bound to the presynaptic boutons. Hence, loss of cadherins would result in collapse of these spines that may affect laterally diffusing AMPAR that get recruited post LTP (Herring and Nicoll, 2016).

On the other hand, if high SO LTP results from higher proportion of similarly potentiated synapses and if absence of cadherins-6, 9, and 10 reduces this proportion (keeping the quantal size unchanged), then it can be argued that these cadherins function as a second wave of effector molecules. This can be tested by checking if overexpression of cadherin-2 in CA1 neurons can rescue the SO LTP phenotype of $Cdh9^{-/-}$ or $Cdh6^{-/-}$;$Cdh10^{-/-}$ slices.

Does high LTP comprise greater activation of silent synapses?

As mentioned above, high SO LTP can result from increased activation of silent synapses in the SO. This can be measured directly by performing experiments similar to those that led to the discovery of the role of silent synapses in LTP (Isaac et al., 1995; Liao et al., 1995). Briefly, voltage clamped CA1 neurons need to be stimulated (either in SR or SO layer) at an intensity that would evoke no synaptic response at -70mV holding potential but evoke positive responses at +40 mV holding potential. In these situations, the responses at +40mV result from silent synapses. LTP induction in these neurons results in synaptic responses at -70 mV that indicate activated silent synapses (that now have AMPARs). If SO LTP measured using this protocol is higher than SR LTP, it will indicate that activation of higher proportion of silent synapses contribute to high SO LTP levels. Interestingly, if cadherin knockout slices affect SO LTP by specifically reducing the activation of silent synapses in SO layer, it will beg the question why they do not affect the SR silent synapses (as evident from a lack of SR LTP phenotype in the knockouts). In such scenarios, it may be argued that SO silent synapses are in some way different than SR silent synapses. However, this argument is also difficult to justify given

that cadherin-9 knockouts have SR LTP phenotype when the LTP levels are artificially increased using picrotoxin (Figure 5.1). One alternative possibility could be that silent synapses differ in their "silence" and some may require higher levels of depolarization to be activated and these are the synapses regulated by the cadherins-6, 9, and 10.

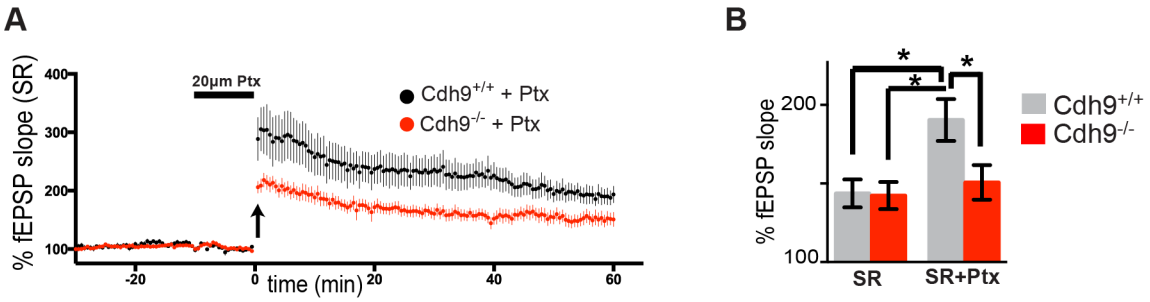

Figure 5.1: Cadherin-9 functions in artificially increased SR LTP.

(A) Mean CA1 SR LTP timecourse in $Cdh9^{+/+}$ and $Cdh9^{-/-}$ slices in the presence of of picrotoxin (Ptx) before and during TBS (arrow). **(B)** Quantification of mean SR LTP in $Cdh9^{+/+}$ and $Cdh9^{-/-}$ slices in the absence (first two columns) and presence (last two columns) of picrotoxin. Note that picrotoxin addition causes significant increase in SR LTP in wildtype slices.

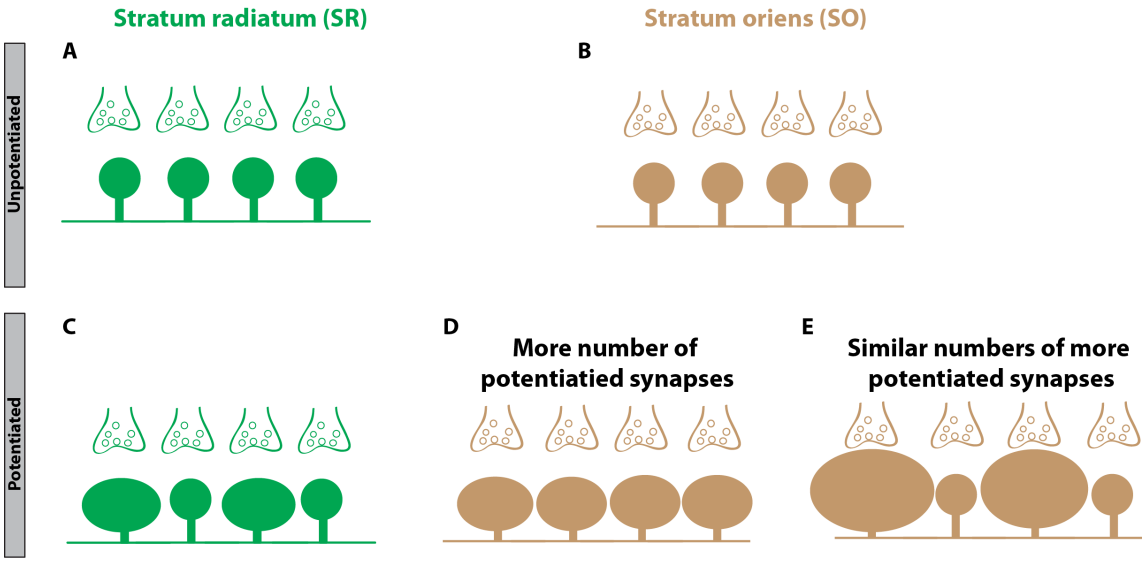

Figure 5.2: Connecting enhanced functional LTP to structural LTP.

(A, B) Schematic of unpotentiated SR **(A)** and SO synapses **(B)**. **(C)** Schematic of the same SR dendrite undergoing LTP. Note that the first and third synapse (from left) are shown to undergo potentiation. For SO synapses, two distinct possibilities are depicted for the enhanced potentiation compared to SR **(D, E)**. **(D)** Schematic showing potentiation of all four SO synapses as compared to only two synapses in the SR. **(E)** Schematic depicting enhanced potentiation of the first and third SO synapse resulting in 'very big headed' spines.

References

Arai, A., Black, J., and Lynch, G. (1994). Origins of the variations in long-term potentiation between synapses in the basal versus apical dendrites of hippocampal neurons. Hippocampus *4*, 1–9.

Bekkers, J.M., and Stevens, C.F. (1990). Presynaptic mechanism for long-term potentiation in the hippocampus. Nature *346*, 724–729.

Benson, D.L., and Huntley, G.W. (2012). Synapse adhesion: a dynamic equilibrium conferring stability and flexibility. Curr. Opin. Neurobiol. *22*, 397–404.

Bourne, J.N., and Harris, K.M. (2010). Coordination of size and number of excitatory and inhibitory synapses results in a balanced structural plasticity along mature hippocampal CA1 dendrites during LTP. Hippocampus *21*, 354–373.

Bozdagi, O., Shan, W., Tanaka, H., Benson, D.L., and Huntley, G.W. (2000). Increasing numbers of synaptic puncta during late-phase LTP: N-cadherin is synthesized, recruited to synaptic sites, and required for potentiation. Neuron *28*, 245–259.

Bozdagi, O., Wang, X.B., Nikitczuk, J.S., Anderson, T.R., Bloss, E.B., Radice, G.L., Zhou, Q., Benson, D.L., and Huntley, G.W. (2010). Persistence of coordinated long-term potentiation and dendritic spine enlargement at mature hippocampal CA1 synapses requires N-cadherin. J. Neurosci. *30*, 9984–9989.

Chen, H.X., Otmakhov, N., and Lisman, J. (1999). Requirements for LTP induction by pairing in hippocampal CA1 pyramidal cells. J. Neurophysiol. *82*, 526–532.

Golding, N.L., Staff, N.P., and Spruston, N. (2002). Dendritic spikes as a mechanism for cooperative long-term potentiation. Nature *418*, 326–331.

Gordon, U., Polsky, A., and Schiller, J. (2006). Plasticity compartments in basal dendrites of neocortical pyramidal neurons. J. Neurosci *26*, 12717–12726.

Herring, B.E., and Nicoll, R.A. (2016). Long-term potentiation: From CaMKII to AMPA receptor trafficking. Annu. Rev. Physiol. *78*, 351–365.

Isaac, J.T.R., Nicoll, R.A., and Malenka, R.C. (1995). Evidence for silent synapses: Implications for the expression of LTP. Neuron *15*, 427–434.

Larkman, A.U., Jack, J., and Stratford, K.J. (1997). Quantal analysis of excitatory synapses in rat hippocampal CA1 In Vitro during low-frequency depression. J. Physiol. *505*, 457-471.

Larkman, A., Stratford, K., and Jack, J. (1991). Quantal analysis of excitatory synaptic action and depression in hippocampal slices. Nature *350*, 344–347.

Levy, J.M., Chen, X., Reese, T.S., and Nicoll, R.A. (2015). Synaptic consolidation

normalizes AMPAR quantal size following MAGUK loss. Neuron *87*, 534–548.

Liao, D., Hessler, N.A., and Malinow, R. (1995). Activation of postsynaptically silent synapses during pairing-induced LTP in CA1 region of hippocampal slice. Nature *375*, 400–404.

Liao, D., Jones, A., and Malinow, R. (1992). Direct measurement of quantal changes underlying long-term potentiation in CA1 hippocampus. Neuron *9*, 1089–1097.

Markram, H., Lübke, J., Frotscher, M., and Sakmann, B. (1997). Regulation of synaptic efficacy by coincidence of postsynaptic APs and EPSPs. Science *275*, 213–215.

Matsuzaki, M., Honkura, N., Ellis-Davies, G.C.R., and Kasai, H. (2004). Structural basis of long-term potentiation in single dendritic spines. Nature *429*, 761–766.

Mendez, P., De Roo, M., Poglia, L., Klauser, P., and Muller, D. (2010). N-cadherin mediates plasticity-induced long-term spine stabilization. J. Cell Biol. *189*, 589–600.

Patel, S.D., Ciatto, C., Chen, C.P., Bahna, F., Rajebhosale, M., Arkus, N., Schieren, I., Jessell, T.M., Honig, B., Price, S.R., et al. (2006). Type II cadherin ectodomain structures: implications for classical cadherin specificity. Cell *124*, 1255–1268.

Tai, C.-Y., Mysore, S.P., Chiu, C., and Schuman, E.M. (2007). Activity-regulated N-cadherin endocytosis. Neuron *54*, 771–785.

Tang, L., Hung, C.P., and Schuman, E.M. (1998). A role for the cadherin family of cell adhesion molecules in hippocampal long-term potentiation. Neuron *20*, 1165–1175.

Xu-Friedman, M.A., and Regehr, W.G. (2000). Probing fundamental aspects of synaptic transmission with strontium. J. Neurosci. *20*, 4414–4422.